Collagen expression in renal fibrosis

Von der Medizinischen Fakultät der Rheinisch-Westfälischen Technischen Hochschule Aachen zur Erlangung des akademischen Grades einer Doktorin der Medizin genehmigte Dissertation

Vorgelegt von

Paula Marie Tyra

aus Henstedt-Ulzburg

Berichter: Universitätsprofessor Dr. med. Peter Boor, PhD
Universitätsprofessor Dr. med. Jürgen Floege

Tag der mündlichen Prüfung: 12.05.2021

Diese Dissertation ist auf den Internetseiten der Universitätsbibliothek online verfügbar

Contents

List of Abbreviations

AD	**A**d**e**nine nephropathy
BCA	**B**icinchoninic **A**cid **A**ssay
cDNA	**C**omplementary **D**eoxyribo**n**ucleic **A**cid
COPD	**C**hronic **O**bstructive **P**ulmonary **D**isease
CKD	**C**hronic **K**idney **D**isease
DAB	3,3′-**D**i**a**mino**b**enzidine
DAPI	4′,6-**D**i**a**midino-2-**p**heny**l**indole
EDS	**E**hlers-**D**anlos **S**yndrome
ECM	**E**xtra**c**ellular **M**atrix
EDTA	**E**thylene**d**iamine**t**etraacetic **a**cid
eGFR	**E**stimated **GFR**
EGFR	**E**pidermal **G**rowth **F**actor **R**eceptor
EMT	**E**pithelial-**m**esenchymal **T**ransition
FA	**F**olic **A**cid
FACIT	**F**ibril-**a**ssociated **c**ollagens with **i**nterrupted **t**riple **h**elices
GBM	**G**lomerular **B**asement **M**embrane
GFR	**G**lomerular **F**iltration **R**ate
IgG	**I**mmuno**g**lobulin **G**
IF	**I**mmuno**f**luorescence
IHC	**I**mmuno**h**isto**c**hemistry
ISEMF	**I**ntestinal **S**ub**e**pithelial **M**yo**f**ibroblasts
I/R	**I**schemia **R**eperfusion
kDa	**K**ilo**da**lton
NC	**N**on-**C**ollagenous
MMP	**M**atrix **M**etallo**p**rotease
NFDM	**N**on**f**at **D**ry **M**ilk
PAS	**P**eriodic **A**cid **S**chiff
PBS	**P**hosphate **B**uffered **S**aline
PCR	**P**olymerase **C**hain **R**eaction
PMSF	**P**henyl**m**ethyl**s**ulfonyl **f**luoride
RT-qPCR	**R**everse **T**ranscriptase **q**uantitative **PCR**
SD	**S**tandard **D**eviation
SDS	**S**odium **D**odecyl **S**ulfate

SLRP	**S**mall **L**eucine **R**ich **P**roteoglycan
TGF-β	**T**ransforming **G**rowth **F**actor-β
TLR	**T**oll-**L**ike **R**eceptor
TTBS	**T**ween **T**ris-**B**uffered **S**aline
UUO	**U**nilateral **U**reteral **O**bstruction
VEGF	**V**ascular **E**ndothelial **G**rowth **F**actor
VEGF-R	**VEGF-R**eceptor
vWF-A	**V**on **W**illebrand **f**actor type **A**
WT	**W**ild **T**ype

Chapter 1
Introduction

1.1 Chronic kidney disease and fibrosis

1.1.1 Kidney anatomy and function

The kidneys are two bean-shaped retroperitoneal organs. They consist of urine-forming structures (nephrons and collecting tubes) and urine-collecting structures (renal calyces and renal pelvis). The kidney is responsible for the homeostasis of the blood, the excretion of metabolic waste products, and foreign substances. It also has endocrine functions such as the production of erythropoietin, vitamin D3 and renin (Benninghoff & Drenckhahn, 2008).
The kidney is made up of cortex and medulla and in human it is divided into several renal lobes. These consist of a medullary segment, called the renal pyramid, and are surrounded by renal cortex, called columns. The pyramids extend to the renal papilla that empties urine into minor then major calyces, which then empty into the renal pelvis (Benninghoff & Drenckhahn, 2008).
The nephron is the structural and functional unit of the kidney. Each human adult kidney contains around one million nephrons. Each nephron consists of a renal corpuscle and a renal tubule. The renal corpuscle is composed of a tuft of capillaries called a glomerular tuft and an encompassing Bowman's capsule. The capillaries are stabilized by extracellular matrix (ECM)-producing mesangial cells, together called mesangium. The filtration of the blood takes place in the renal corpuscle through a filtration barrier, which consists of the endothelium of the capillaries, a thick basal lamina, and the podocytes. The resulting ultrafiltrate is called primary urine. In the tubule system, the ultrafiltrate is concentrated by reabsorption of low-molecular components and water, and active excretion of metabolic waste products. Between the tubules, there is the interstitium consisting of fibroblasts surrounded by ECM and resident dendritic immune cells (Welsch, 2006). Figure 1.1 shows a periodic acid Schiff (PAS) staining of a murine cortex section, which closely resembles the human cortex morphology.

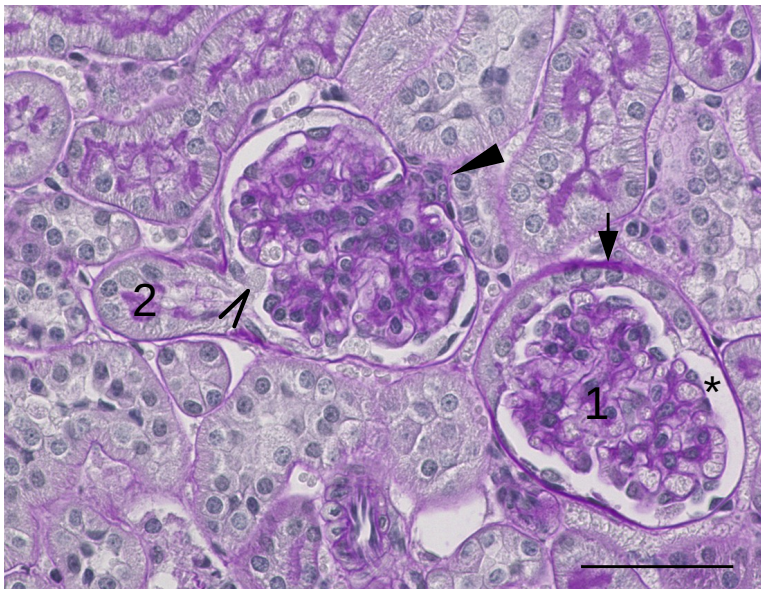

FIGURE 1.1: **Periodic acid Schiff (PAS) staining of a murine kidney cortex section.** 1: glomerulus, 2: proximal tubule *: Bowman's space, arrow: parietal layer of Bowman's capsule, closed arrow head: capillary pole, open arrow head: tubular pole. Adapted from Breitkopf, 2020. Scale bar: 50 µm.

1.1.2 Chronic kidney disease

Definition and epidemiology

Chronic kidney disease (CKD) is defined as the presence of kidney damage and decreased kidney function for three months or more. According to international guidelines, CKD can be classified into five stages using the glomerular filtration rate (GFR), which is pathologically reduced at $< 60\,\text{ml} / \text{min} / 1.73\,\text{m}^2$, and the extend of albuminuria (National Kidney Foundation, 2002). GFR and albuminuria allow to estimate the risk of patients with CKD to adverse outcomes, like progress-ion to end-stage renal disease, cardiovascular disease, hospitalization, or death (Romagnani et al., 2017).
The prevalence of all stages of CKD varies between 11.7 – 15.1 %, for stages 3 – 5 the prevalence is 9.2 – 12.2 % (Hill et al., 2016). The most common underlying diseases associated with CKD are diabetes mellitus and hypertension, which have a high prevalence in high-income countries (Romagnani et al., 2017). The 5-year survival of patients on dialysis is 40 – 50 %. Once dialysis begins, future life expectancy is only 1/3 of the life expectancy of that of the age-matched and sex-matched general population. For patients receiving a kidney transplant, 5-year survival increases between 86 – 93 % (Romagnani et al., 2017).
There is still no effective treatment for CKD. Key strategies are managing the

complications, like renal anemia, arterial hypertension and mineral bone disorder, and slowing down the progression of loss of kidney function. Dialysis and kidney transplantation are used for kidney replacement therapy. In 2008, an estimated 1.77 million patients worldwide received dialysis (Lameire & Van Biesen, 2010). Dialysis is not only associated with higher mortality but also with a lower quality of life due to the uremic symptoms and a time-consuming procedure (Romagnani et al., 2017). CKD is not only a significant economic burden on affected individuals, especially in developing countries, but causes also high costs on health care. People with end-stage kidney disease make up 0.1 – 0.2% of the total population and cause 2 – 3 % of the healthcare expenditure in developed nations. The econo-mic costs associated with milder forms of CKD are harder to evaluate but are even higher. In 2007, in the USA 27 % of the total Medicare budget was used for expenditures on CKD (Jha et al., 2013).

Pathomechanisms of CKD

Chronic injury e.g. caused by diabetes, high blood pressure or recurrent glomerulonephritides leads to pathological wound healing with fibrosis as the common end-point of failed repair and recovery. The pathological fibrosis results in glomerulosclerosis, tubular atrophy and dilatation, tubulointerstitial fibrosis, and a reduction in capillary density (see 1.1.3) (Boor et al., 2010; Webster et al., 2017).

1.1.3 Fibrosis

Mechanisms of fibrosis

Fibrosis is the final common pathological feature of most chronic inflammatory diseases. Fibrosis, or scarring, is defined as the accumulation of excess ECM components in and around inflamed or damaged tissue, which can lead to permanent scarring and organ malfunction (Karsdal et al., 2016; Wynn & Ramalingam, 2012). More precisely, Schaefer, 2018 defines fibrosis "as a degenerative process of connective tissues with excessive accumulation of a collagen-rich ECM characterized by abnormal crosslinking".
Rockey et al., 2015 propose four major phases of the fibrogenic response, which can also be adapted for the kidney (Genovese et al., 2014). First, a stimulus leads to damage of epithelial or endothelial cells. This leads to inflammation, with the recruitment of immune cells that release mediators and cytokines. These in turn recruit and activate effector cells, fibroblasts or myofibroblasts; the second phase.

The third phase is the production of ECM by the effector cells. In this wound environment, they produce cytokines, growth factors, and ECM proteins, which lead to a further autocrine amplification of this process. The fourth phase emerges and overlaps with the third: the deposition and insufficient resorption of ECM promotes progression to fibrosis and ultimately to end-organ failure (Rockey et al., 2015; Mack, 2018).
Common features of fibrosis in all organs are that acute and chronic inflammation trigger fibrosis (Wynn & Ramalingam, 2012; Mack, 2018). The ECM proteins that make up the fibrotic scar are very similar between the organs, consisting mainly of collagen I and III, fibronectin, and basement membrane proteins such as laminin (Rockey et al., 2015). The molecular processes and the cells driving fibrosis are wide-ranging and complex and will not be discussed further in this thesis (Boor et al., 2010; Zeisberg & Neilson, 2010; Mack, 2018; Schaefer, 2018).

Renal fibrosis

Renal fibrosis is, at the beginning, probably a beneficial response to injury, however, very little data exist support this notion. Maintaining of the injurious condition results in pathological fibrosis. This characterizes nearly all progressive kidney diseases (Boor et al., 2010). The location of the initial injury determines the primary fibrosis localization. The fibrotic process can be initiated in the glomerulus causing glomerulosclerosis or in the tubulointerstitium resulting in tubulointerstitial fibrosis (Schaefer, 2018; Rockey et al., 2015).
Tubulointerstitial fibrosis is the final common pathway for all kidney diseases (Webster et al., 2017; Zeisberg & Neilson, 2010). Tubulointerstitial damage is closely associated with a reduction in GFR (Rodríguez-Iturbe et al., 2005). It is characterized by excessive deposition of ECM, mainly collagen. The accumulation of fibroblasts in the injured tissue correlates with the fibrosis risk. However, the origin of the collagen-producing cells is not yet clearly understood. Inflammatory cells, growth, and inflammation factors maintain the fibrosis process. The role of tissue proteases that could cut up the excessive ECM is contradictory, complex, and unclear (Zeisberg & Neilson, 2010).
Glomerulosclerosis often results from inflammation due to glomerular immune complex deposition leading to glomerulonephritis (Rockey et al., 2015) or activated epithelial cells in response to hypertension or diabetes (Webster et al., 2017). Since only tubulointerstitial kidney damage models were used in this work, the pathomechanism of glomerulosclerosis will not be discussed further.

Another phenomenon that always accompanies renal fibrosis is capillary rarefaction and thus also hypoxia. Hypoxia promotes fibrosis, and leads to further damage to the kidney (Boor et al., 2010). In summary, once the fibrotic process has begun, a vicious circle occurs that ultimately leads to a loss of kidney function.

1.2 Extracellular matrix

ECM is the term for the organic matter between most cells (Mecham, 2011). It is a three-dimensional network of cross-linked secreted proteins, which forms a structural scaffold around the cells and the basement membranes (Hobeika et al., 2017). The ECM is not an amorph scaffold, it is a highly dynamic structure, constantly remodeled, with multiple functions. The ECM influences cell migration (Charras & Sahai, 2014) and embryonic development like the vascular branching morphogenesis (Mettouchi, 2012). The ECM also interacts with the resident cells, with specific proteins, and transduces signals into the cells. ECM proteins also influence the communication between cells by binding to soluble growth factors and regulating their distribution, activation, and presentation to cells (Hynes, 2009).

1.2.1 Composition of the ECM

The ECM is composed of water, polysaccharides, and a large variety of proteins. The proteins of the ECM can be divided into two main groups: proteoglycans and fibrous proteins. These proteins have some common characteristics: they all are very large; molecular masses of 100 - 1000 kDa (kilodaltons) are frequent. They are also mainly multidomain proteins, a domain being a homologous unit. Different or equal domains can be detected multiple times in one protein. These domains can be very characteristic for a protein group, for example the collageneous domain, which is common for all collagens (Mecham, 2011).
The main fibrous proteins are collagens, elastin, fibronectin, and laminins. Collagens are the most abundant proteins in mammals. This group will be discussed in more detail in the following sections. Elastin gives tissues the required elasticity, which is limited by the collagen fibrils. Fibronectin is crucial for the organization of the ECM and mediates cell attachment. Other fibrous ECM proteins are tenascins (Alberts et al., 2014).

Bioinformatic tools and experimental approaches have been used to characterize the ECM proteins, called the matrisome (Naba et al., 2016). The tissue distribution of the extracellular proteins is not fully known and changes between the organs (Naba et al., 2016). A good example is the recent characterization of the glomerular ECM by proteomic analysis of laser-captured microdissected glomeruli (Hobeika et al., 2017).

Proteoglycans

Proteoglycans are a subgroup of glycoproteins with a high content of carbohydrates, which fill the majority of the renal extracellular interstitial space (Iozzo & Schaefer, 2015). Proteoglycans consist of a core protein with glycosaminoglycans, unbranched polysaccharide chains composed of repeating disaccharide units, covalently linked to it (Alberts et al., 2014). 43 different genes and a much higher number of proteoglycans, due to alternative splicing, are known. Proteoglycans are mainly localized extracellularly (Iozzo & Schaefer, 2015). Due to the GAG chains these molecules are very hydrophilic. This way, they maintain normal tissue hydration (Chakravarti et al., 1998) and give the ECM resistance to compression forces (Frantz et al., 2010).
One can differentiate three main families of proteoglycans: small leucine-rich proteoglycans (SLRPs), modular proteoglycans, and cell-surface proteoglycans. The SLRPs, the largest class of proteoglycans, are characterized by a relatively small protein core of 36-42 kDa and a central region constituted by leucine-rich repeats (Iozzo & Schaefer, 2015). The repeats in the protein core are biologically active components of the ECM. SLRPs do not only bind to various collagens, but also fulfill signaling functions, binding to and activating growth factor receptors, e.g. the epidermal growth factor receptor (EGFR) or the transforming growth factor β (TGF-β) receptor (Schaefer & Schaefer, 2010; Frantz et al., 2010). In renal fibrosis, they can act as a reservoir of profibrotic growth factors like TGF-β (Genovese et al., 2014).

Collagens & the collagen superfamily

Collagens are trimeric molecules composed of three polypeptide α-chains, which contain the repeated sequence $(G\text{-}X\text{-}Y)_n$, X being frequently proline and Y hydroxyproline. These repeats allow the formation of a triple helix, which is characteristic for the collagen superfamily (Karsdal, 2016). This family consists of 28 members that are numbered in order of discovery with roman numerals. At least

45 known collagen genes code for the individual collagen polypeptides called α-chains. Three of these α chains form a collagen molecule. A collagen molecule consists of three identical (homotrimer) or different (heterotrimer) α-chains. A single collagen type can have multiple chain compositions, e.g. [$\alpha1(V)_2\alpha2(V)$, $\alpha1(V)\alpha2(V)\alpha3(V)$, $\alpha1(V)_3$] (Mecham, 2011).
Collagens are ECM proteins and predominantly located in the interstitial and basement membrane matrix. According to their characteristics, collagens can be clustered in different groups. In the literature, multiple classifications can be found. A summary of the broadly used, different collagen subfamilies is given in Table 1.1 (modified from (Mecham, 2011).).
Fibrillar collagens contain a long uninterrupted triple-helical domain (Ricard-Blum, 2011). The fibril-forming collagen subfamily includes collagens I, II, III, V, XI, XXIV and XXVII. These collagens can be subdivided into three different subclasses. Collagen I, II, and III are the most abundant proteins in vertebrates and are the main component of all collagen fibrils. Collagen V and XI are quantitatively minor collagens that co-assemble with the main collagens. They retain portions of the N-terminal propeptide and are involved in the regulation of fibril assembly (Wenstrup et al., 2004). Collagen XXIV and XXVII are not that well described yet and have shorter helical regions that are interrupted (Mecham, 2011).
Fibril-associated collagens with interrupted triple helices (FACITs) are collagens where the triple-helical, collagenous domain is interrupted by multiple non-collagenous (NC) domains. These domains participate in structural assembly, confer biological activities, and are frequently repeated within the same collagen molecule. An example is the von Willebrand domain, which is found in collagens VI, VII, XII, XIV, XX, XXI, XXII, and XXVIII (Ricard-Blum, 2011). FACITs include collagen IX, XII, XIV, XVI, XIX, XX, XXI, XXII. Collagen IX, XII, XIV, and XX are classified as classical FACITs. They do not form fibrils themselves, but rather associate with the surface of fibril-forming collagens as single molecules (Karsdal, 2016). All these collagens have a large N-terminal NC domain that projects into the interfibrillar space. In this way, the surface properties of collagen fibrils can be modulated. FACIT-like collagens include collagens XVI, XIX, XXI, XXII. These collagens are localized at basement membrane zones or interfacial regions separating different tissue types (Mecham, 2011).
Collagen IV, VIII, and X belong to the network-forming collagens, whose common feature is network formation. Collagen IV is the main component of basement membranes. Collagen VIII is a major component located in the subendothelial regions of blood vessels (MacBeath et al., 1996) and in Descemet's membrane

TABLE 1.1: Suprastructural organization of collagens.

Classification	Collagen types	Collagen genes (human & murine)	Supramolecular structure
Fibrillar collagens			
Fibril-forming collagens	I	COL1A1, COL1A2	Striated fibrils
	II	COL2A1	
	III	COL3A1	
Regulatory fibril-forming collagens	V	COL5A1, COL5A2, COL5A3	Striated fibrils, retain regulatory, non-collagenous N-terminal domains
	XI	COL11A1, COL11A2	
	XXIV	COL24A1	unknown
	XXVII	COL27A1	
FACITs			
FACIT collagens	IX	COL9A1, COL9A2, COL9A3	Associated with fibril,
	XII	COL12A1	Other interactions
	XIV	COL14A1	
	XX	COL20A1	
FACIT-like collagens	XVI	COL16A1	Interfacial regions,
	XIX	COL19A1	basement membrane zones
	XXI	COL21A1	
	XXII	COL22A1	
Network-forming collagens			
Basement membrane collagen	IV	COL4A1, COL4A2, COL4A3, COL4A4, COL4A5, COL4A6	Chicken-wire network with lateral association
Network-forming collagens	VIII	COL8A1, COL8A2	Hexagonal lattices
	X	COL10A1	
Transmembrane collagens			
	XIII	COL13A1	Transmembrane and shed soluble ecto domains
	XVII	COL17A1	
	XXIII	COL23A1	
	XXV	COL25A1	
Multiplexins			
	XV	COL15A1	Basement membrane proteoglycans, cleaved C-terminal domains influence angiogenesis
	XVIII	COL18A1	
Other collagens			
Beaded filament-forming collagen	VI	COL6A1, COL6A2, COL6A3, COL6A4, COL6A5, COL6A6[1]	Beaded filaments, networks
Anchoring fibrils	VII	COL7A1	Laterally associated antiparallel dimers with collageneous domains
Others	XXVI	COL26A1	
	XXVIII	COL28A1	

[1]COL6A4 is only found in mouse but not in human (Gordon & Hahn, 2010)

(the basement membrane separating corneal endothelial cells from corneal stroma). Collagen X is only found in hypertrophic cartilage (Schmid et al., 1990). Transmembrane collagens include collagen XIII, XVII, XXIII and XXV. These collagens have a dual function as cell surface receptors and as matrix components. They contain an N-terminal intracellular domain, a single transmembrane region, and a large extracellular C-terminus. If the C-terminus is cut off by limited proteolysis, they can signal to cells as soluble molecules. Collagen XIII and XVII are components of focal adhesions and hemidesmosomes, respectively. Collagen XXIII is also part of cell adhesions and collagen XXV is brain-specific (Franzke et al., 2005).
Collagen XV and XVIII are multiplexins. They have a central collagenous domain flanked by NC-domains containing a thrombospondin domain in the C-terminus. When cleaved, endostatin is generated with anti-angiogenic properties (Mecham, 2011). They are also counted as proteoglycans and found associated with basement membranes (Iozzo & Schaefer, 2015).
The other collagens (VI, VIII, XXVI, XXVIII) do not easily fit into any of the previous categories. Whereas collagen VI has a ubiquitous tissue distribution, collagen VII is the major component of anchoring fibrils that tether the epidermal basement membrane to the underlying dermis. Collagen XXVI is expressed in testes and ovaries whereas collagen XXVIII is expressed by dorsal root ganglia and peripheral nerves (Gordon & Hahn, 2010).

1.2.2 Exemplary collagens

In this thesis, I decided to investigate one or two exemplary collagens from each group in more detail. Each chosen collagen will be discussed briefly and the current state of research on the role of collagen in the kidney will be presented.

Collagen V (fibrillar collagen)

Collagen V is a fibrillar collagen, more specifically a regulatory fibril-forming collagen (Karsdal, 2016). The α-chains are encoded by three different genes, *COL5A1, COL5A2, COL5A3* (Fichard et al., 1995). Mutations of *COL5A1* and *COL5A2* are responsible for the Ehlers-Danlos syndrome (EDS) (Bowen et al., 2017). Three different isoforms of collagen V are known: $\alpha1(V)_2$ $\alpha2(V)$, $\alpha1(V)_3$ and $\alpha1(V)\alpha2(V)\alpha3(V)$, the $\alpha1(V)_2\alpha2(V)$ isoform being the most abundant (Wenstrup et al., 2004).

After intracellular assembling, procollagen V is secreted and the N- and C-terminal propeptides are cleaved by propeptidases. Collagen V associates with the fibrillar collagen I, III, and VI into heterotypic fibrils (Birk, 2001). Collagen V is normally present in the ECM of tissues that express collagen I. It is therefore present in several parenchymal organs, like the kidney (Mak et al., 2016). It is essential for embryonic development. *Col5a1*$^{-/-}$ homozygous mutant mice die early in embryogenesis, due to the lack of mesenchymal fibrils (Wenstrup et al., 2004). Collagen V is a forming part of large collagen bundles and closely associated with the surface of type I collagen fibers (Martinez-Hernandez et al., 1982). It controls the initiation of collagen fibril assembly and regulates the diameter of these collagen I fibrils (Wenstrup et al., 2004) through partial retention of the α1(V)-N-propeptide (Birk, 2001). This peptide emerges at the surface of these fibrils and interacts with multiple ECM proteins, like collagen VI (See section 1.2.2) (Malfait et al., 2010). *In vitro*, increased collagen V levels appear to modify the stiffness of the ECM by changing ECM fibril organization (Birk et al., 1990; Breuls et al., 2009). Collagen V is known to be overexpressed in most forms of organ fibrosis, e.g. liver fibrosis (Mak et al., 2016).

Collagen XVI (FACIT-like collagen)

Collagen XVI is a member of the family of fibril-associated collagens with interrupted triple helices (FACITs). Collagen XVI is synthesized by various cell types, like keratinocytes or fibroblasts (Grässel et al., 1999), and expressed in several tissues like the kidney, the skin, arterial walls, the heart or the intestine (Karsdal, 2016; Kassner et al., 2003; Ratzinger et al., 2010). In mouse kidneys, collagen XVI is expressed in the cortex and medulla, particularly by the convoluted tubules, the collecting tubules, and in the arcuate arteries (Lai & Chu, 1996).
The function and regulation of collagen XVI are not yet well understood. As FACIT, collagen XVI is associated not only with other collagens but with other molecules of the ECM. In the skin, collagen XVI may anchors microfibrils to the basement membrane (Grässel et al., 1999). Collagen XVI also interacts with α2 integrins. There, it induces the formation of focal adhesions plaques, an important component of the signaling mechanisms of integrins. Eble et al., 2006 hypothesized that this collagen-integrin interaction connects cells with specialized fibrils and thus contributes to the organization of connective tissue.

Collagen XIX (FACIT-like collagen)

Collagen XIX is also a member of the FACIT family (Myers et al., 1994; Inoguchi et al., 1995) forming a homotrimer of three α1(XIX) chains. During embryonic development, *Col19a1* transcripts can be detected in almost all tissues, but *Col19a1* is preferentially and transiently expressed in differentiating muscle cells (Sumiyoshi et al., 2001). The expression of collagen XIX in adult mice is limited to a few tissues (Sumiyoshi et al., 1997; Sumiyoshi et al., 2001). Collagen XIX is localized in the basement membrane zone of vascular, neuronal, mesenchymal, and epithelial tissues (Myers et al., 1997). It is expressed in the spleen, the basement membrane zone of ductal and vascular structures of the liver and also in the placenta, colon, and skin (Myers et al., 1997), and in the brain, more specifically in the hippocampus (Sumiyoshi et al., 2001).
The function of collagen XIX is not well identified. Sumiyoshi et al., 2001 suspect that collagen XIX may be involved in muscle differentiation. Collagen XIX null mice developed a megaesophagus and a disorder of NO-dependent relaxation of the esophagus. The authors suggest that the collagen XIX-rich basement membrane is essential for the neuromuscular junction of the sphincteric muscle and the transdifferentiation from smooth to skeletal muscle (Sumiyoshi et al., 2004). Ramont et al., 2007 could show that the NC1(XIX) domain decreased tumor growth *in vivo* through inhibition of melanoma cell invasive properties and tumor angiogenesis (like decreased VEGF-expression) in a mouse melanoma model.

Collagen VIII (network forming collagen)

Collagen VIII is a network-forming collagen. It is encoded by two different genes (*COL8A1, COL8A2*). The α-chains can form stable homotrimers $(\alpha 1(\mathrm{VIII}))_3$ or $(\alpha 2(\mathrm{VIII}))_3$ (Illidge et al., 1998). After being secreted, collagen VIII undergoes supramolecular assembly into hexagonal lattices (Sherratt et al., 2004). Vastatin is the NC-C-terminal fragment (NC1) of collagen VIII. It is an endogenous antiangiogenic matrikine, a matrix-originating peptide with a cytokine activity, (Karsdal et al., 2017; Shen et al., 2016; Li et al., 2017). In cell culture, vastatin inhibits bovine aortic endothelial cell proliferation and causes cell apoptosis (Xu et al., 2001).
Collagen VIII is expressed mainly in large arteries, most strongly detected in the subendothelial region, but also found throughout the elastin-rich tunica media. It is also found in the heart, brain, liver, lung, and muscle, always associated

with the organ vessels (Kittelberger et al., 1990). Finally, it is a prominent component of Descemet's membrane (Sherratt et al., 2004). Collagen VIII is strongly associated with arteriogenesis and repair mechanisms after vascular injuries. It influences the migration, proliferation, apoptosis, and differentiation of key cells in the development of artherosclerosis (Plenz et al., 2003). Type VIII collagen is elevated in the serum of patients with diseases associated with angiogenesis and vascular remodeling, like COPD (chronic obstructive pulmonary disease) or different cancers (Larsen et al., 2016). Collagen VIII expression is not only elevated in multiple atherosclerosis models (Plenz et al., 2003) but seems also to be a primary regulator of smooth muscle cell migration and invasion from the media to the intima after vascular injury. These cells are responsible for the expansion of the ECM and the development of atherosclerosis (Hou et al., 2000).
Collagen VIII also influences fibrosis, e.g. in myocardial remodeling following pressure overload. In mice with only heart hypertrophy without heart failure, collagen VIII expression is increased, whereas it is decreased in mice with heart failure (Skrbic et al., 2013). In heart failure models, like aortic banding, mice with collagen VIII knockout show less fibrosis, but this leads to ventricle dilatation and early mortality (Skrbic et al., 2015).

Collagen XXIII (transmembrane collagen)

Collagen XXIII is a member of the transmembranous subfamily of collagens. Collagen XXIII is a homotrimer and a type II transmembrane protein consisting of an amino-terminal cytoplasmic domain, a transmembrane domain, and three collagenous domains flanked by a short NC-domain. Collagen XXIII has a limited tissue distribution. It is mainly expressed in the lung, cornea, brain, skin, tendon and kidney (Koch et al., 2006). Collagen XXIII can be cleaved by furin, forming multimers in the ECM. The cleavage of Collagen XXIII is tissue-dependent. Whereas in lung cells collagen XXIII is mainly present in the full-length form, in cells in brain tissue the shed-variant dominates (Veit et al., 2007).
The role of collagen XXIII has not been well studied yet. So far, there are mainly results regarding the alteration of collagen XXIII expression in various cancers (Banyard et al., 2003). It is upregulated in prostate cancer (Banyard et al., 2007) as well as in non-small cell lung cancer (Spivey et al., 2010). Collagen XXIII seems to have dual functions as a matrix component and a cell surface receptor (Franzke et al., 2005). In the skin, collagen XXIII interacts with integrin $\alpha_2\beta_1$ and can induce integrin $\alpha_2\beta_1$-dependent attachment and spreading of keratinocytes. Veit et al.,

2011 postulate a role for collagen XXIII in cell-cell adhesion. A study from Spivey et al., 2012 suggests that in lung cancer cells collagen XXIII has a role in mediating metastasis of cancer cells by facilitating cell-cell and cell-matrix adhesion.

Collagen VI (other collagens)

Collagen VI is the only beaded filament collagen (see Table 1.1) and is a ubiquitous component of connective tissues. It is encoded by six different genes (*COL6A1, COL6A2, COL6A3, COL6A4, COL6A5* and *COL6A6*) (Fitzgerald et al., 2008), which respectively code for the polypeptide chains α1, α2, α3, α4, α5, and α6. Collagen VI is a heterotrimer composed of α1α2αx chains, where x is mostly α3 (Gara et al., 2011). In the extracellular space, collagen VI trimers associate end-to-end and form beaded filaments. These filaments associate laterally, forming beaded microfibrils (Cescon et al., 2015). Endotrophin is the C-terminal fragment of the α3(VI) chain. This fragment is released by cleavage of the C-terminal propeptide (Karsdal et al., 2017) and it is a marker for collagen VI formation (Fenton et al., 2017).
Collagen VI has a ubiquitous tissue distribution (Cescon et al., 2015). It is also widely present in human and murine kidneys (Zhu et al., 1994; Hobeika et al., 2017; Gara et al., 2011). Due to its complex structure collagen VI can bind multiple components of the ECM. It is widely distributed in connective tissues and anchors the basement membrane to the underlying connective tissue (Colombatti et al., 1995). For example, collagen VI is one of the major components of muscle ECM. Mutations in collagen VI genes lead to Ullrich congenital muscular dystrophy, Bethlem myopathy, and myosclerosis myopathy (Kirschner et al., 2005; Jöbsis et al., 1996; Merlini et al., 2008).
The expression of collagen VI is increased in multiple fibrotic diseases, like scleroderma, fibrosis of lungs, heart and adipose tissue, or in liver fibrosis. Collagen VI serum concentration is elevated in chronic liver fibrotic disease; it seems to be a good indicator of early fibrogenesis in the liver. Collagen VI levels are significantly elevated in the heart after myocardial infarction, but also in hypertrophic cardiomyopathy (Mak et al., 2014). After myocardial infarction in *Col6a1*$^{-/-}$ mice, the absence of collagen VI improves the cardiac function, structure, and remodeling (Chilian et al., 2012). *COL6A5* is also upregulated in the kidney in response to heart failure (Melenovsky et al., 2018).

1.2.3 The ECM of the kidney

The ECM in healthy kidneys

The interstitium represents a small portion of the healthy kidney, only 7 - 9 % of the cortex volume in rats. In the medulla, the volume increases from the outside to the inside (Skorecki et al., 2016). The composition of ECM differs between various functional kidney compartments. The glomerulus contains the glomerular basement membrane (GBM), the Bowman's capsule, and the mesangial ECM. The tubulointerstitium contains the basement membranes of the tubules and peritubular capillaries and the interstitial ECM. Finally, further ECM is located in the large vessels (Genovese et al., 2014). All of these ECM differ in their composition (Bülow & Boor, 2019)
The GBM, as well as the other basement membranes in the kidney (tubular, urothelial, and endothelial), is mainly composed of laminin, collagen IV, nidogen, and sulfated proteoglycans (Karsdal, 2016). It acts as a filtration barrier between the vascular system and the urinary space (Skorecki et al., 2016). The basement membrane collagen IV is produced by epithelial cells, in the kidney by the tubular epithelial cells and vascular endothelial cells as well as from the podocytes (Razzaque et al., 1995). The composition of each basement membrane differs (Bülow & Boor, 2019).
The Bowman's capsule is composed of a visceral epithelial layer, an associated basement membrane, and a parietal layer with its basement membrane. It delimits the Bowman's space, or the urinary space (Skorecki et al., 2016) (See Figure 1.1.
The mesangial ECM is produced by the mesangial cells and supports the three-dimensional structure of the glomerulus. The ECM also contributes to the cell response to mechanical stress via cell-matrix interaction. In healthy kidneys its major components are collagen type IV and V, fibronectin, laminin A, B1, and B2, chondroitin sulfate and sulfated proteoglycans, nidogen, and biglycan (Schlondorff & Banas, 2009).
The interstitial matrix has various functions, initially essential for morphogenesis, it gives the kidney its mechanical stability. It is also involved in the regulation of cell adhesion, chemotaxis of inflammatory cells, and so forth. It is mainly composed of collagens, in particular, collagen type I, III, V, VI, VII and XV (Genovese et al., 2014).

The ECM in renal fibrosis

Increased deposition and alteration in EC M is the hallmark of renal fibrosis. This is best described for the tubulointerstitial fibrosis but less well-known for the other ECM compartments including the basal membranes. The activated fibroblasts synthesize and deposit large quantities of ECM proteins, mainly collagen type I and III, fibronectin, and hyaluronic acid (Frantz et al., 2010). In renal fibrosis, fibroblasts acquire the myofibroblast phenotype, thus promoting the formation of more rigid collagen bundles that give the tissue a higher mechanical stability (Tomasek et al., 2002). But fibrosis is not only the accumulation of excessive ECM, but the ECM also changes in composition and orientation. An example of the change in composition is the relative decrease in collagen IV (absolute increase) in favor of the interstitial collagen I, III, and V (Karsdal et al., 2017). Besides, depending on the type of damage, the accumulation of collagen is positively or negatively associated with renal function. Buchtler et al., 2018 were able to show that in mice with unilateral ureter obstruction (UUO, see 3.3.1), collagen I production was important for maintaining renal function, whereas it had negative effects in the model of adenine-induced nephropathy.
Under pathological conditions, the homeostasis of ECM production and degradation is disturbed. This leads to changes in the quantity and quality of the ECM as well as in the composition and quantity of the collagens (Karsdal et al., 2017). Changes in transcriptional regulation, mRNA stabilization and many other effects often lead to increased collagen expression in fibrosis. The induction of various enzymes, such as lysyl oxidases, leads to increased post-translational modifications, cross-linking and stabilization of collagen fibrils (Ricard-Blum et al., 2018). The increased and altered release of turnover products can not only be used as non-invasive biomarkers (Genovese et al., 2014; Boor & Floege, 2015) but also influence their environment. They can have negative feedback and thus prevent further fibrosis or promote further inflammation (Karsdal et al., 2017). ECM provides clues and signals for the cells, e.g. the gene expression of primary fibroblasts was more influenced when cultured on ECM from patients with primary idiopathic pulmonary fibrosis or control patients than by the origin of the cells themselves (Parker et al., 2014). In summary, the role of ECM in the fibrosis process is complex and only incompletely understood.

Chapter 2
Motivation and aims

The ECM is an essential and active component in fibrosis. A better understanding of ECM therefore would not only help to identify new pathomechanisms leading to the loss of kidney function, but also potentially enable to find new targets for therapeutics. Also, ECM proteins carry great potential as non-invasive diagnostic markers for fibrosis. For instance urinary endotrophin (peptide of collagen VI) predicts the disease progression in patients with CKD (Rasmussen et al., 2017) and the turnover of type III collagen reflects disease severity in patients with IgA nephropathy (Genovese et al., 2016). Even more interestingly, ECM proteins can also be used for non-invasive imaging of fibrosis (Sun et al., 2019; Jacobson et al., 2015; Baues et al., 2020).
The changes in renal fibrosis are mainly described for the most abundant and well-known collagens and ECM proteins. The regulation of ECM in renal fibrosis is incompletely discribed, and somewhat limited to the few most commonly analyzed collagens, i.e. collagen I, III and IV. Therefore, the aim of my study was to analyze the expression and regulation of ECM components in two different steps:

- A comprehensive analysis of ECM changes using publicly available datasets, including RNA-Arrays and Protein-Arrays.
- Changes in expression of selected collagens were analyzed in three different murine kidney fibrosis models.

Chapter 3
Materials and methods

3.1 Materials

A complete overview of the used materials is given in Appendix 3.1. All used devices are listed in Table A.1. All consumables and reagents are listed in Table A.2 and A.3, respectively. In Table A.4, the used software is indicated. For a better readability, the different materials will not be referred explicitly in the following.

3.2 *In silico* analysis of already published data

3.2.1 Analysis of gene expression datasets with Geo2R

First, publicly available gene expression data sets were analyzed to get an overview of the regulation of the genes coding for extracellular matrix proteins in CKD. Therefore, in the database Geo-DataSets suitable datasets were searched using the keyword "kidney", as from the year 2010. This database is managed by NCBI (National Center for Biotechnology Information) with original submitter-supplied records. The datasets were chosen according to the relevance for the topic CKD and availability in the appropriate format. Additionally, the datasets were selected with regard to the species (Mus musculus) analyzed, and animal models of CKD used. To select the animal models of CKD the extensive lists of animal models provided by Rabe & Schaefer, 2016 and Yang et al., 2010 were consulted. The finally selected datasets are described in Appendix B.1. In Appendix B.2 a short overview and explanation of the different animal models used are given.
The datasets allowed to detect changes in gene expression between two different groups, e.g. healthy vs. diseased mice. Therefore, all animals undergoing the same experimental design were attributed to one group in a dataset. Table B.1 gives an overview of the defined groups. The selected datasets were analyzed with the Limma package of R (Smyth, 2004), embedded in Geo2R, an interactive web tool provided by NCBI (https://www.ncbi.nlm.nih.gov/geo/geo2r/). This program allows to perform statistical tests to compare the defined groups. It applies multiple-testing corrections on p-values to help to correct for the occurrence of false positives (Smyth et al., 2010). The test was run with default parameters (an exemplary calculation is shown in Appendix B.3) and saved as CSV-data. The

threshold for significance was set to 5 % with respect to the adjusted p-value. The results were expressed using a binary logarithmic scale. The results were generated for all collagens known to date.
The analyzed data-sets are listed in the table B.1. In addition, further models or points in time were analyzed, which did not yield any significant results. They are listed in Section B.1. On microarrays, each gene can be represented by multiple probes, representing different exons of the gene, sometimes even characterizing different splice variants (Stalteri & Harrison, 2007). Since the goal is to determine a trend of up- or down-regulation and the probes for the same gene were mostly strongly correlated, the decision was made to summarize the probes. Even though, this is a strong simplification, which holds many pitfalls (Stalteri & Harrison, 2007). This data is only used to determine a trend and will not be processed further. Since different types of microarrays have been used, gene regulation can only be compared within one dataset but not among different datasets. For the analysis, the data have been arranged in heat maps. This allows to detect consistent trends of up- or down-regulation across datasets. It should not lead the viewer to quantitatively compare the regulation between different datasets.

3.2.2 Multi-omics analysis of fibrotic kidneys in two mouse models by Pavkovic et al., 2019

Pavkovic et al., 2019 analyzed changes in CKD using mRNA sequencing and mass spectrometry. They used two classical CKD models at several points in time: on the one hand folic acid induced nephropathy (confer B.2), on the other hand, UUO (confer 3.3.1 for details). The results generated and normalized were presented in an easy-to-use tool, the Mouse Kidney Fibromics browser (http://hbcreports.med.harvard.edu/fmm/). This was analyzed for collagen. The results are given as normalized abundance (log2 counts) of molecules in each mouse model.

3.3 *In vivo* experiments

To verify the regulation of matrix proteins, several *in vivo* experiments have been conducted. All animal experiments were approved by the local review boards

(Landesministerium für Umwelt- und Verbraucherschutz NRW). They were performed in accordance with the guidelines for care and use of laboratory animals. The animals were held in rooms with constant temperature and humidity, 12 h/12 h light / dark cycles, and had free access to water and food. All surgeries were performed under anesthesia by ketamine (14 mg/g body weight) and xylazine (8 mg/g body weight). Temgesic (0.1 mg/kg body weight), an analgesic medication, was injected every 8 h for three days after the operation. All surgeries were kindly performed by Dr. rer. nat. Barbara Klinkhammer.

3.3.1 Unilateral ureteral obstruction model

First, ten 10-week-old Balb/c mice and six C57Bl/6N-mice underwent unilateral ureteral obstruction (UUO). After anesthesia with ketamine and xylazine under sterile conditions, a median incision of the lower abdomen was performed. The left ureter was prepared from the surrounding tissue and ligated by cauterization. The incision was closed layer by layer with continuous peritoneal and skin sutures (Peng et al., 2015; Zeisberg et al., 2005). Four animals underwent a sham operation as control. The animals were kept warm until recovery using a heating lamp and were examined twice daily for wound control and infection. The kidneys were harvested ten days or 14 days after the operation.

3.3.2 Ischemia-reperfusion model

Ischemia-reperfusion (I/R) was applied on ten 10-week-old Balb/c mice and six C57Bl/6N mice. After left lateral incision of the skin and muscle, the left renal artery and vein were clamped with a micro-serrefine clip. This operation was performed on a heating pad set to 37 °C (warm ischemia) and body temperature was measured rectally throughout the kidney ischemia. After 30 minutes the obstruction was released and the incision sewed with two layers. The ischemia and subsequent reperfusion were verified macroscopically and were present in ten out of twelve animals. The other two animals were therefore excluded from further analysis. Four animals underwent a sham operation. The kidneys were harvested 21 days after surgery.

3.3.3 Adenine nephropathy model

Adenine nephropathy was induced in 16 12-week-old C57BL6/N mice by administration of an adenine-rich diet (supplemented with 0.2 % adenine). Eight

mice were killed on day 7 and eight mice on day 21 after diet start. Seven mice were used as healthy control for day 7 and six mice for day 21. Adenine induces crystal formation that leads to tubular obstruction and interstitial fibrosis (Rabe & Schaefer, 2016; Jia et al., 2013).
In all experiments, kidneys were taken and immediately processed for further analysis. If not analyzed immediately, all samples apart from fixed tissues for histology and immunohistochemistry were stored at -80 °C.

3.3.4 Kidney fixation and sample preparation

Kidney harvest. The mice were anesthetized and euthanized by injection of physiological saline into the left ventricle of the heart. The kidneys were removed. Portions of the decapsulated kidneys were snap-frozen for further protein analysis. Samples for mRNA analysis were stored in RNAlater solution for 24 h at 4 °C and then stored at -80 °C until further processing. Portions of the kidneys were fixed for 24 h at 4 °C in methacarn solution (see Table 3.1).

TABLE 3.1: Methacarn.

Methanol	600 ml
Chloroform	300 ml
Acetic acid (100 %)	100 ml

Tissue embedding and slide sectioning. The fixed tissues were dehydrated in increasing concentrations of methanol, followed by 100 % isopropanol, in an embedding machine. Finally, the samples were embedded in paraffin and kept at room temperature. The kidneys were then cut into 1 µm sections with a Leica SM 2000 R microtome by Cherelle Timm and Simon Otten and transferred onto a glass slide. They were then dried at 50 °C overnight.

3.4 mRNA expression

3.4.1 RNA extraction from tissues

After defrosting the tissue stored in RNAlater, to stabilize the RNA, approximately 30 mg of tissue were cut off. The samples were placed in 600 µl RLT lysis buffer from the Qiagen RNeasy Kit transposed with 10 µl β-mercaptoethanol. The RNA isolation was performed according to the manufacturer's protocol.
Briefly, the tissue was disrupted and homogenized in the vibrator mill for five

minutes at a frequency of 25/minute, until the lysate was uniformly homogeneous. The homogenate was given in QIAshredders and centrifuged at 14 000 rpm for three minutes at room temperature to remove cell walls and organelles. The flow-through was removed and pipetted in a new microtube. 600 µl of 70 % ethanol was added to the flow-through. The mixture was given to an RNeasy spin column and centrifuged for 15 s at 10 000 rpm. The RNA was bound by the membrane of the column and separated from the remaining lysates. A washing step followed. The DNA of the column was digested with 75 µl DNase mastermix (10 µl of DNAse I stock solution and 70 µl RDD buffer) and incubated for 15 minutes at room temperature.
After washing with RW1 buffer, the column was rinsed two times with 500 µl RPE-buffer and centrifuged at 10 000 rpm for 15 s in the first step, and two minutes in the second step. The column was transferred on a new collection tube and centrifuged for one minute at full speed to dry-out the membrane. Thereafter, the RNA was eluted in RNAse-free water by centrifuging the column for on minute at 10 000 rpm. The obtained RNA concentration was measured with the microvolume spectrophotometer NanoDrop 2000.

3.4.2 cDNA-synthesis

To analyze the RNA expression of different genes *via* reverse transcriptase quantitative polymerase chain reaction (RT-qPCR) complementary DNA (cDNA) needs to be synthesized. Therefore, RNA was reversely transcribed using the M-MLV reverse transcriptase (*moloney-monkey leukemia virus*-reverse transcriptase) as follows.
1 µg RNA was filled up to 20 µl with distilled water and then incubated for 10 minutes at 75°C in a thermocycler to denature the RNA. The RNA samples were immediately cooled on ice to prevent the reforming of secondary structures. 10.2 µl mastermix (Table 3.2) was added and the samples were shortly centrifuged. The samples were incubated 10 minutes at 25°C followed by incubation at 42°C for 60 minutes. During the incubation, the random primer binds randomly to sites throughout the mRNA. The reverse transcriptase synthesizes one complementary strand of DNA hybridized to the original mRNA strand (O'Connel, 2002). The cDNA samples were stored at -20°C until further processing.

TABLE 3.2: cDNA synthesis mastermix (for one sample).

Master mix	
Random primer (240 ng/µl)	1.0 µl
First strand buffer (5x)	6.0 µl
dNTP-Mix	1.5 µl
RNAsin	0.7 µl
M-MLV-RT	1.0 µl
M-MLV RT 5x Reaction Buffer (provided)	
Tris-HCl pH 8.3	250 mM
KCl	375 mM
$MgCl_2$	15 mM
DTT	50 mM

3.4.3 Real-time quantitative PCR (RT-qPCR)

The real-time quantitative PCR allows to quantify the gene expression of a gene of interests relatively to housekeeping genes, i.e. non-regulated genes with stable RNA expression. To this end, specific sequences within the cDNA templates are amplified using a polymerase and thermal cycling. The PCR product is monitored at each cycle via SYBR green. This fluorescent dye intercalates in double-stranded DNA of the PCR product. The fluorescent signal increases in direct proportion to the number of PCR product molecules. This allows to determine the initial quantity of target mRNA. The used primers are listed in Table 3.3. Primers that could not be established successfully are listed in Table 3.4. For each reaction 0.75 µl cDNA was amplified in a 25 µl volume using the RT-qPCR Core Kit for SYBR green I. The cDNA was added to the mastermix, specified in Table 3.5. Each sample was assayed in duplicate. *Gapdh* and *Actb* were used as housekeeping genes (Cui et al., 2009). 25 µl of PCR reaction mix was transferred into each well of a 96-well reaction plate. The plate was sealed, centrifuged briefly, and loaded into the ABI Prism 7300 sequence detection system. The reactions were run according to the schedule shown in Table 3.6. The measurement results were evaluated using the $\Delta\Delta C_T$ method. To calculate the initial DNA copy number the threshold Cycle [C_T] from the target gene and *Gapdh* of each sample were read out. C_T is the number of the first PCR-cycle where a significant fluorescent signal can be measured. This means, as the template amount decreases, the cycle number at which significant amplification can be detected, is increased. ΔC_T, the difference between $C_{TTarget}$ and C_{TGAPDH} was calculated, for each sample. Then $\Delta\Delta C_T$, the difference between $\Delta C_{TGroupX}$, e.g. UUOd10, and $\Delta C_{TControl}$,

was calculated. Since the DNA copy number increases exponentially, the relative change of expression with respect to the control group can be calculated with $Expression = 2^{-\Delta\Delta C_T}$.

TABLE 3.3: Primer used for RT-qPCR.

Gene	Forward primer	Reverse primer
Col1a1	TCGCTTCACCTACAGCACCC	TGACTGTCTTGCCCCAAGTTC
Col2a1	GGGCAGACTGCAAAATAAAATC	GCGTCTGACTCACACCAGATAG
Col3a1	TGAAGATGTCGTTGATGTGCAG	GCAGTGGTATGTAATGTTCTGGGAG
Col4a1	CCTTCCTGCAGTCTTCCTAAAA	CAGTGAGCTCAGCTATCATTGG
Col5a1	CACTTACATCTGCCAGAACTCG	CTGGTTGAAGGACAACTCTTCC
Col6a1	AGTGGCTAGTCCTTCCACTCTG	TGGATTGATTCTGACAGGACAC
Col7a1	ACCTTGGGACCTGAGTCTAACA	AGGACAGTCAGCCATACTTGGT
Col8a1	ATGGATAGATGCCTGGAGTGAT	ATCTCCACAGATGACTGCTTCA
Col12a1	TTCACAGTGGAGGATTTTGATG	TGCCAACTCTTGCTCAATTCTA
Col13a1	CTGCAGAAGAGAGAAGGGAAAG	ATCGGAGTACGCCAAAGTAAGA
Col14a1	AATTTGGTGGCTACAAACTGCT	CTTTTGTTGCAGTGTTCTGGAG
Col15a1	GCTTTTTAACAATTGGGACTCG	ACCGTCAAAGGAGTAGATTGGA
Col16a1	TGGGAGACATGGTGAATTATGA	AGCCATCCTCTCATCAAACAGT
Col17a1	GACACCACACTAGACCCAGACA	CTTCCTCAGCATCAGGAGTTCT
Col18a1	AAACTACTGGGGCTACAGGTCA	ACAGGACGATGTAGCTGTTGTG
Col19a1	CAAGGGAGAAATTGGTGAAAAG	TCAAACCATCTTGTCCATTGAG
Col24a1	GGACCTTAATCAGCCACAGTTC	AAGAGGATTCTTGATGCTGCTC
Col25a1	TATCAGAGCTCAGGTTGCTGAA	GACGACCTTTGGTAAAGTCTGC
Col27a1	GTTGGAAATCCTAGAACGATGC	TCTGTCTGGTTTTCTTGGAGGT
Gapdh	GGCAAATTCAACGGCACAGT	AGATGGTGATGGGCTTCCC
Actb	CAACGAGCGGTTCCGATG	GCCACAGGATTCCATACCCAA

TABLE 3.4: Not successfully established primer.

Gene	Forward primer	Reverse primer
Col9a1	CTTGTCCATGGAAGGAAGGTAG	TCAAACTCCTGGGAAGAGGATA
Col10a1	GGTTCATGGGATGTTTTATGCT	GGCGTATGGGATGAAGTATTGT
Col11a1	CTGGTTTACCTGGTCTCAAAGG	GGAGGACCAATCAATCCAATTA
Col20a1	ACCGTCAGAGTCACCTGTTTTT	GCTAGGAGCTTTCTGTGTGGTT
Col22a1	CTCTATGAACAAGCTGGTGCTG	ATTGAAACCAGCATGAGGAACT
Col23a1	GACGGCATTCCTGGACTAAAG	TGTCACCTTGTTCTCCCTTGAG
Col26a1	TGGCTGGTGCTTGGTCTC	CGAGGGTGGTGTTTTCTGTTC
Col28a1	GAAGACTCCAGGAAAGCAGTGT	AGAAGACAGAAGGCAACGTCTC

3.5 Histology and morphology

3.5.1 Periodic acid schiff (PAS)

Periodic acid Schiff staining allows the evaluation of renal morphology and damage. Schiff's reagent reacts with glycoproteins in the basal lamina and allows the

TABLE 3.5: Mastermix for RT-qPCR with SYBR green (per sample).

Reaction buffer (10x)	2.5 µl
$MgCl_2$ (50 mM)	1.75 µl
Forward primer (1 pmol)	1.25 µl
Reverse primer (1 pmol)	1.25 µl
dNTPs (5 mM)	1.0 µl
SYBR Green I	0.75 µl
cDNA template	0.75 µl
Taq-Polymerase (0.025 U/µl)	0.125 µl
A. inject	15.625 µl

TABLE 3.6: Thermal cycling conditions for RT-qPCR in ABI Prism 7300 sequence detection system.

Stage	Function	Temperature	Time (mm:ss)
Hold		50 °C	2:00
Hold	Polymerase activation	95 °C	10:00
Cycle (40 cycles)	Denaturation	95 °C	0:15
	Annealing and elongation	60 °C	1:00

assessment of basal membranes (Suvarna et al., 2013). The slides were counterstained with hematoxylin, which reacts with the negatively charged nuclei.
Paraffin was removed by washing the slides in xylene for 3 x 5 minutes. They were rehydrated by washing in decreasing concentrations of ethanol (100 % ethanol for 3 x 2 minutes, 90 % ethanol for 2 x 2, and 70% ethanol for 2 minutes). After rinsing with phosphate-buffered saline (PBS) (see Table 3.7), the slides were incubated in a freshly prepared 2 % periodic acid solution for 30 minutes. They were soaked in distilled water and placed in the dark in Schiff's reagent for 1 h. After washing in lukewarm tap water for 5 minutes, the slides were counterstained in a previously filtered hematoxylin solution for 4 minutes. Afterwards they were rinsed in tap water for 5 minutes and blued in tris buffer pH 8.3 (see Table 3.8). Finally, the slides were dehydrated and mounted with Roti-Histokitt.

TABLE 3.7: Phosphate buffered saline (PBS)

Na_2HPO_4	5.92 g (42 mM)
KH_2PO_4	1.72 g (13 mM)
NaCl	28.8 g (0.5 M)
A. dest	add to 1 l
pH 7.2-7.4	adjust with NaOH

TABLE 3.8: Tris buffer pH 8.3.

Tris	6.1 g (0.05 M)
NaCl	11.69 g (0.2 M)
A. dest	add 500 ml
pH 8.3	adjust with HCl
A. dest	add to 1 l

3.5.2 Immunohistochemistry

Immunohistochemistry allows to detect specific proteins by using antibodies directed against these proteins. The different antibodies used for staining are listed in Table 3.9.

TABLE 3.9: Primary antibodies used for immunohistochemistry.

Name	Host species	Supplier	Catalog-No.	Dilution
Collagen I	goat (polyclonal)	Southern Biotech (Birmingham USA)	1310-01	1/100
Collagen III	goat (polyclonal)	Southern Biotech (Birmingham, USA)	1330-01	1/100
Collagen V	rabbit (polyclonal)	Abcam (Cambridge, UK)	ab7046	1/100
Collagen VI	rabbit (monoclonal)	Abcam (Cambridge, UK)	ab182744	1/200
Collagen VIII	rabbit (polyclonal)	Thermo-Fischer Scientific (Rockford, USA)	PA5-37109	1/50
Collagen XIX	rabbit (polyclonal)	Thermo-Fischer Scientific (Rockford, USA)	PA5-23977	1/200

After deparaffinizing and hydrating the tissue sections as described above, an antigen retrieval with Tris EDTA pH 9 (see Table 3.10) for 5 minutes in the microwave was performed for collagen VI and VIII antibodies. For the other antibodies no further blocking or antigen retrieving steps were required. The endogenous peroxidase was blocked with 3 % H_2O_2 for 10 minutes. Then, the primary antibodies, diluted as described in Table 3.9 in 1 % BSA-PBS, were applied. After incubation for 1 h in a wet chamber at room temperature, the slides were washed in PBS two times for 5 minutes. Thereafter, the secondary antibody was applied (see Table 3.11) for 30 minutes at room temperature. For collagen V, the secondary antibody was diluted 1/400.

After two washing steps in PBS, the slides were incubated with an avidin-biotin-complex for half an hour. Colorimetric detection with 3-3-Diaminobenzidin (DAB)

TABLE 3.10: Tris EDTA pH 9.

Tris	1.21 g (10 mM)
EDTA	0.37 g (1 mM)
A. dest	add to 1 l
pH 9	adjust with 1N sodium hydroxide
Tween 20	0.5 ml

TABLE 3.11: Secondary antibodies and controls.

Name	Host species	Supplier	Dilution
Secondary antibodies			
a-goat	rabbit	Vector (Burlingame, USA)	1/300
a-rabbit	goat	Vector (Burlingame, USA)	1/300
IF antibodies			
a-rabbit alexa 647	donkey	Jakson (Ely, UK)	1/100
a-mouse IgG2a Alexa 488	goat	Thermo-Fischer Scientific (Rockford, USA)	1/100
a-goat Alexa 488	donkey	Jackson (Ely, UK)	1/100
Control IgG-antibodies			
Rabbit IgG	rabbit	Dako (Santa clara, USA)	adapted
Goat IgG	goat	Santa Cruz (Oregon, USA)	adapted

(see Table 3.12) was performed for 10 minutes at 37°C. The slides were counterstained with methyl green (see Table 3.13) for 4 minutes. The sections were dehydrated and mounted with Roti-Histokitt.

TABLE 3.12: DAB.

DAB (Working solution)	
Tris buffer pH 7.6	175 ml
DAB (stock solution)	4.0 ml
8% Nickel(II) chloride	1.8 ml
H_2O_2 (30 %)	180 µl
Tris buffer pH 7,6	
Tris	6.1 g (0.05 M)
NaCl	11.69 g (0.2 M)
A. dest	add 500 ml
pH 7.6	adjust with HCl
A. dest	add to 1.0 l
DAB Stocksolution	
DAB	10.0 g
A. dest	1.0 l
8 % Nickel(II)chloride (working solution)	
$NiCl_2$	2.0 g
A. dest	25.0 ml

TABLE 3.13: Methyl green (working solution)

Methyl green	20 g
Acetic acid (0.1 M)	735 ml
Na-Acetate	265 ml

Staining with all antibodies was established in a standardized matter. For a more extensive overview of the used techniques and unsuccessful establishments confer to Appendix C.1. For negative controls, substitution of phosphate-buffered saline solution or irrelevant matched IgG (see Table 3.11) in place of the primary antibodies was used.
For morphometric analyses, the sections were scanned with a whole-slide scanner. 15 to 50 images at x 40 magnification from cortex and medulla were obtained with the imaging software NDP.view. The positively stained area of each slide was quantified with ImageJ.

3.5.3 Immunofluorescence

Immunofluorescence (IF) enables the simultaneous detection of different proteins. The secondary antibodies are coupled to fluorescent molecules that can be excited by different wavelengths and can thus be differentiated. The steps up to the application of the first secondary antibody are identical to immunohistochemistry, except for the H_2O_2 blocking (confer Section 3.5.2). After washing the slides twice in PBS, it has to be worked in the dark. A fluorescently labeled secondary antibody was applied for 30 minutes at room temperature (see Table 3.11). After washing in PBS twice for 5 minutes, the slides were incubated with a second first antibody (for dilution confer Table 3.9) for one hour at room temperature. The corresponding secondary antibody was then applied for 30 minutes at room temperature. After washing the slides twice for 5 minutes in PBS. 4',6-diamidino-2-phenylindole (DAPI), diluted 1 / 10 000 with distilled water, was pipetted on the slides and incubated for 3 minutes. Thereafter, the slides were mounted with immumount, let dry for 30 minutes at room temperature and stored in the dark at 4° C. Pictures were taken with a Biorevo BZ9000 fluorescence microscope (Keyence, Neu-Isenburg, DE).

3.6 Protein analysis

Urea buffer

Since urea is effective in disrupting hydrogen bonds aiding protein unfolding and denaturation, collagens were solubilized with high concentrated urea. A 6 M urea solution was prepared (see Table 3.14). To obtain the working buffer, per 1 ml urea solution 10 µl inhibitor cocktail was added. 600 µl urea working solution were added to each sample. The samples were crushed in the vibrator mill for 2 minutes. Afterwards, they were put three times for 10 s in the ultrasound bath, in between they were cooled on ice for 2 minutes. They were then incubated for 30 minutes at 4°C and centrifuged for 10 minutes at 10 000 rpm. The supernatant was carefully transferred in new tubes and frozen at -80°C.

TABLE 3.14: Urea buffer.

Tris	50 mM
Urea	6 M
NaCl	50 mM
EDTA	5 mM
A. dest	add to 1 l
Adjust to pH 7.5	

3.6.1 Bicinchoninic acid assay

The protein concentration was determined using the colorimetric bicinchoninic acid assay (BCA). A standard curve with 2 mg/ml albumin was prepared (see Table 3.15). The assay was performed according to manufacturer specifications. 10 µl of sample in doublet and in dilution 1/5 and 1/10 were pipetted, then 200 µl of working solution filled in each well. After incubating the samples for 30 minutes at 37°C, the absorption at 562 nm was measured with a microplate reader photometer. This measurement method is very robust and in particular is not affected by urea (Walker, 1996).

3.6.2 SDS-PAGE

For the quantification of protein expression, the protein lysates were separated in a denaturated SDS-polyacrylamide gel with electrophoresis. The samples were heated and denaturated with β-mercaptoethanol (reducing conditions), thereby

TABLE 3.15: Albumin standard.

Standard	Concentration	Preparation
1	2 mg/ml	60 µl
2	1 mg/ml	30 µl from standard 1 + 30 µl H_2O
3	0.5 mg/ml	30 µl from standard 2 + 30 µl H_2O
4	0.25 mg/ml	30 µl from standard 3 + 30 µl H_2O
5	0.125 mg/ml	30 µl from standard 4 + 30 µl H_2O
6	0.062 mg/ml	30 µl from standard 5 + 30 µl H_2O
7	0.031 mg/ml	30 µl from standard 6 + 30 µl H_2O
8	0 mg/ml	30 µl H_2O

the proteins unfold and SDS binds in a ratio of 1.4 / 1. The proteins acquire a negative charge, proportional to the length of the polypeptide chain (Roy & Kumar, 2014).

Equal amounts of protein (40 µg) were filled up to 15 µl with distilled water. 5 µl of reducing sample buffer (see Table 3.16) were added to each sample. The samples were boiled for 5 minutes, then put on ice and shortly centrifuged. Afterwards, they were applicated to the wells of a 1.5 mm 4-12 % Bis-Tris gel. This gel was placed in the Novex electrophoreses system, which was filled up with running buffer (50 ml MOPS or MES SDS running buffer (20 x) + 950 ml H_2O). The running buffer was chosen according to the target protein size: For proteins < 70 kDa MES buffer was used, for proteins > 70 kDa MOPS. As a standard 6 µl Spectra Multicolor Broad or High range protein ladder were used (depending on the target protein size). The electrophoresis took place at 130 V for 90 minutes.

TABLE 3.16: Sample Buffer (4x).

A. dest	2.4 ml
Sample buffer (4x)	2.4 ml
Glycerol	2 ml
SDS (10 %)	2 ml
β-mercaptoethanol	1 ml
Bromphenol blue (1 %)	200 µl
EDTA (0.5 M)	40 µl

3.6.3 Western Blot

The samples were transferred to a 0.45 µm nitrocellulose membrane. After washing the gel in TTBS (see Table 3.17 (A)), gel and nitrocellulose membrane were given in the blot system, with a cooling unit and cold transfer buffer (see Table 3.17 (B)). The transfer took place at 100 V for 60 minutes (target proteins <

70 kDa) or 70 minutes (target proteins > 70 kDa). The membrane was washed four times for 5 minutes in TTBS, then the background was blocked for 1 hour at room temperature with 5 % non-fat dry milk powder (NFDM) in TTBS. The membranes that were later incubated with the collagen VIII antibody were blocked with Roti-Block. After washing the blot four times for 5 minutes in TTBS, it was

TABLE 3.17: Tris-buffered saline with Tween (TTBS) and Transfer buffer.

(A) Tris-buffered saline with Tween (TTBS).

NaCl (5 M)	60 ml
Tris (1 M, pH 8)	20 ml
Tween-20	1 ml
A. dest	add to 2 l

(B) Transfer buffer.

Tris	6.06 g (25 mM)
Glycin	28.8 g (190 mM)
Methanol 20%	400 ml
A. dest	add to 2 l

incubated with the primary antibody overnight at 4°C diluted 1/1000 in TTBS (see Table 3.18). Antibodies against collagen I, V, and VI were diluted in 2.5 % NFDM in TTBS. The following day, the membrane was washed four times for 5 minutes and incubated with the corresponding secondary antibody (see Table 3.19) diluted 1/10 000 in TTBS.

TABLE 3.18: Primary antibodies.

Name	Host species	Supplier	Catalog-Nr.
Collagen I	goat (polyclonal)	Southern Biotech (Birmingham, USA)	1310-01
Collagen V	rabbit (polyclonal)	Abcam (Cambridge, UK)	ab7046
Collagen VI	rabbit (monoclonal)	Abcam (Cambridge, UK)	ab182744
Collagen VIII	rabbit (polyclonal)	Thermo-Fischer Scientific (Rockford, USA)	PA5-37109
Collagen XIII	sheep (polyclonal)	R&D systems (Wiesbaden-Norderstadt)	AF4627
Collagen XVI	rabbit (polyclonal)	Thermo-Fischer Scientific (Rockford, USA)	PA5-38893
Collagen XIX	rabbit (polyclonal)	Thermo-Fischer Scientific (Rockford, USA)	PA5-23977
Collagen XXIII	rabbit (polyclonal)	Abcam (Cambridge, UK)	ab204578
GAPDH	mouse (monoclonal)	Santa Cruz (Oregon, USA)	sc-32233

TABLE 3.19: Secondary antibodies.

Name	Host species	Supplier	Catalog-Nr.
a-goat	rabbit	Dako (Santa clara, USA)	P0449
a-rabbit	goat	Dako (Santa clara, USA)	P0448
a-mouse	horse	Vector (Burlingame, USA)	PI-2000

The bound antibody was visualized with ECL used according to the manufacturer's specifications. In cases of very low protein expression Lumi-Light, a more

sensitive reagent, was used. The horseradish-peroxidase, coupled with the secondary antibody, catalyzes the ECL-substrate conversion. The membrane was placed bubble-free between two projector foils. The film was exposed for up to 30 minutes to the membrane in a dark room and then developed.
To allow a quantification, GAPDH (36-40 kDa) was used as loading control. The antibody complex was removed by stripping the membrane with stripping buffer (see Table 3.20), adding 25 µl β-mercaptoethanol per 100 ml, for 30 minutes at 56°C.
After incubation for 1 h at room temperature with 5 % NFDM in TTBS, the membrane was incubated overnight at 4°C with the GAPDH antibody (see Table 3.18, 1/1000 in TTBS). The following day GAPDH was visualized. The quantification was done with ImageJ and the healthy kidneys were identified as "1".
Western Blot for all antibodies was established in a standardized matter. For a more extensive overview of the used techniques and unsuccessful establishment confer to Appendix C.2. For negative controls, substitution of TTBS in place of the primary antibodies was used.

TABLE 3.20: Stripping buffer.

1M Tris-HCl	
Tris	121.14 g
HCl	adjust to pH 6.8
10 % SDS	
SDS	20 g
A. dest	200 ml
Stripping buffer (working solution)	
1 M Tris-HCl pH 6.8	62.5 ml
10 % SDS	200 ml
A. dest	add to 1 l

3.7 Statistical analysis

All statistical analyses were performed with Graph PadPrism. All data are presented as mean ± standard deviation (SD). All data were checked for normal distribution. The two-tailed unpaired Student's t-test was applied for comparison of continuous variables between two groups. For not normal distributed data Mann-Whitney U test was used. Statistical significance was defined as $p < 0.05$.

3.8 Ethics statement for human sample material

For the collection and anonymous use of human kidney biopsies, there is a positive vote from the ethical committee of RWTH University No. EK 240/11 and No. EK 244/14.

Chapter 4
Results

4.1 Overview of changes in collagen expression in publicly available data sets

4.1.1 Geo2R mRNA expression

To gain an overview of changes in collagen expression in CKD, freely available data sets of high-throughput gene expression arrays were analyzed in the Gene Expression Omnibus (GEO) using the web tool Geo2R. The analyzed data sets are listed in the table B.1. The results are displayed as a heat map in figure 4.1. For the analysis of these results, it should be mentioned again that the results are only comparable with each other within an identical data set, i.e. a GEO accession number. It is noticeable that a significant change in collagen expression is often observed rather late in the course of renal damage. In the model of interferon-induced lupus nephritis (GSE86444), significant changes can be observed especially from the seventh week (D.4 in figure 4.1). Also in the UUO model, significant changes in gene expression are only observed at a later stage. GSE96101 can be mentioned as an example, in which significant changes in gene expression are found mainly from UUO day 3 (M.4 in figure 4.1). At late points in time such as UUO day 8 (K in figure 4.1) or UUO day 14 (N in figure 4.1) a significant upregulation of many collagens is found.
In the figure 4.1, the collagens were arranged according to families for a detailed review of the different collagen families confer table 1.1. It can be observed that the fibril-forming collagens are upregulated in almost all cases and this also at an early stage of CKD. *Col5a1, Col5a2, Col5a3* and *Col11a1*, regulatory fibril-forming collagens, are mostly upregulated, while *Col11a2, Col24a1* and *Col27a1* hardly seem to be significantly up- or downregulated. FACITs and FACIT-like collagens tend to be upregulated or not regulated. Exceptions being *Col19a1, Col20a1* and *Col22a1*, whose expressions are mostly not significantly regulated, and if so, they are rater downregulated. Whereas most network-forming collagens are upregulated, *Col4a3, Col4a4* and *Col4a5* are mainly downregulated in CKD. The picture is not uniform for transmembrane collagens. While the expression of *Col13a1* and *Col25a1* is rarely significantly altered, *Col17a1* is mostly upregulated and *Col23a1*

is in some cases significantly downregulated. The multiplexins as well as the beaded-filament-forming collagens, anchoring and other collagens tend to be upregulated.
In summary, almost all collagen families are upregulated. The exceptions are *Col19, 20, 22* (FACIT-like collagens), *Col4a3, Col4a4, Col4a5* (network forming collagens) and *Col23*. These are mostly downregulated. The results are particularly significant at the late disease stages in the animal models.

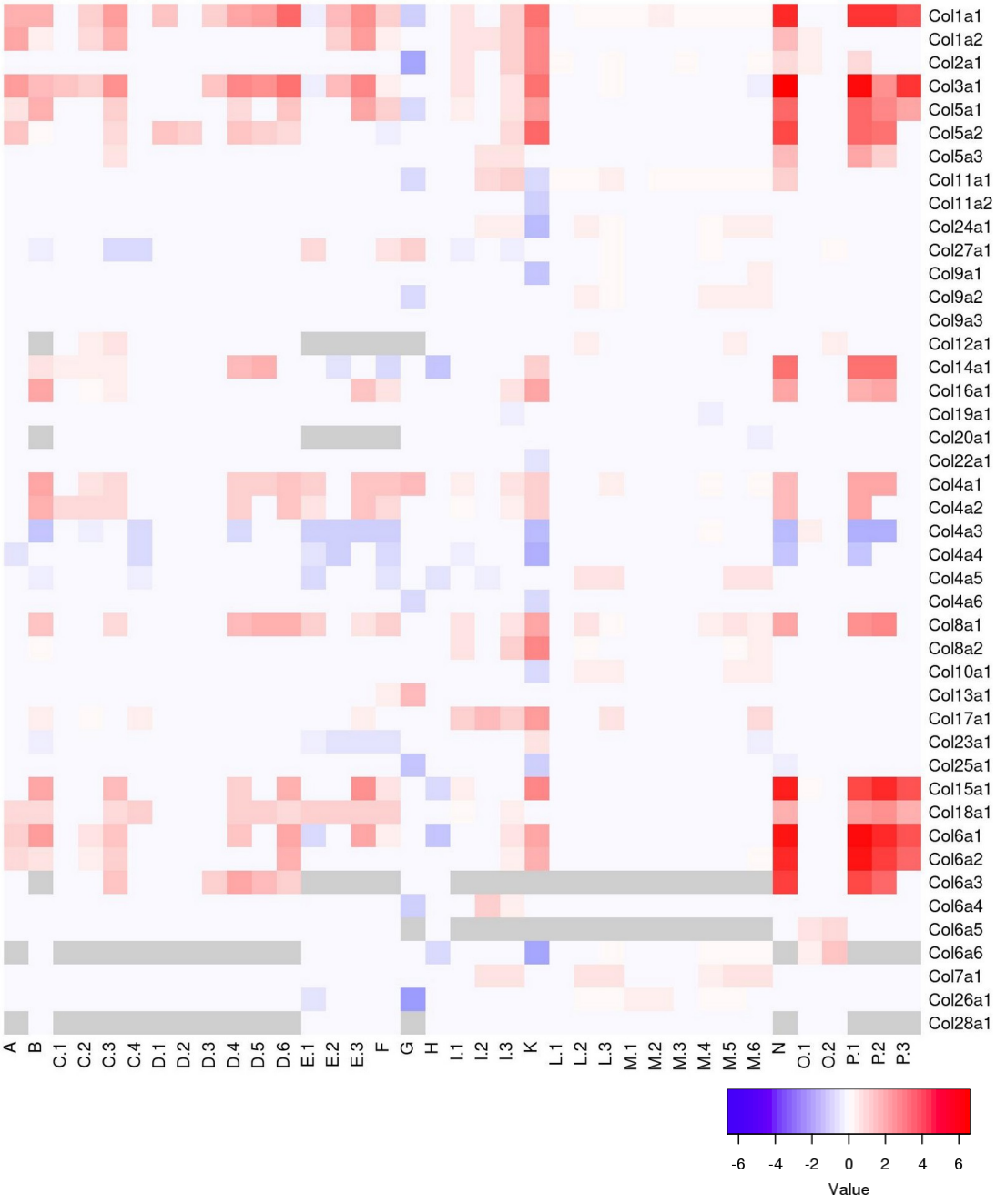

FIGURE 4.1: **Changes in gene expression of collagens in different murine fibrosis models.** The collagens are classified according to collagen families. The results are expressed using a binary logarithmic scale, $p < 0.05$. Non-significant changes are shown in white, upregulation is shown in red, downregulation in blue, missing values in gray. **A**: HIV-associated nephropathy (GSE35226). **B**: Alport model (GSE85409). **C**: Lupus nephritis (GSE32583). **D**: Lupus nephritis (GSE86444). **E**: I/R (17.5 minutes) (GSE87024). **F**: I/R day 1 (d1) (17.5 minutes) (GSE87023). **G**: I/R 6 h (45 minutes) (GSE39548). **H**: I/R bilateral (28 min) 1 d (GSE52004). **I**: UUO (GSE36496). **J**: UUO d3(GSE42303). **K**: UUO d8 (GSE38117). **L**: reversible UUO (GSE96102). **M**: UUO (GSE96101). **N**: UUO d14 (GSE121190). **O**: Hypertension (GSE54015). **P**: FA (GSE121190). The extensive list of the analyzed data sets is provided in table B.1.

4.1.2 Multi-omics analysis of fibrotic kidneys in two mouse models from Pavkovic et al., 2019

The data provided by Pavkovic et al., 2019 were analyzed for changes in collagen expression in mRNA (Figure 4.2) and protein (Figure 4.3). Figure 4.2 shows changes in gene expression in a folic acid and UUO time course. In both models there is a trend towards upregulation of gene expression with the duration of the model. The trends are more evident in the UUO model than in the folic acid model. As with the analysis of the data sets using Geo2R, the fibrillar collagens and the regulatory fibril-forming collagens are upregulated. While in the UUO model the gene expression of *Col11a2, Col24a1*, and *Col27a1* increases, in the folic acid model there is no clear trend. Also the FACITs are mostly upregulated, the exception is *Col19a1*, which shows a downregulation in the UUO time course, the regulation in the folic acid time course is less clear. *Col20a1* and *Col22a1,* which were mainly downregulated in the previous analysis, show an increased expression. A similar result as with the FACITs can be observed with network-forming collagens. Exceptions being the expression of *Col4a3, Col4a4*, and *Col4a5* in the UUO model, which seems to decrease over time. In the case of transmembrane collagens, the picture is mixed. While the mRNA expression of *Col13a1* and *Col17a1* seems to increase over time in the UUO model, no trend can be seen in the folic acid model. *Col23a1* and *Col25a1* show increased expression over time in the folic acid model, while it is decreasedin the UUO model. The multiplexins as well as the beaded-filaments-forming collagens, anchoring, and other collagens are upregulated. The exceptions are *Col6a6* in the UUO model and *Col7a1* in the folic acid model. Figure 4.3 shows changes in collagen frequency in mass spectrometry in folic acid and the UUO model over time. For many collagens, no values at all could be determined. This is probably due to the very low expression of the proteins in the kidney. An increase in the frequency of the measured collagens can be observed. Except for *Col4a3* in both models and *Col6a6* in the UUO time course, this is identical to the measured gene expression level data.
In summary, most collagens in CKD mouse models are upregulated. Therefore, for each collagen family one or more exemplary collagens were selected and analyzed in detail. In addition, as far as antibodies were available, collagens that were downregulated in these array results were analyzed in more detail.

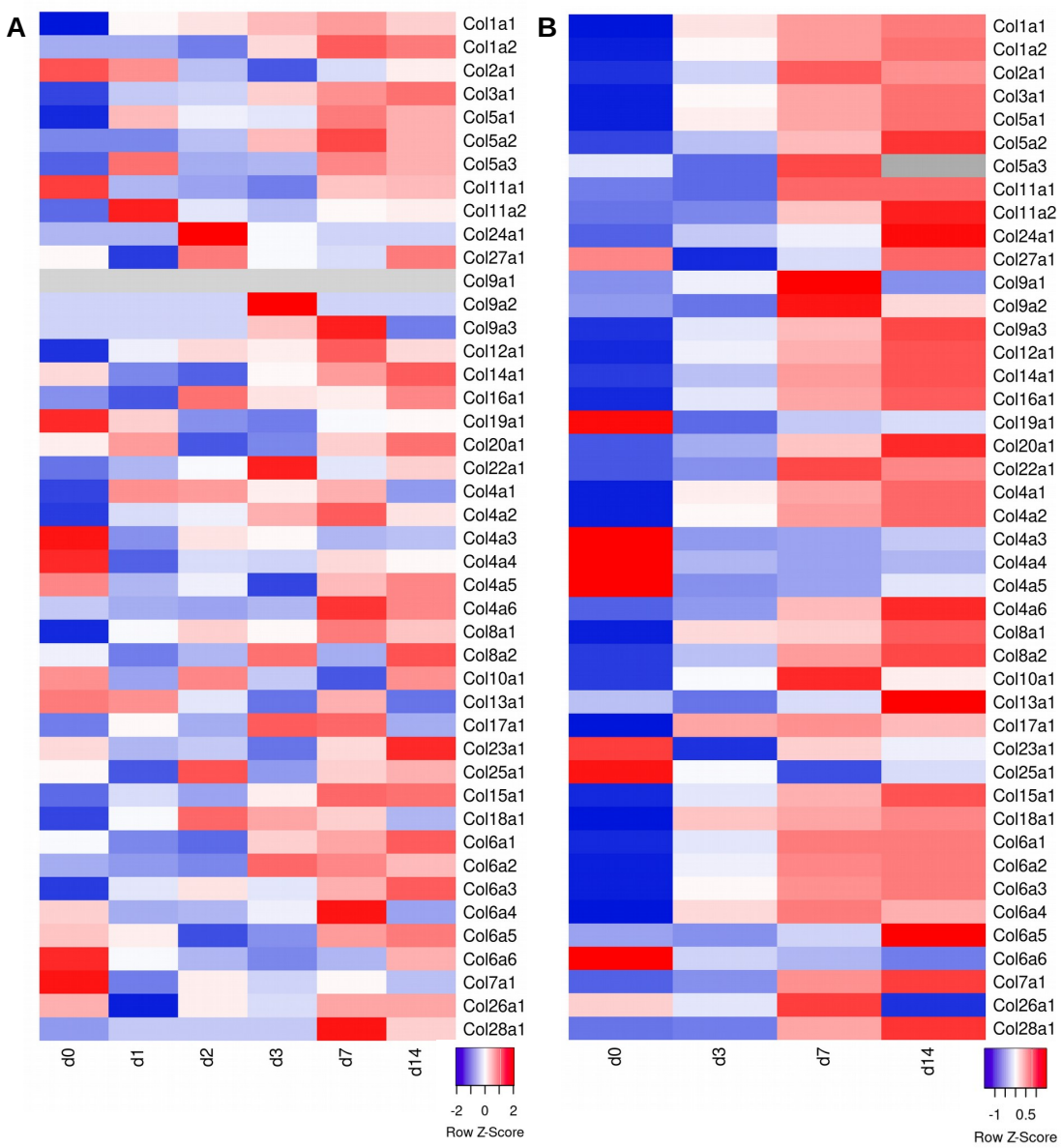

FIGURE 4.2: **Heat map of changes in collagen mRNA expression in folic acid and unilateral ureteral obstruction model in mice. A**: FA (time points: d0, d1, d2, d7 and d14). **B**: UUO (time points: d0, d3, d7 and d14). Values are raw z-scores of the log2 normalized abundance for each molecule. Gray color: missing values. The collagens are classified according to collagen families.

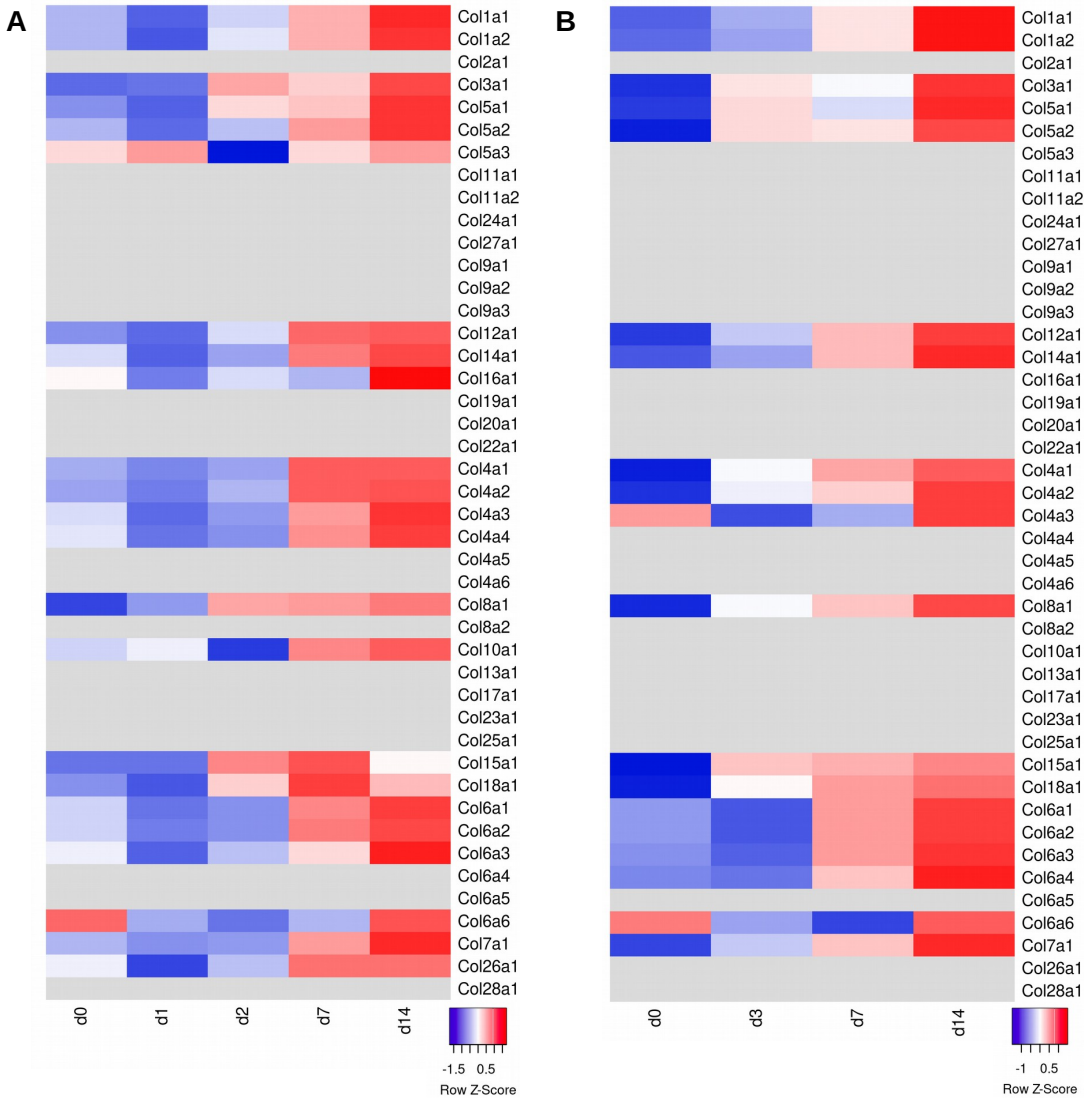

FIGURE 4.3: **Changes in collagen abundance in folic acid and unilateral ureteral obstruction model in mice.** **A**: FA (time points: d0, d1, d2, d7 and d14). **B**: UUO (time points: d0, d3, d7 and d14). Values are raw z-scores of the log2 normalized abundance for each molecule. Gray color: missing values. The collagens are classified according to collagen families.

4.2 Fibrillar collagens

4.2.1 Fibrillar collagens

Changes in gene expression levels of fibrillar collagens were analyzed using the examples of *Col1a1* and *Col3a1*. Figure 4.4 shows a significant upregulation of both collagens in all investigated models, up to a 447-fold increase.

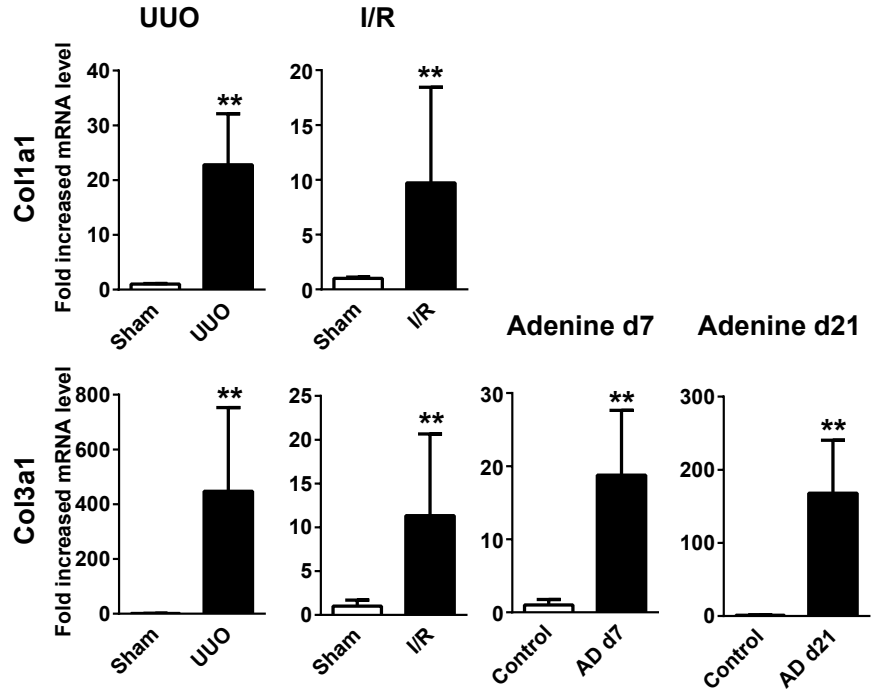

FIGURE 4.4: **Gene expression levels in different renal fibrosis models of the fibrillar collagens Col1a1 and Col3a1 in mice.** UUO, I/R, adenine day 7 and day 21 model showed a significant upregulation of *Col1a1* and *Col3a1* expression in comparison to untreated control animals. **: $p < 0.01$, $n(\text{sham}_{\text{UUO}}) = 5$, $n(\text{UUO}) = 5$; $n(\text{sham}_{\text{I/R}}) = 5$, $n(\text{I/R}) = 5$; $n(\text{control}_{\text{AD d7}}) = 7$, $n(\text{AD d7}) = 8$; $n(\text{control}_{\text{AD d21}}) = 7$, $n(\text{AD d21}) = 8$.

The expression of collagen I was also significantly increased, up to 3.6-fold, in western blot in all investigated renal fibrosis models, as shown in Figure 4.5. Immunohistochemistry showed significant increases in collagen III in all animal models in both the kidney cortex and medulla (Figure 4.6). The increase of collagen III positive area was up to 24-fold in the cortex and 32-fold in the medulla in the UUO model.

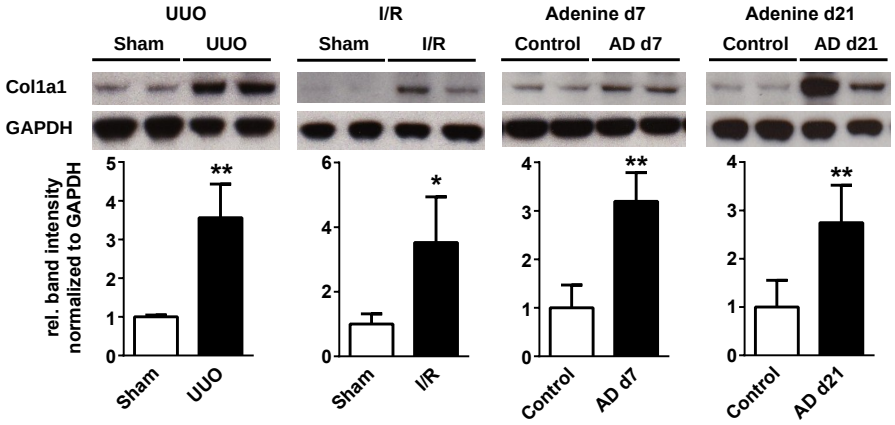

FIGURE 4.5: **Collagen I expression in renal fibrosis models in mice.** UUO, I/R, adenine day 7 and adenine day 21 model showed a significant upregulation of collagen I in comparison to untreated control animals. *: $p < 0.05$, **: $p < 0.01$, $n(\text{sham}_{\text{UUO}}) = 4$, $n(\text{UUO}) = 6$; $n(\text{sham}_{\text{I/R}}) = 4$, $n(\text{I/R}) = 4$; $n(\text{control}_{\text{AD d7}}) =,7$, $n(\text{AD d7}) = 8$; $n(\text{control}_{\text{AD d21}}) = 7$, $n(\text{AD d21}) = 8$.

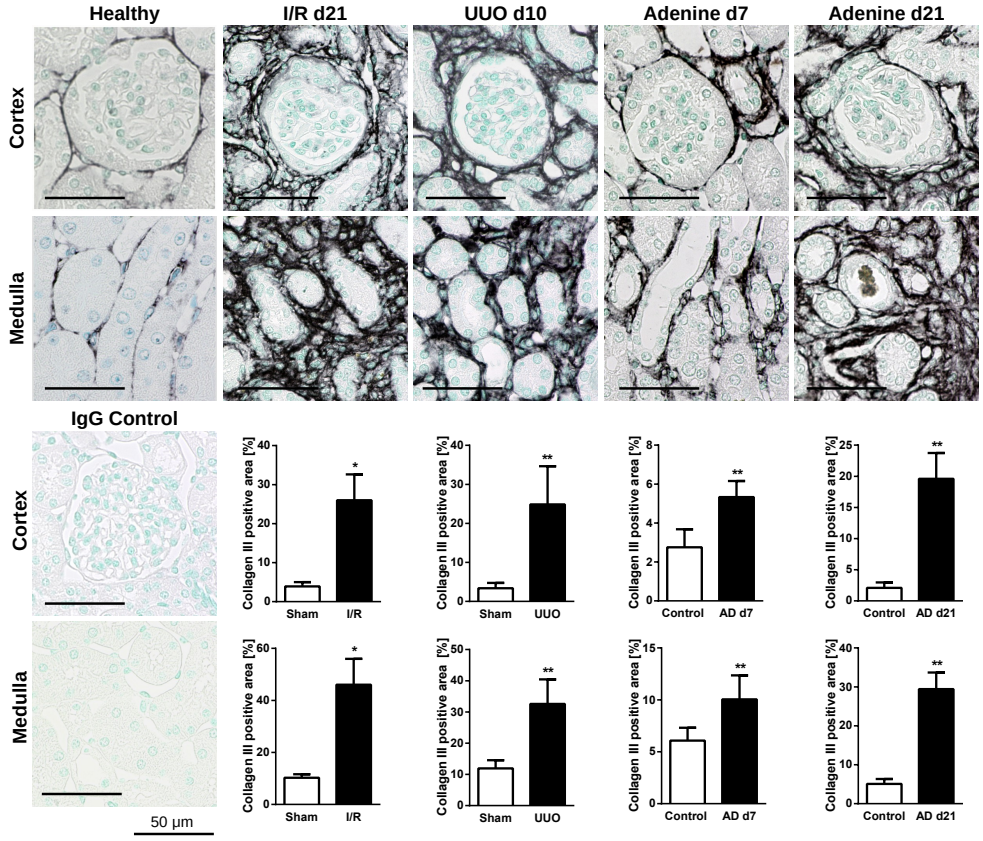

FIGURE 4.6: **Expression of collagen III in immunohistochemistry staining in renal fibrosis models in the cortex and medulla of mouse kidneys.** Quantification of collagen III positive area showed a significant increase of collagen III in the medulla and cortex in I/R, UUO and adenine day 7 and day 21 model in comparison to untreated control animals. *: $p < 0.05$, **: $p < 0.01$. Nuclear staining with methyl green. Nonspecific IgG used as control. Scale bare: 50 µm. $n(\text{sham}_{\text{UUO}}) = 4$, $n(\text{UUO}) = 6$; $n(\text{sham}_{\text{I/R}}) = 4$, $n(\text{I/R}) = 4$; $n(\text{control}_{\text{AD d7}}) = 5$, $n(\text{AD d7}) = 8$; $n(\text{control}_{\text{AD d21}}) = 5$, $n(\text{AD d21}) = 7$.

4.2.2 Fibril regulating collagens

A significant upregulation of *Col5a1* in all renal fibrosis models could be observed (Figure 4.7), while *Col24a1* did not show any significant changes in mRNA levels. *Col27a1* was significantly downregulated in all animal models except adenine day 21. In the UUO model, the gene expression of *Col27* was reduced by 90 %.

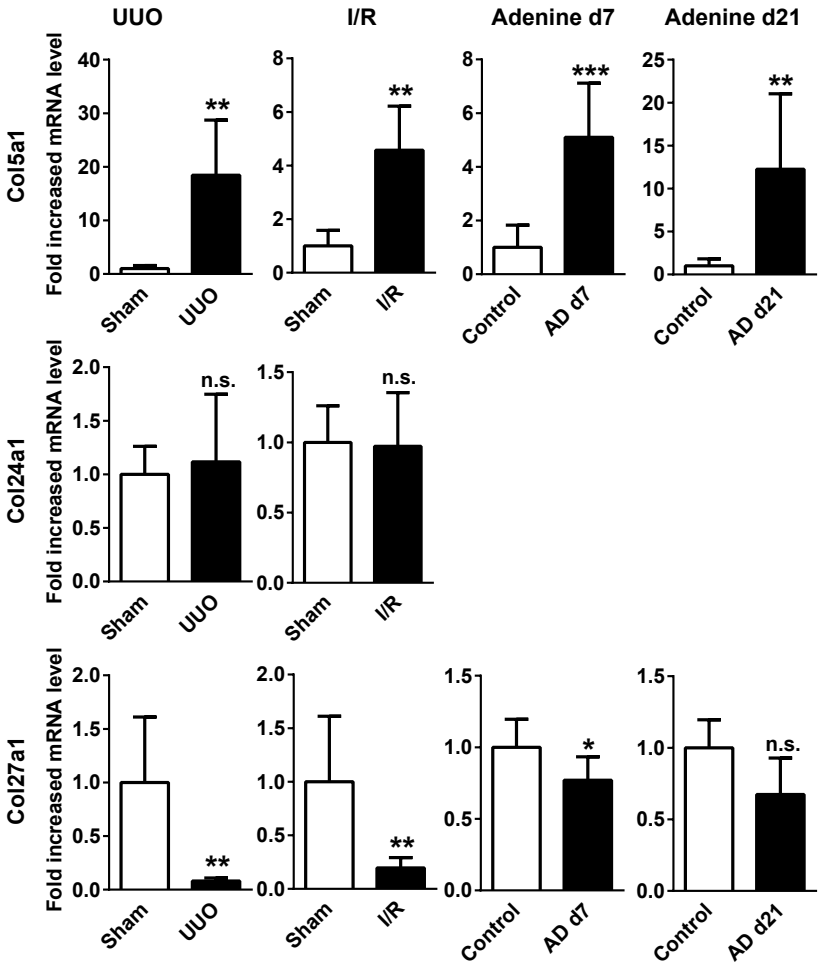

FIGURE 4.7: **Gene expression levels in different renal fibrosis models of the fibril regulating collagens *Col5a1, Col24a1, Col27a1*.** *Col5a1* was significantly upregulated in UUO, I/R, adenine day 7 and day 21 in comparison to untreated control animals. *Col24a1* was not regulated and *Col27a1* was downregulated in all models except for adenine d21. *: $p < 0.05$ **: $p < 0.01$, ***: $p < 0.001$, n.s.: not significant. $n(sham_{UUO}) = 5$, $n(UUO) = 5$; $n(sham_{I/R}) = 5$, $n(I/R) = 5$; $n(control_{AD\ d7}) = 7$, $n(AD\ d7) = 8$; $n(control_{AD\ d21}) = 7$, $n(AD\ d21) = 8$.

The upregulation could be confirmed in western blot and immunohistochemistry. In western blot, a significant increase of collagen V in all late fibrosis timepoints (UUO, I/R and adenine day 21 model), up to 6-fold in I/R model, as

shown in Figure 4.8, could be observed.

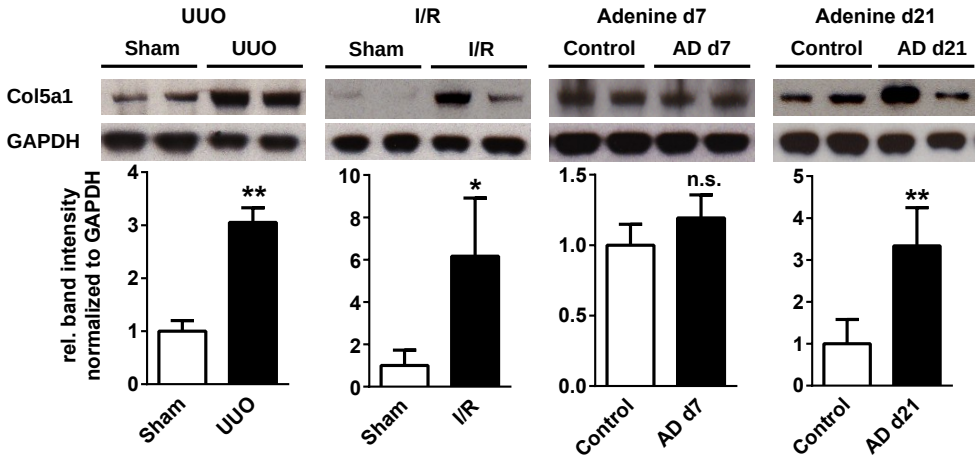

FIGURE 4.8: **Collagen V expression in renal fibrosis models in mice.** In UUO, I/R and adenine day 21 collagen V was significantly upregulated. *: $p < 0.05$, **: $p < 0.01$, n.s.: not significant. $n(\text{sham}_{\text{UUO}}) = 4$, $n(\text{UUO}) = 6$; $n(\text{sham}_{\text{I/R}}) = 4$, $n(\text{I/R}) = 4$; $n(\text{control}_{\text{AD d7}}) = 5$, $n(\text{AD d7}) = 8$; $n(\text{control}_{\text{AD d21}}) = 5$, $n(\text{AD d21}) = 8$.

Figure 4.9 shows a significant expansion of collagen V positive area in the medulla in all models up to 3-fold. The amount of collagen V was also significantly higher in the cortex in UUO and adenine day 21 model compared to healthy kidneys.

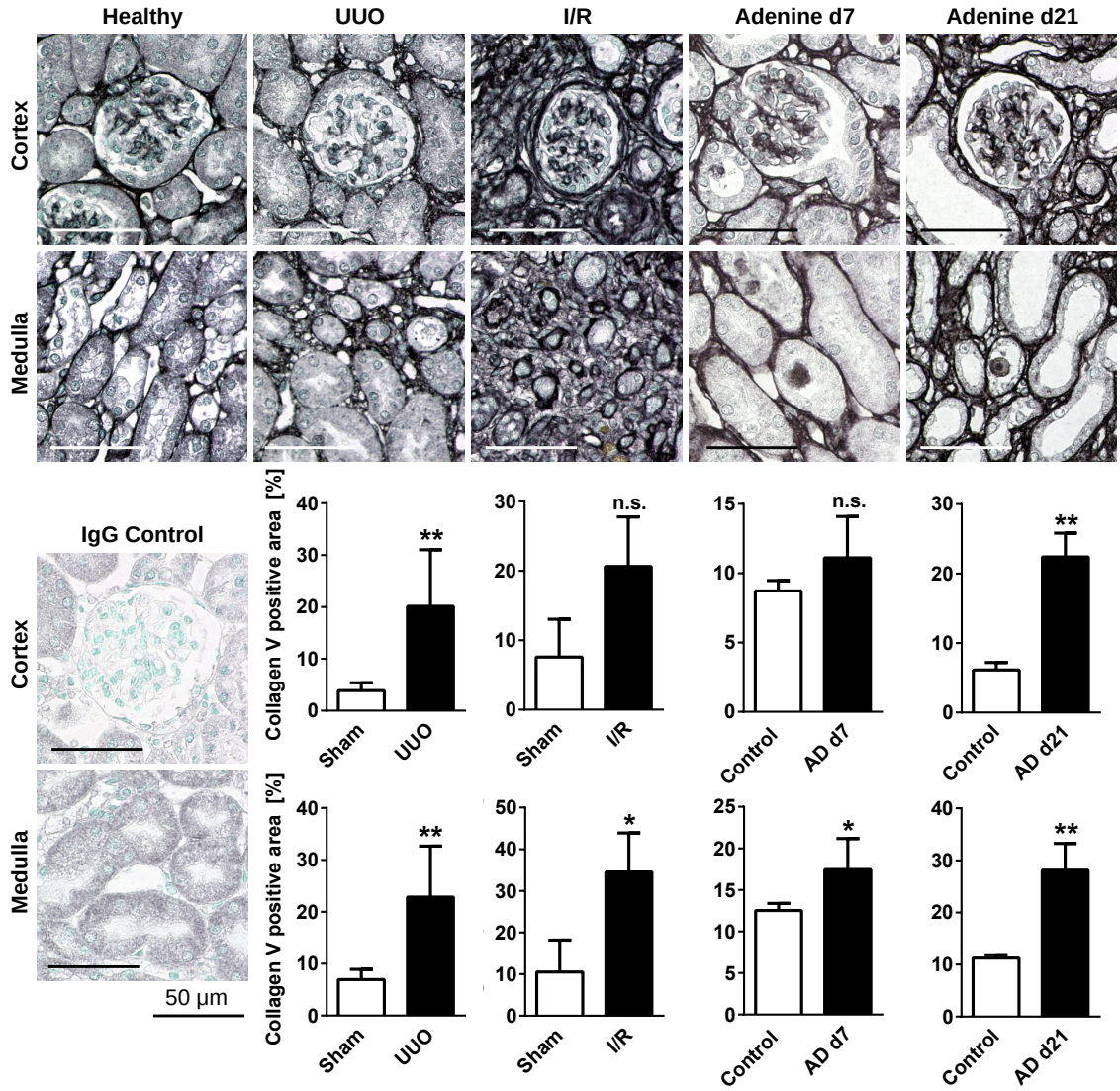

FIGURE 4.9: **Expression of collagen V in immunohistochemistry staining in renal fibrosis models in the cortex and medulla of mouse kidneys.** Quantification of collagen V positive area showed a significant increase of collagen V in the medulla of all models in comparison to untreated control animals. In the cortex collagen V was significantly upregulated in the UUO and adenine day 21 model. *: $p < 0.05$, **: $p < 0.01$, n.s.: not significant. Nuclear staining with methyl green. Nonspecific IgG used as control. Scale bare: 50 µm. $n(\text{sham}_{\text{UUO}}) = 4$, $n(\text{UUO}) = 6$; $n(\text{sham}_{\text{I/R}}) = 4$, $n(\text{I/R}) = 4$; $n(\text{control}_{\text{AD d7}}) = 5$, $n(\text{AD d7}) = 8$; $n(\text{control}_{\text{AD d21}}) = 4$, $n(\text{AD d21}) = 7$.

In the human kidney, collagen V was expressed in the mesangium of the glomeruli and near the Bowman's capsule as shown in Figure 4.10. Besides, collagen V could be detected in the renal interstitium. As shown in Figure 4.11, collagen V colocalized with collagen I.

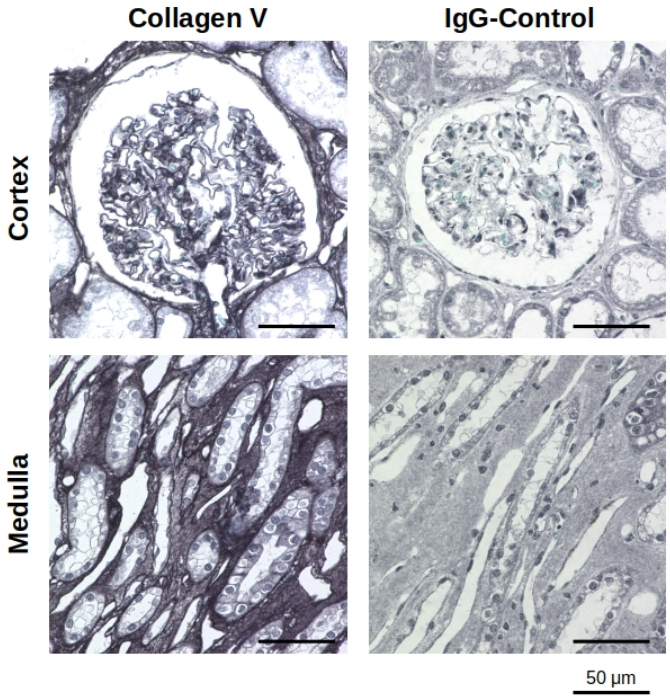

FIGURE 4.10: **Immunohistochemistry staining of collagen V expression in the cortex and medulla of healthy human kidneys.** In humans, collagen V was expressed in the glomerular mesangium, near the Bowman capsule and in the interstitium. Nonspecific IgG used as control. Scale bare: 50 µm

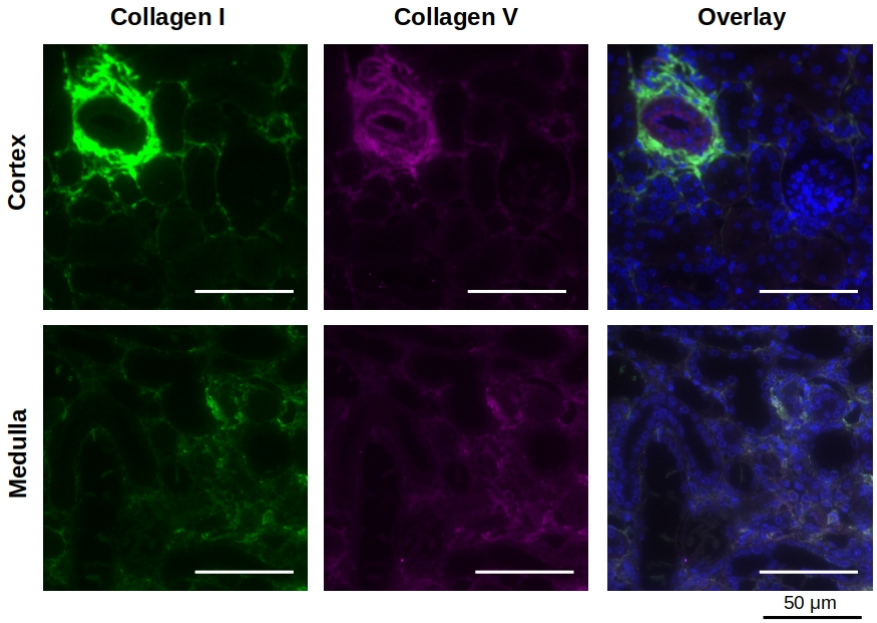

FIGURE 4.11: **Collagen V and collagen I expression in the UUO day 7 model in mouse kidney.** Collagen I and V were expressed in the kidney interstitium in cortex and medulla. The expression was pronounced around vessels. collagen I; collagen V: DAPI. Scale bar: 50 µm.

4.3 FACITs

As examples of fibril-associated collagens with interrupted triple helices (FACITs) RT-qPCR from *Col12a1, Col14a1, Col16a1* and *Col19a1* could be successfully established. *Col14a1* and *Col16a1* were found to be higher expressed in all renal damage models studied, except I/R (Figure 4.12). *Col14* was upregulated up to 4-fold in the adenine day 21 model, *Col16a1* even up to 10-fold. For *Col12a1*, increased mRNA expression was observed in the adenine day 7 and day 21 model, up to 108-fold. In the I/R model, however, the expression was significantly reduced by 90 %. *Col19a1* gene expression was significantly decreased by 88 % in the UUO model.

4.3.1 Collagen XVI

The protein expression of collagen XVI was analyzed in more detail (Figure 4.13). Three bands were detected in the western blot. A 213 kDa band representing the intact collagen chain and a 180 kDa band representing collagen XVI without non-collagenous domain 11 (NC11) domain were detected (Ratzinger et al., 2010). Also, a 60 kDa band was detected, which most likely represents a non-specific band from the antibody (Bedal, 2015). While the protein level of the 213 kDa form was significantly increased only in the UUO and adenine day 7 model, the level of the 180 kDa form was increased up to 25-fold in all models. The 60 kDa fragment was significantly augmented in all fibrosis models up to 2-fold, only in the adenine day 7 model it was significantly decreased by 27 %.

4.3.2 Collagen XIX

Changes in protein expression of collagen XIX were also investigated further (Figure 4.14). Three bands could be detected. The 140 kDa band representing the collagen chain. The 50 and 40 kDa bands are representing proteolytic products of collagen XIX (Oudart et al., 2013). Collagen XIX was significantly decreased up to 84 % in the UUO and I/R model. The protein level of the 50 kDa proteolytic fragment was significantly increased by 80 % in the UUO model and down-regulated by 45 % in the adenine day 21 model. The level of 40 kDa fragment was decreased in the UUO, I/R, and adenine day 21 model up to 46 %.

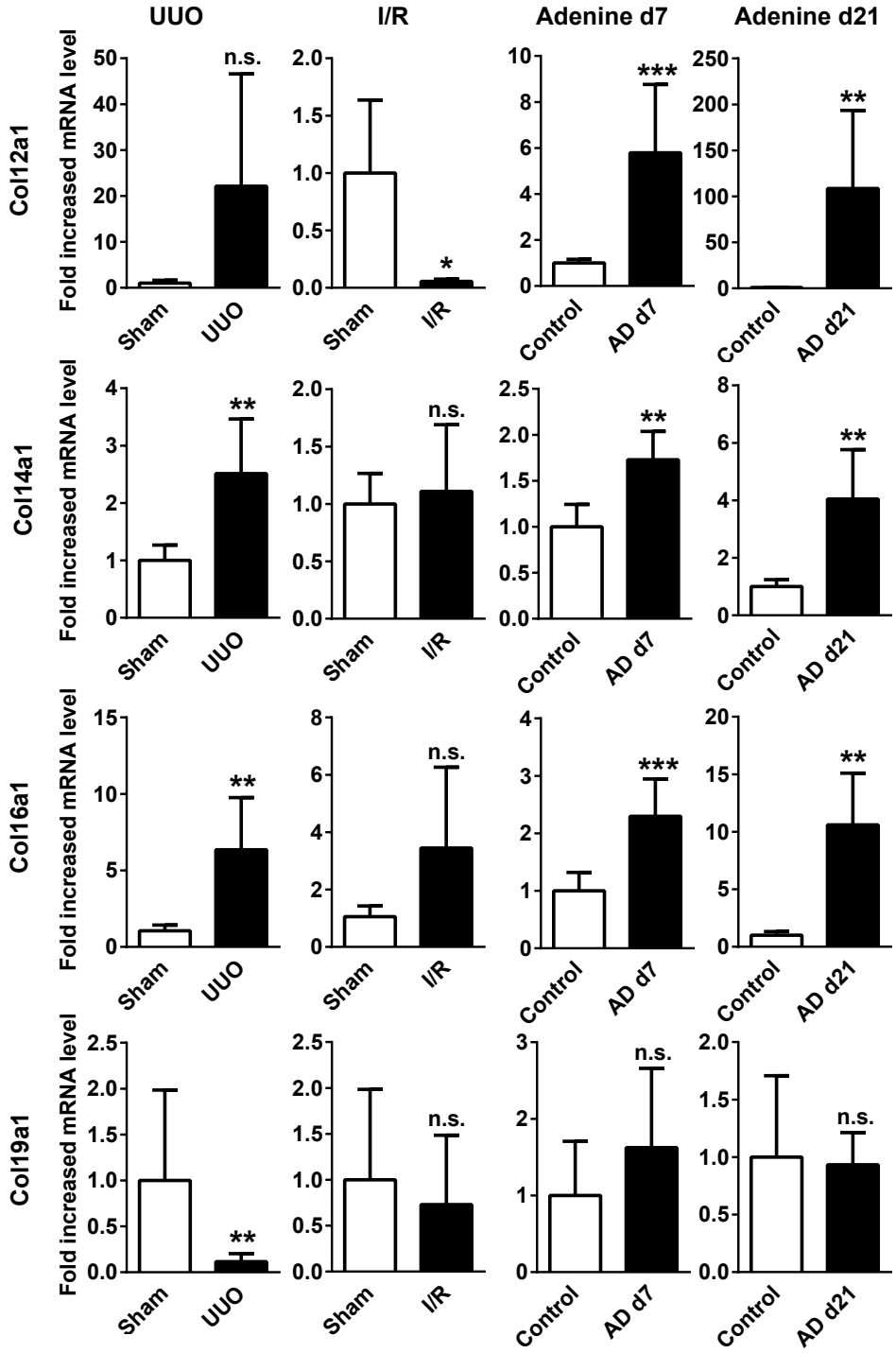

FIGURE 4.12: **Gene expression levels in different renal fibrosis models of the FACITs *Col12a1, Col14a1, Col16a1, Col19a1* in mice.** *Col12a1* was significantly upregulated in the adenine day 7 and day 21 model, it was downregulated in the I/R model in comparison to untreated control animals. *Col14a1* and *Col16a1* were upregulated in the UUO, adenine day 7 and day 21 model. *Col19a1* was significantly downregulated in the UUO model. *: $p < 0.05$ **: $p < 0.01$, ***: $p < 0.001$, n.s.: not significant. $n(\text{sham}_{\text{UUO}}) = 5$, $n(\text{UUO}) = 5$; $n(\text{sham}_{\text{I/R}}) = 5$, $n(\text{I/R}) = 5$; $n(\text{control}_{\text{AD d7}}) = 7$, $n(\text{AD d7}) = 8$; $n(\text{control}_{\text{AD d21}}) = 7$, $n(\text{AD d21}) = 8$.

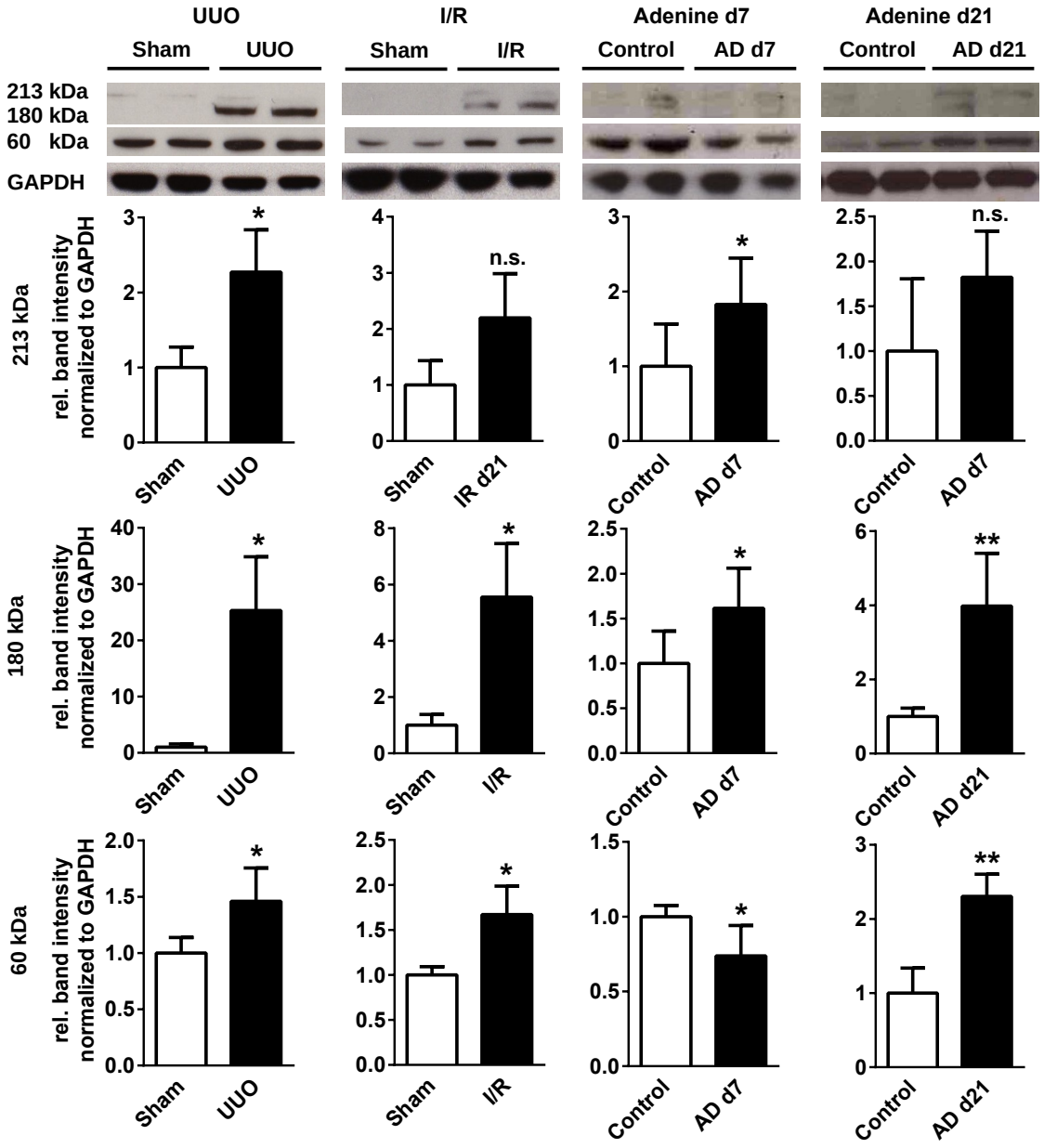

FIGURE 4.13: **Collagen XVI expression in renal fibrosis models in mice.** Three different bands could be detected: The 213 kDa and 180 kDa form of collagen XVI and a 60 kDa unspecific fragment. The 210 kDa form of collagen XVI was significantly upregulated in the UUO and adenine day 7 model in comparison to untreated control animals. The 183 kDa form was significantly upregulated in all models, the 60 kDa fragment was upregulated in the UUO, I/R and adenine day 21 but downregulated in adenine day 7. *: $p < 0.05$, **: $p < 0.01$, n.s. not significant; $n(\text{sham}_{\text{UUO}}) = 4$, $n(\text{UUO}) = 6$; $n(\text{sham}_{\text{I/R}}) = 4$, $n(\text{I/R}) = 4$; $n(\text{control}_{\text{AD d7}}) = 5$, $n(\text{AD d7}) = 7$; $n(\text{control}_{\text{AD d21}}) = 5$, $n(\text{AD d21}) = 8$.

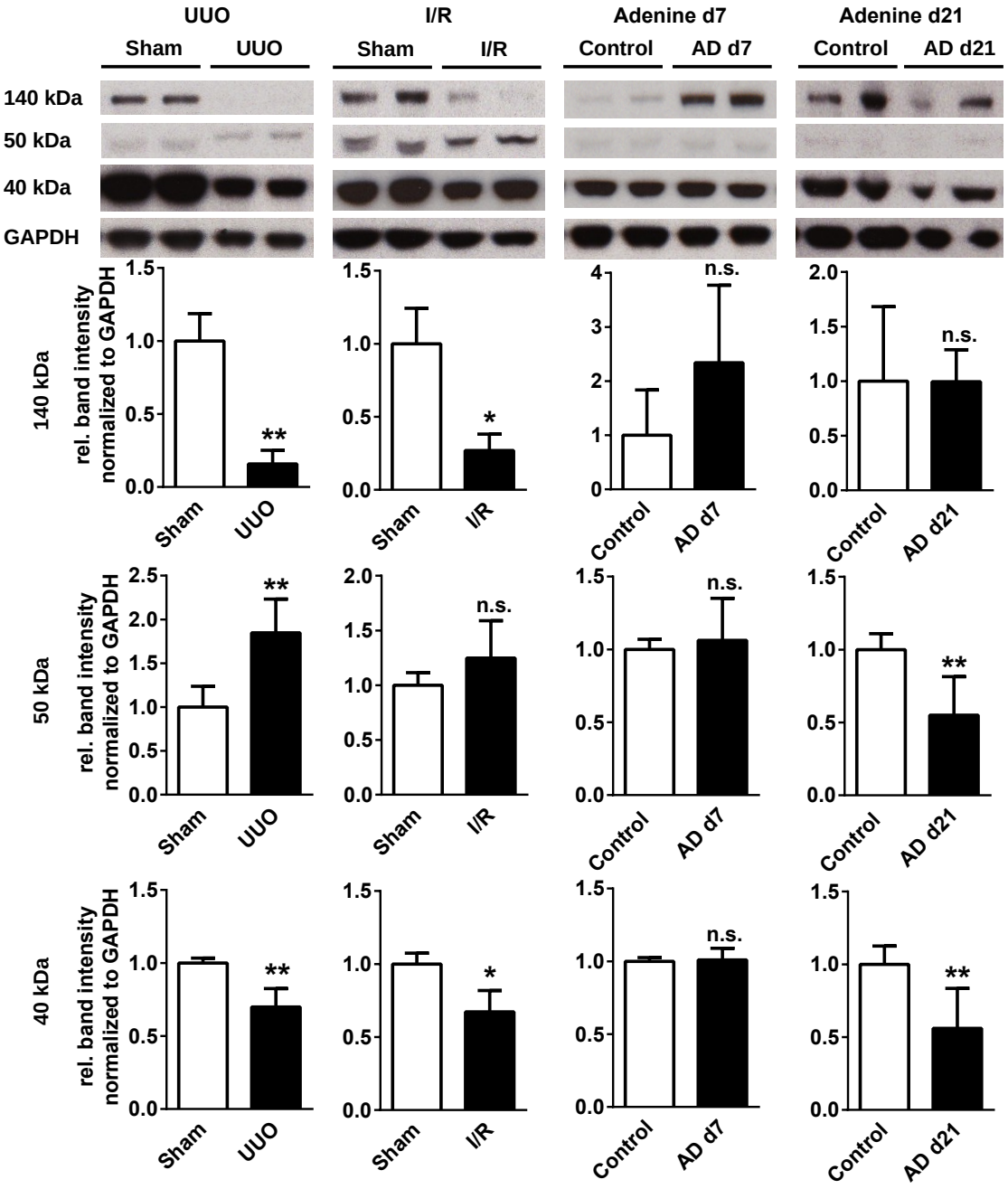

FIGURE 4.14: **Collagen XIX expression in renal fibrosis models in mice.** Three different bands were detected: 140, 50 and 40 kDa. The 140 kDa form was significantly downregulated in the UUO and I/R model in comparison to untreated control animals. The 50 kDa fragment was upregulated in the UUO model and downregulated in the adenine day 21 model. The 40 kDa fragment was downregulated in all models except for adenine day 7. *: $p < 0.05$, **: $p < 0.01$, n.s.: not significant; $n(\text{sham}_{\text{UUO}}) = 4$, $n(\text{UUO}) = 6$; $n(\text{sham}_{\text{I/R}}) = 4$, $n(\text{I/R}) = 4$; $n(\text{control}_{\text{AD d7}}) = 5$, $n(\text{AD d7}) = 8$; $n(\text{control}_{\text{AD d21}}) = 5$, $n(\text{AD d21}) = 8$.

The expression pattern of collagen XIX was further explored with immunohistochemistry (Figure 4.15). Collagen XIX was expressed very specifically in the

vascular smooth cells of the arterioles cells. It was shown by immunofluorescence (Figure 4.16) that the cells expressing α-smooth muscle actin do not express collagen XIX.

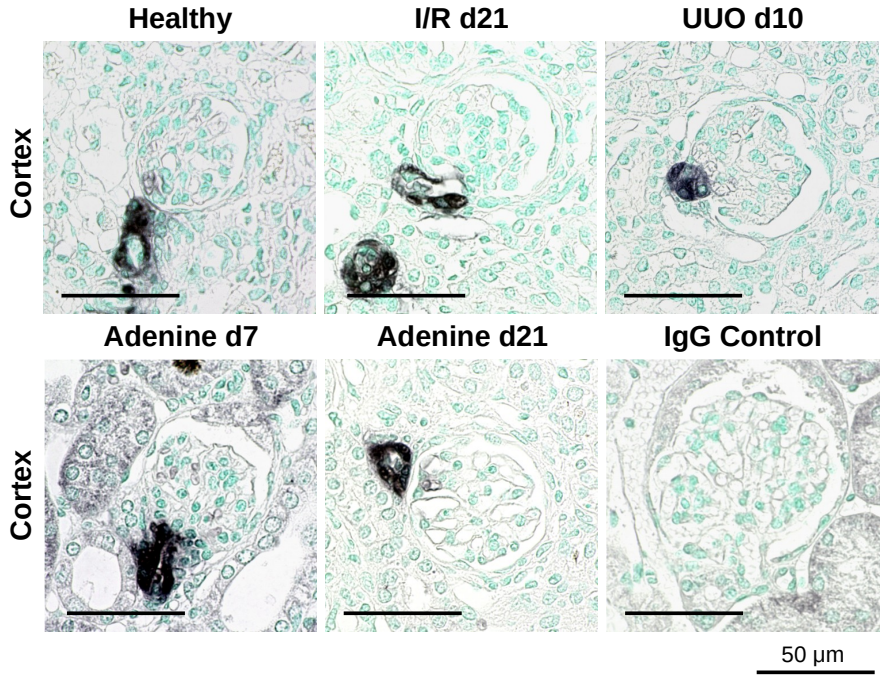

FIGURE 4.15: **Expression of collagen XIX in immunohistochemistry staining in renal fibrosis models.** Collagen XIX was expressed adjacent to the vascular smooth muscle cells of the arterioles. Nuclear staining with methyl green. Nonspecific IgG used as control. Scale bare: 50 µm.

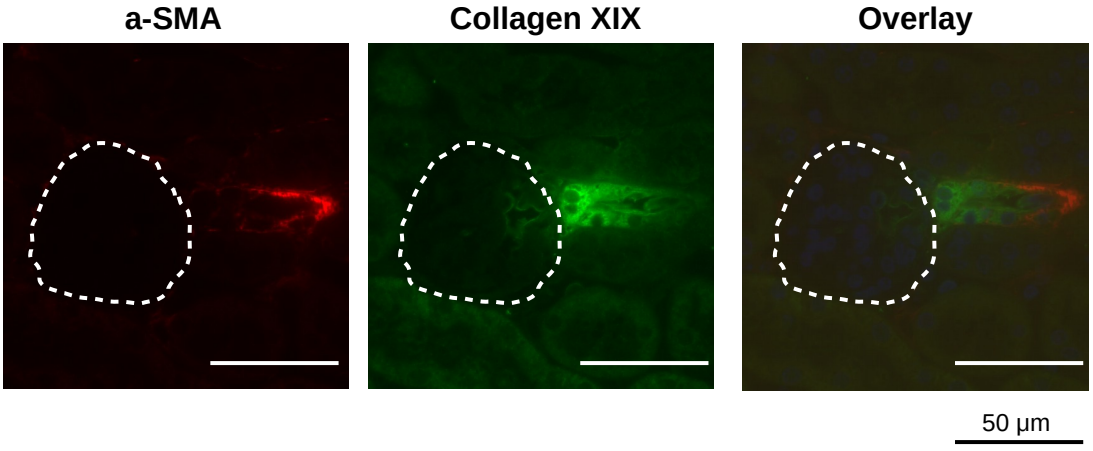

FIGURE 4.16: **Immunofluorescence of collagen XIX and alpha-smooth muscle actin (SMA).** Collagen XIX was expressed adjacent to the cells expressing α-SMA. Staining: α-SMA, Collagen XIX. Scale bar: 50 µm.

4.4 Network forming collagens

To investigate the regulation of network forming collagens, the gene expression levels of *Col4a1, Col8a1* and *Col10a1* were analyzed (Figure 4.17). *Col4a1* was significantly upregulated in the UUO model and the *Col8a1* gene level was increased in all analyzed models up to 32-fold. *Col10a1* gene expression was not significantly altered.

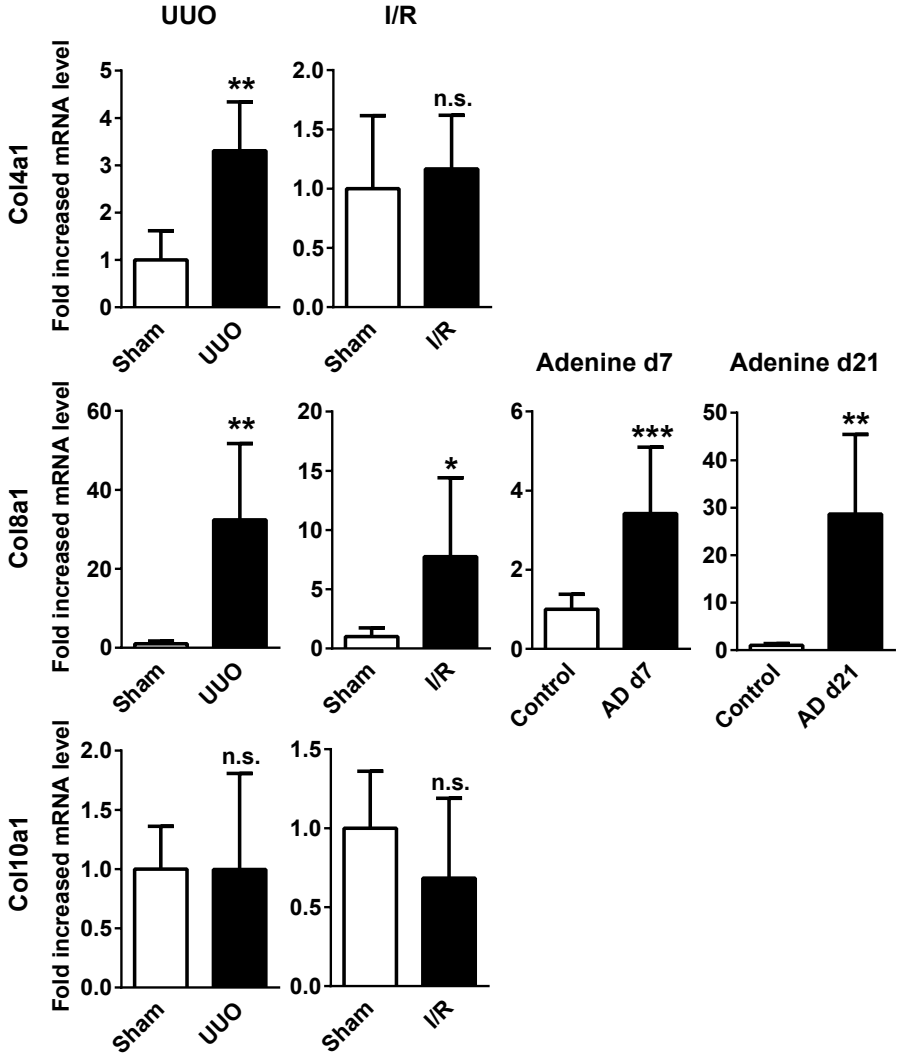

FIGURE 4.17: **Gene expression levels in different renal fibrosis models of the network forming collagens *Col4a1, Col8a1, Col10a1.*** *Col4a1* was significantly upregulated in the UUO model in comparison to untreated control animals. *Col8a1* was significantly upregulated in the UUO, I/R, adenine day 7 and day 21 model. *Col10a1* was not regulated in the UUO and I/R model. *: $p < 0.05$ **: $p < 0.01$, ***: $p < 0.001$, n.s.: not significant. $n(sham_{UUO}) = 5$, $n(UUO) = 5$; $n(sham_{I/R}) = 5$, $n(I/R) = 5$; $n(control_{AD\ d7}) = 7$, $n(AD\ d7) = 8$; $n(control_{AD\ d21}) = 7$, $n(AD\ d21) = 8$.

The collagen VIII protein level was further examined by western blot (Figure 4.18). Four bands could be detected, the band corresponding to a protein size of 235 kDa represents the trimeric form of the protein, the 140 kDa band the dimeric form and the 73 kDa band the monomeric form (Sherratt et al., 2004). The band corresponding to a protein mass of 50 kDa corresponds to a proteolytic form of collagen VIII (Kapoor et al., 1988). It could be shown that the alpha chain (73 kDa) as well as the dimeric and trimeric form were mostly upregulated. The dimeric form, 140 kDa could not be detected in the adenine day 21 model. The trimeric form was significantly increased up to 2.2-fold in the UUO, I/R, and adenine day 21 model. The level of the dimeric form was increased in the UUO and I/R model up to 3-fold. The monomeric form was increased up to 4.2-fold in the UUO, I/R, and adenine day 7 model. The 50 kDa proteolytic form was significantly decreased up to 79 % in the I/R and adenine day 21 model (one sample had to be excluded due to artifacts while developing).
The immunohistochemical staining (Figure 4.19) confirmed the western blot results. In the renal cortex the collagen VIII positive area was significantly increased in all fibrosis models except adenine day 7. The UUO model showed up to an 8-fold increase in percentage of collagen VIII positive area. In the medulla, collagen VIII positive area was increased in the I/R and adenine day 21 model up to 11-fold. In healthy kidneys, there was hardly any staining in the cortex. In the medulla, staining was mainly localized around the loop of henle. There was a strong staining around the vessels (not shown here).

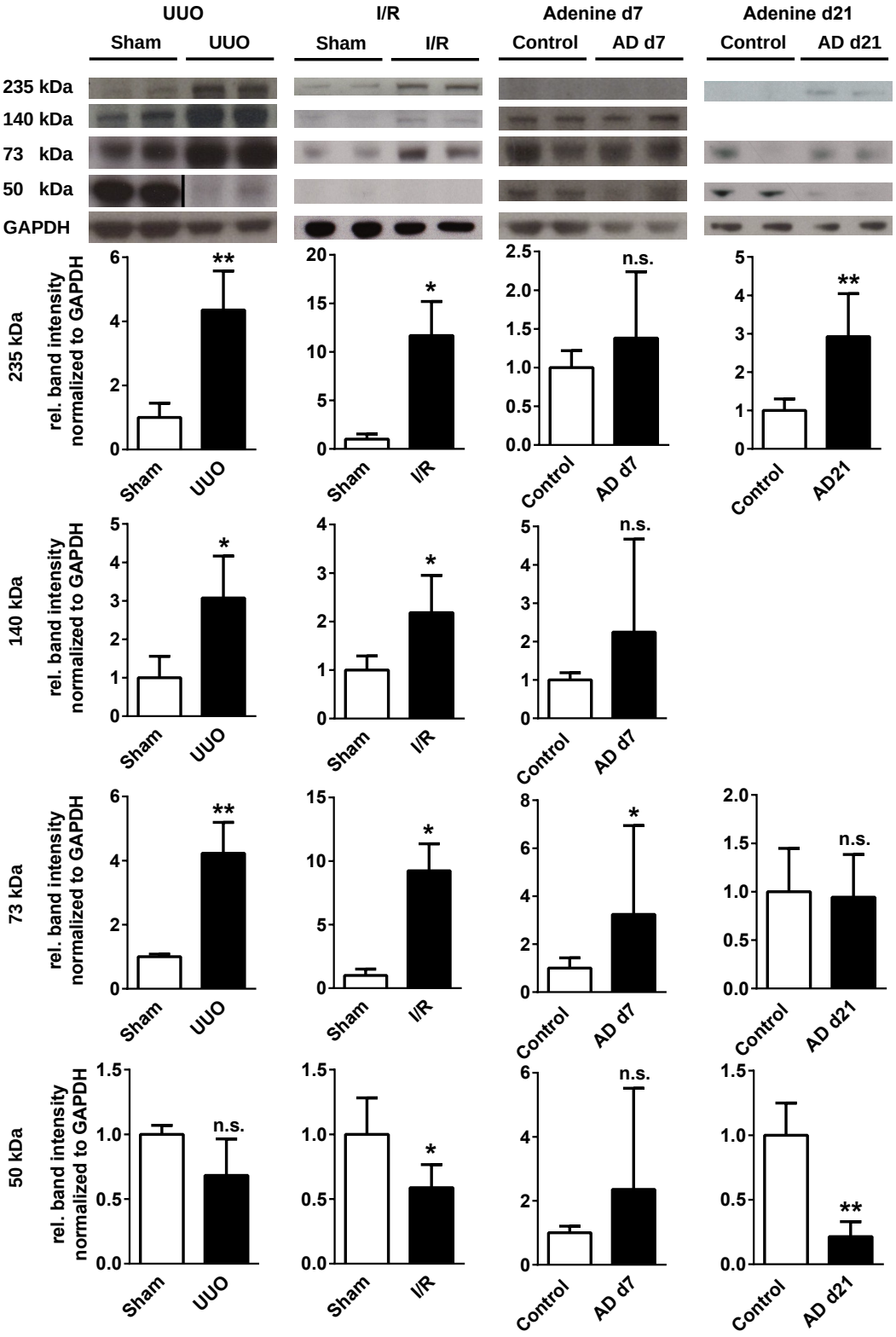

FIGURE 4.18: **Collagen VIII expression in renal fibrosis models in mice.** Four bands were detected: 235, 140, 73 and 50 kDa. The 235 kDa form of collagen VIII was significantly upregulated in the UUO, I/R and adenine day 21 model in comparison to untreated control animals. The dimeric 140 kDa form was upregulated in the UUO and I/R model and could not be detected in the adenine day 21. The 73 kDa monomer was upregulated in all models except for the adenine day 21 model. The proteolytic 50 kDa fragment was downregulated in all models except for the adenine day 7 model. *: $p < 0.05$ **: $p < 0.01$, n.s.: not significant; $n(\text{sham}_{\text{UUO}}) = 4$, $n(\text{UUO}) = 6$; $n(\text{sham}_{\text{I/R}}) = 4$, $n(\text{I/R}) = 4$; $n(\text{control}_{\text{AD d7}}) = 5$, $n(\text{AD d7}) = 8$; $n(\text{control}_{\text{AD d21}}) = 5$, $n(\text{AD d21}) = 8$.

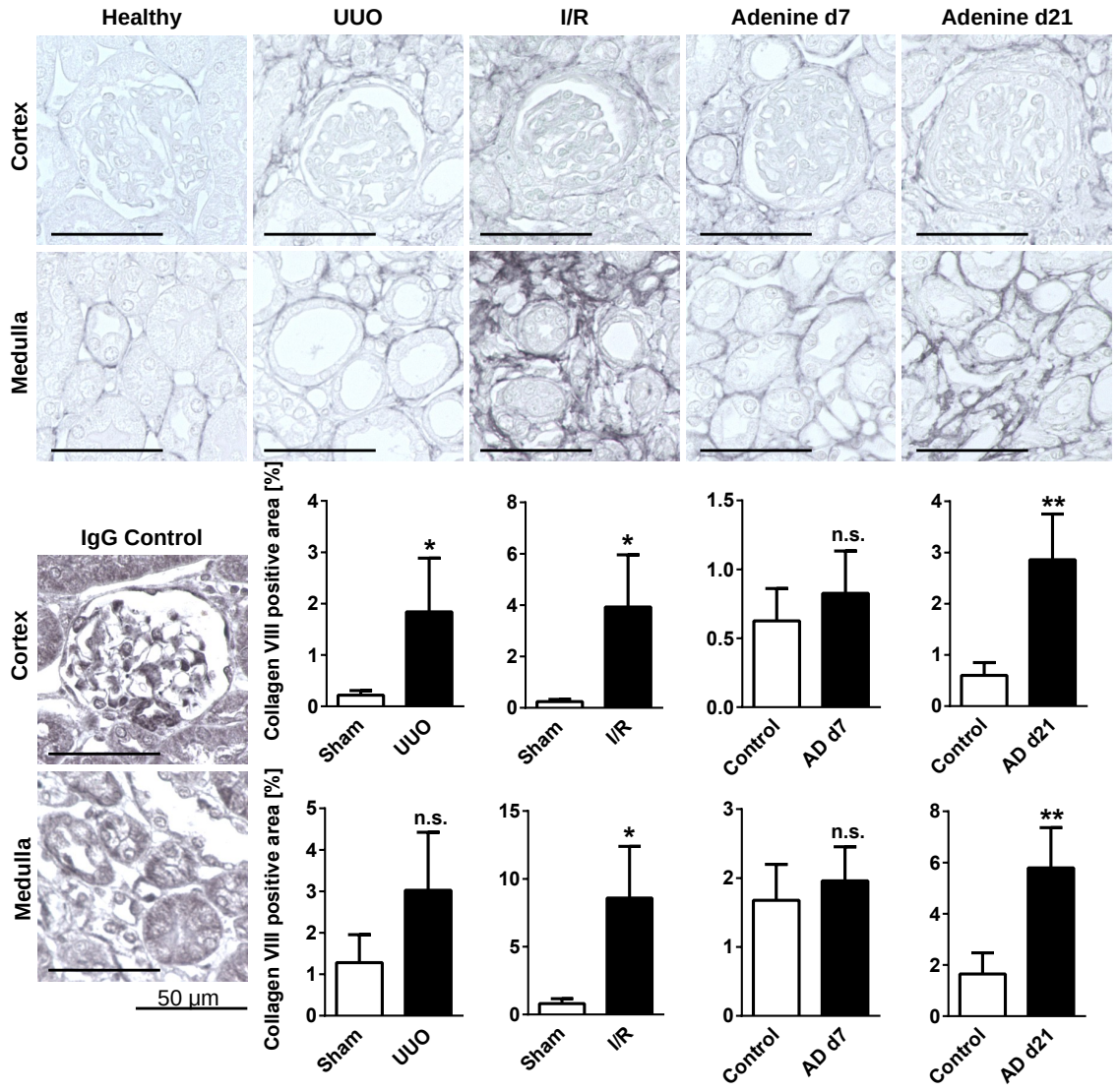

FIGURE 4.19: **Expression of collagen VIII in immunohistochemistry staining in renal fibrosis models in the cortex and medulla of mouse kidneys.** Quantification of collagen VIII positive area showed a significant increase of collagen VIII in the cortex in all models except for adenine day 7 in comparison to untreated control animals. In the medulla collagen VIII was significantly upregulated in the I/R and adenine day 21 model. *: $p < 0.05$, **: $p < 0.01$, n.s.: not significant. Nuclear staining with methyl green. Nonspecific IgG used as control. Scale bare: 50 µm. $n(\text{sham}_{\text{UUO}}) = 4$, $n(\text{UUO}) = 6$; $n(\text{sham}_{\text{I/R}}) = 4$, $n(\text{I/R}) = 4$; $n(\text{cotnrol}_{\text{AD d7}}) = 6$, $n(\text{AD d7}) = 7$; $n(\text{control}_{\text{AD d21}}) = 5$, $n(\text{AD d21}) = 7$.

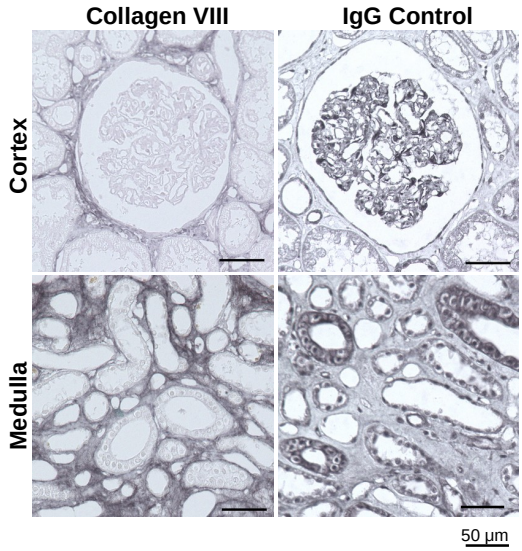

FIGURE 4.20: **Immunohistochemistry staining of collagen VIII expression in the cortex and medulla of healthy human kidneys.** Collagen VIII was expressed in the intersitium, around vessels and discretely aournd the GBM. Nuclear staining with methyl green. Non-specific IgG used as control. Scale bare: 50 µm.

4.5 Transmembrane collagens

In line with the results of the database search, the gene expression of transmembrane collagens was hardly regulated (Figure 4.1). While, as shown in Figure 4.21, *Col13a1* and *Col23a1* were not significantly regulated in any model, *Col17a1* expression was increased up to 5.6-fold, in the UUO, adenine day 7 and day 21 model. *Col25a1* was significantly decreased by 60 % in the UUO model. While no changes in the expression of *Col23* were seen in RT-qPCR, a significant reduction, up to 89 %, of collagen XXIII (52 kDa) could be observed in western blot (Figure 4.22). A second band, with a molecular size of 37 kDa was detected. This corresponds to the size of a predicted splice variant of collagen XXIII, which was significantly increased, up to 3.8-fold, in the I/R and adenine day 21 model compared to healthy kidneys.

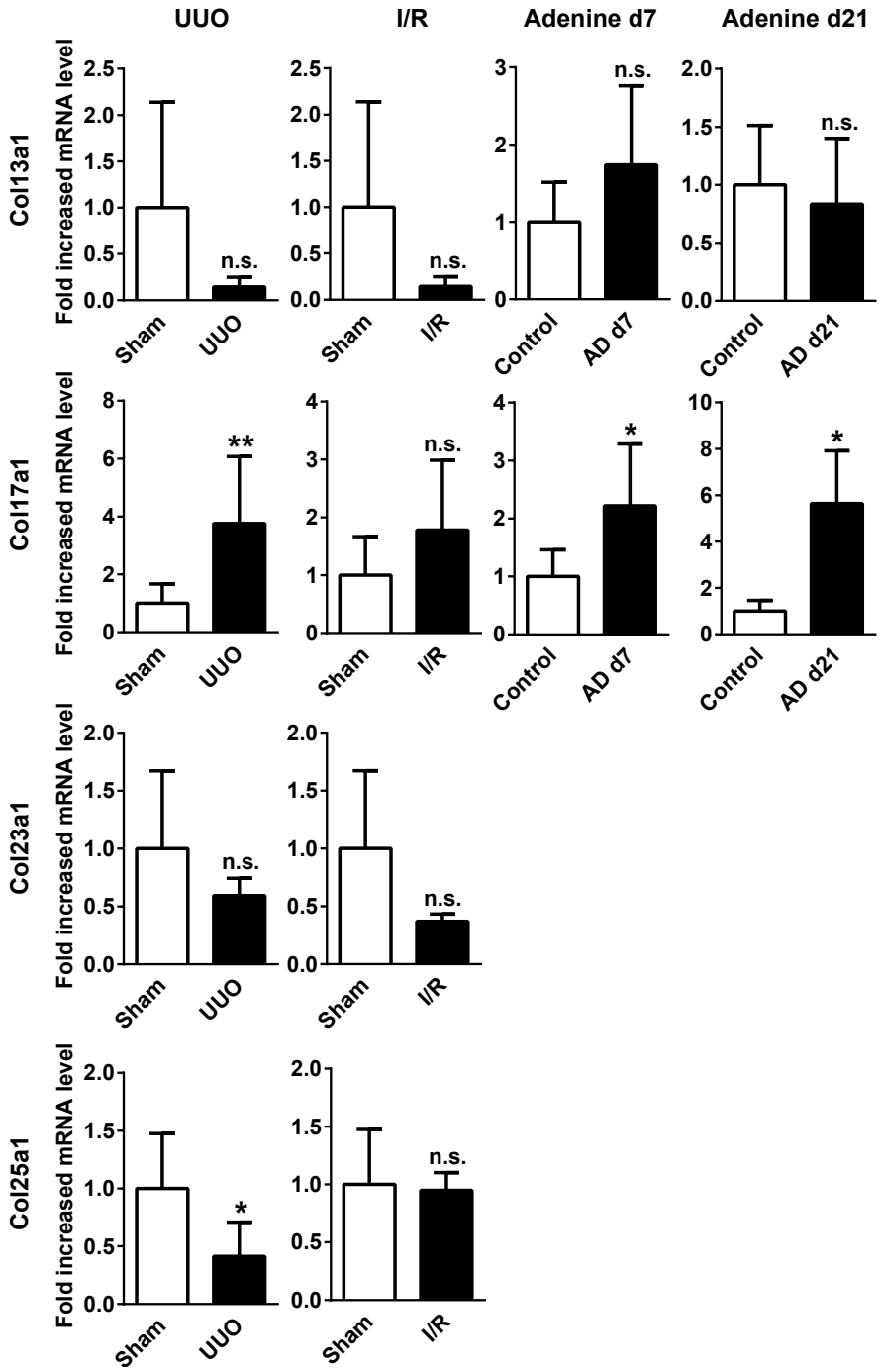

FIGURE 4.21: **Gene expression levels in different renal fibrosis models of the transmembrane collagens *Col13a1, Col17a1, Col23a1* and *Col25a1* in mice.** *Col13a1* and *Col23a1* were not significantly regulated in comparison to untreated control animals. *Col17a1* was significantly upregulated in the UUO, adenine day 7 and day 21 model. *Col25a1* was significantly upregulated in the UUO model. *: $p < 0.05$ **: $p < 0.01$, ***: $p < 0.001$, n.s.: not significant. $n(\text{sham}_{\text{UUO}}) = 5$, $n(\text{UUO}) = 5$; $n(\text{sham}_{\text{I/R}}) = 5$, $n(\text{I/R}) = 5$; $n(\text{control}_{\text{AD d7}}) = 7$, $n(\text{AD d7}) = 8$; $n(\text{control}_{\text{AD d21}}) = 7$, $n(\text{AD d21}) = 8$.

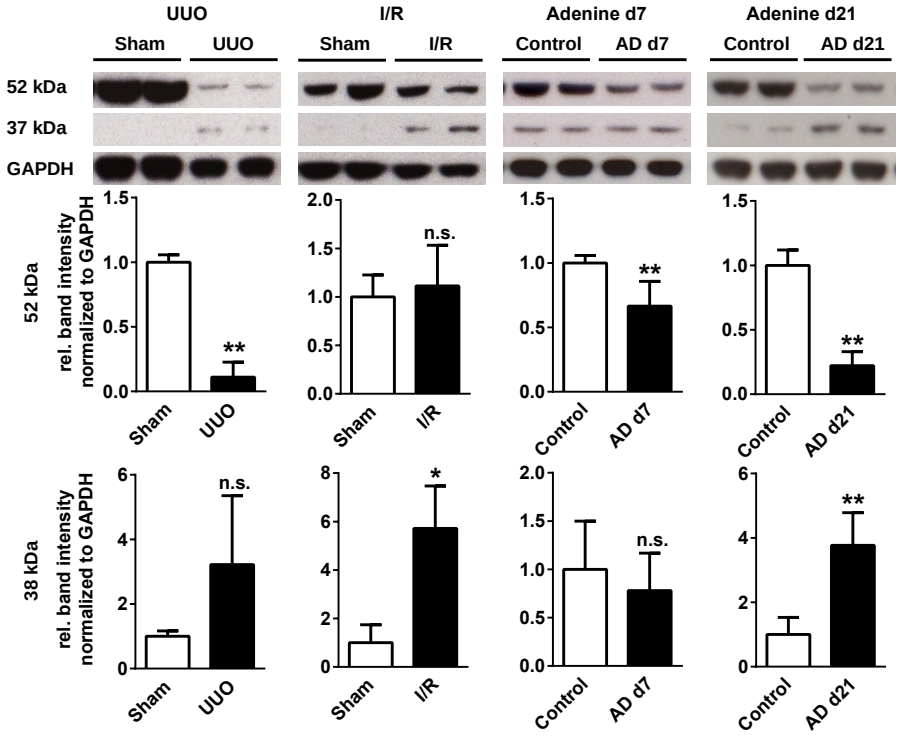

FIGURE 4.22: **Collagen XXIII expression in renal fibrosis models in mice.**. Two bands corresponding to the molecular weight of 52 kDa and 37 kDa were detected. The 52 kDa form of collagen XXIII was significantly downregulated in the UUO, adenine day 7 and day 21 model in comparison to untreated control animals. The 37 kDa splice variant was upregulated in the I/R and adenine day 21 model. *: $p < 0.05$ **: $p < 0.01$, n.s.: not significant; $n(\text{sham}_{\text{UUO}}) = 4$, $n(\text{UUO}) = 6$; $n(\text{sham}_{\text{I/R}}) = 4$, $n(\text{I/R}) = 4$; $n(\text{control}_{\text{AD d7}}) = 5$, $n(\text{AD d7}) = 8$; $n(\text{control}_{\text{AD d21}}) = 5$, $n(\text{AD d21}) = 8$.

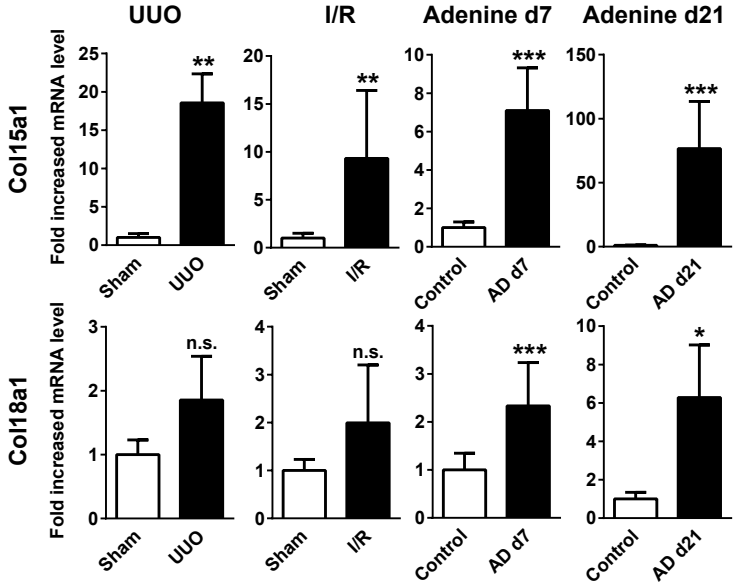

FIGURE 4.23: **Gene expression levels in different renal fibrosis models of the multiplexins *Col15a1* and *Col18a1*.** *Col15a1* was significantly upregulated in the UUO, I/R, adenine day 7 and day 21 model in comparison to untreated control animals. *Col18a1* was significantly upregulated in the adenine day 7 and day 21 model. **: $p < 0.01$, ***: $p < 0.001$, n.s.: not significant. $n(\text{sham}_{\text{UUO}}) = 5$, $n(\text{UUO}) = 5$; $n(\text{sham}_{\text{I/R}}) = 5$, $n(\text{I/R}) = 5$; $n(\text{control}_{\text{AD d7}}) = 7$, $n(\text{AD d7}) = 8$; $n(\text{control}_{\text{AD d21}}) = 7$, $n(\text{AD d21}) = 8$.

4.6 Multiplexins and other collagens

4.6.1 Multiplexins

The gene expression level of *Col15a1* was significantly increased up to 76-fold in all analyzed models (Figure 4.23). *Col18a1* showed a significant upregulation up to 6.3-fold, in the adenine day 7 and day 21 model.

4.6.2 Other collagens

The gene expression levels of *Col6a1* and *Col7a1* were further analyzed as examples for other collagens. As shown in Figure 4.24, *Col6a1* was significantly upregulated up to 24-fold in all analyzed models. *Col7a1* gene expression level was significantly increased up to 17-fold in the UUO, adenine day 7 and day 21 model. The changes in collagen VI protein level were analyzed further (Figure 4.25). The protein level of collagen VI was significantly increased in all analyzed models. The protein amount was increased up to 5.2-fold in the I/R model.
In a second step, the expression of collagen VI was analyzed with immunohistochemistry stainings (Figure 4.26). In the medulla, the amount of collagen VI was significantly increased in all models except for the UUO model. In the I/R model, there was a 4.7-fold increase in percentage of collagen VI positive area. In the cortex, the collagen VI positive area was only significantly augmented up to 2.3-fold in the adenine day 7 and day 21 model. The immunohistochemistry staining of collagen VI in human kidneys (Figure 4.27) showed a similar expression pattern as in murine kidneys. The nonspecific IgG used as control shows an unspecific nuclear staining, which was not observed in the collagen VI staining. A staining in the mesangium of the glomeruli and the interstitium could not be observed, therefore the collagen VI staining in human kidneys can be considered specific.

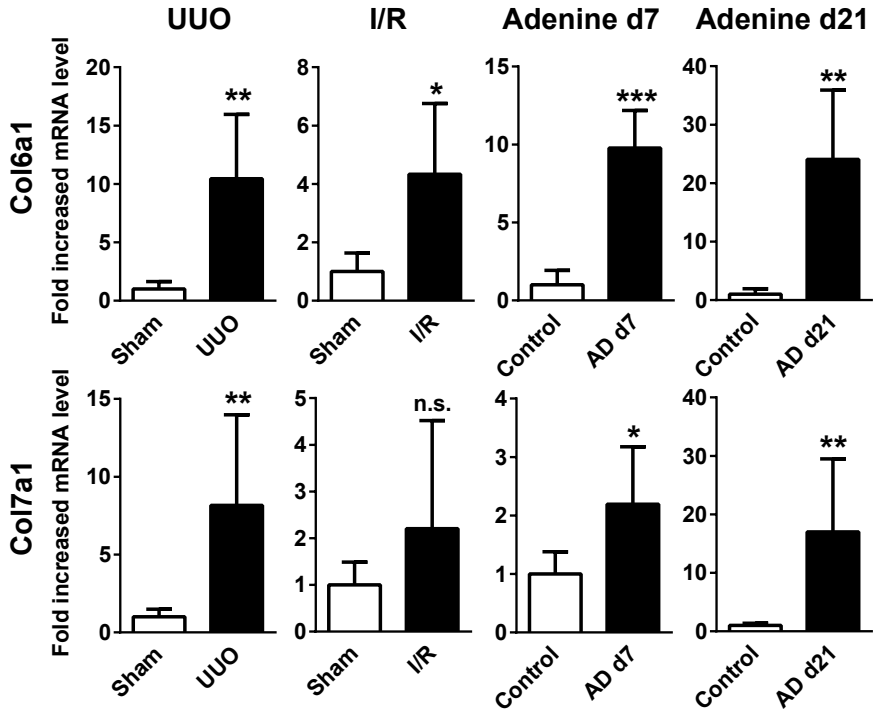

FIGURE 4.24: **Gene expression levels in different renal fibrosis models of other exemplary collagens *Col6a1* and *Col7a1*.** *Col6a1* was upregulated in the UUO, I/R, adenine day 7 and day 21 model in comparison to untreated control animals. *Col7a1* showed a significant higher expression in all analyzed models, except for I/R. *: $p < 0.05$ **: $p < 0.01$, ***: $p < 0.001$, n.s.: not significant. $n(\text{sham}_{\text{UUO}}) = 5$, $n(\text{UUO}) = 5$; $n(\text{sham}_{\text{I/R}}) = 5$, $n(\text{I/R}) = 5$; $n(\text{control}_{\text{AD d7}}) = 7$, $n(\text{AD d7}) = 8$; $n(\text{control}_{\text{AD d21}}) = 7$, $n(\text{AD d21}) = 8$.

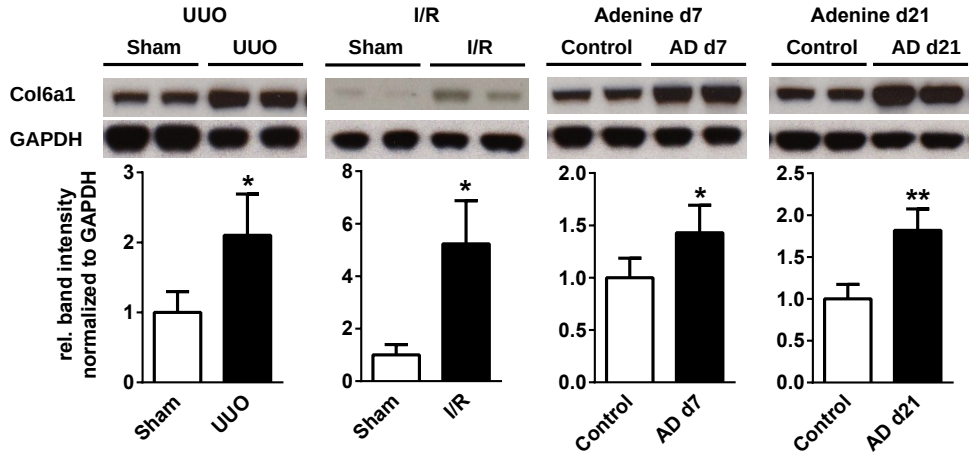

FIGURE 4.25: **Collagen VI expression in renal fibrosis models in mice.** Collagen VI was upregulated in the UUO, I/R, adenine day 7 and day 21 model in comparison to untreated control animals. *: $p < 0.05$ **: $p < 0.01$; $n(\text{sham}_{\text{UUO}}) = 4$, $n(\text{UUO}) = 6$; $n(\text{sham}_{\text{I/R}}) = 4$, $n(\text{I/R}) = 4$; $n(\text{control}_{\text{AD d7}}) = 5$, $n(\text{AD d7}) = 8$; $n(\text{control}_{\text{AD d21}}) = 5$, $n(\text{AD d21}) = 8$.

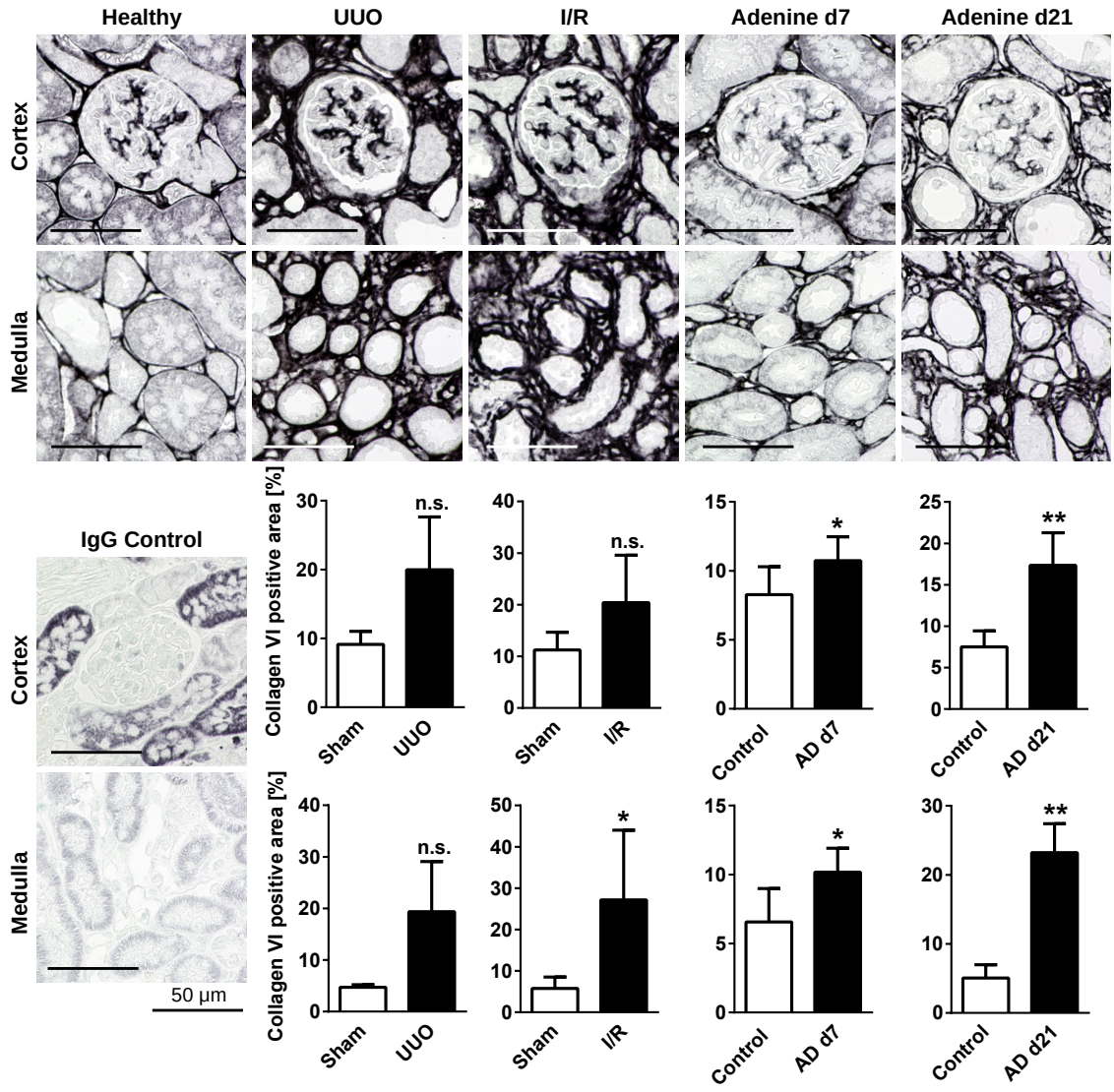

FIGURE 4.26: **Expression of collagen VI in immunohistochemistry staining in renal fibrosis models in the cortex and medulla of mouse kidneys.** Quantification of collagen VI positive area showed a significant increase of collagen VI in the medulla of the I/R, adenine day 7 and day 21 model in comparison to untreated control animals. Collagen VI positive area was significantly higher in the cortex in the adenine day 7 and day 21 model. *: $p < 0.05$, **: $p < 0.01$, n.s.: not significant. Nuclear staining with methyl green. Nonspecific IgG used as control. Scale bare: 50 µm. $n(\text{sham}_{UUO}) = 3$, $n(UUO) = 5$; $n(\text{sham}_{I/R}) = 4$, $n(I/R) = 4$; $n(\text{sham}_{AD7}) = 5$, $n(AD7) = 8$; $n(\text{sham}_{AD21}) = 5$, $n(AD21) = 7$.

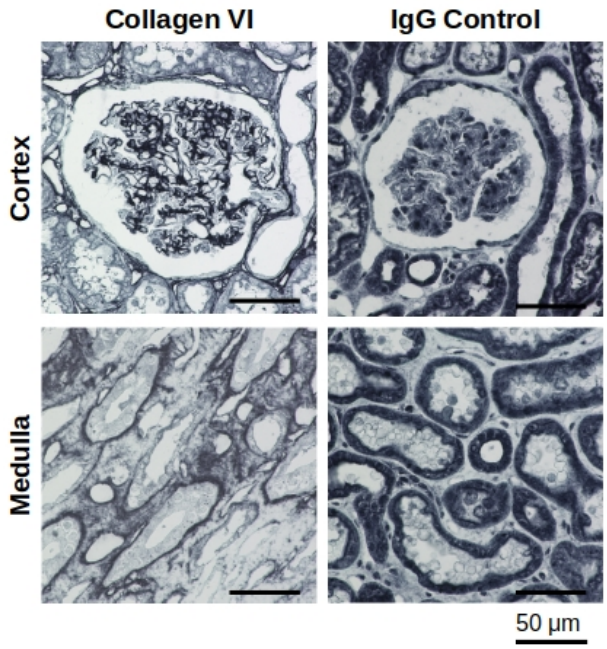

FIGURE 4.27: **Immunohistochemistry staining of collagen VI expression in the cortex and medulla of healthy human kidneys.** In humans, collagen VI was expressed in the glomerular mesangium, as well was in the interstitium. Nuclear staining with methyl green. Nonspecific IgG used as control. Scale bare: 50 µm.

Chapter 5
Discussion

5.1 Fibrillar collagens and collagen V

Renal fibrosis is defined as the excessive deposition of ECM, particularly of the fibrillar collagens (Zeisberg & Neilson, 2010). The increase of fibrillar collagens such as collagen I and III in chronic kidney disease is considered a marker for fibrosis (Boor et al., 2010, Ricard-Blum et al., 2018, Farris & Colvin, 2012). The analyzed arrays as well as in RT-qPCR and western blot showed an increased collagen I and III expression in murine renal fibrosis models. This fits well with already published results (Kuncio et al., 1991; Soylemezoglu et al., 1997). The immunohistochemical staining showed that the accumulation of collagen III is predominantly located in the tubulointerstitium, a key feature of tubulointerstitial fibrosis (Kuncio et al., 1991). Urinary and serum type III collagens are markers of renal fibrosis (Soylemezoglu et al., 1997; Papasotiriou et al., 2015). In IgA-nephropathy, the turnover of type III collagens reflects the disease severity (Genovese et al., 2016).
In murine kidney fibrosis models, collagen V gene expression and the amount of protein was increased. Vleming et al., 1994 were able to show that in human fibrosis the increased collagen V is best correlated with the strength of histopathological changes in human fibrotic kidneys. However, in this work it was shown that collagen III is significantly elevated in both western blot and immunohistochemical staining already in the adenine day 7 model, which was not the case for collagen V. Thus, collagen III seems to be an earlier indicator of fibrosis than collagen V. Collagen V is upregulated in diffuse and nodular diabetic glomerulosclerosis in the GBM and the mesangium of humans (Nerlich et al., 1994; Mason & Wahab, 2003). The immunohistochemistry staining showed a staining pattern similar to already published data. Martinez-Hernandez et al., 1982 show that in rat kidneys, immunolabeled anti-type V collagen is positive on the stromal surface of some vascular basement membranes. Collagen V is present on the basement membrane of peritubular capillaries whereas all tubular basement membranes and Bowman's capsule do not express collagen V. In Alport mice, collagen V is present in the GBM of the glomerulus, whereas in healthy kidneys collagen V is restricted to the mesangium and the subendothelial aspect of the GBM (Kashtan & Kim, 1992).

As described in 1.2.2, collagen V is responsible for the regulation of fibril association and thickness, explaining the co-staining of collagen I and V. Since there is not only an increase of collagen in fibrotic kidneys but also a change in collagen organization, it would be interesting to investigate whether collagen V, through its upregulation, influences the organization of the classical fibrillar collagen I and III. Especially since TGF-β_1, a profibrotic factor, upregulates the transcription of *Col5a2* and inhibits its removal in rat tubular epithelial cells (NRK 52E), as Bertelli et al., 2002 showed.

5.2 FACIT-like collagens: collagen XVI and XIX

Both the array data and the RT-qPCR suggested an upregulation of *Col12a1* and *Col14a1* (more clearly for *Col14a1*). A more detailed investigation of the role of these collagens in fibrosis has not yet been performed (Karsdal, 2016). Tzortzaki et al., 2003 show that collagen XII and XIV were significantly elevated at different time points during bleomycin-induced pulmonary fibrosis.

5.2.1 Collagen XVI

In the murine renal fibrosis models, it was shown that both gene expression and protein level of collagen XVI were increased, especially the variant without the N-terminal globular NC11 domain. The NC11 domain, which can be cleaved by metalloproteases, has a biological effect itself. The approximately 35 kDa sized NC11 domain could not be detected in the western blot, but the significant increase of collagen XVI without the NC11 domain could indicate an increase of the free, biologically active NC11 domain. Bedal, 2015 showed that *NC11* overexpression leads to an induction of VEGFR (vascular endothelial growth factor receptor) 1 and 2 in oral squamous carcinoma cell. This raises the question of whether this is also the case in the kidney, since an important feature of CKD is the rarefaction of capillaries. This rarefaction is caused by an imbalance between pro-angiogenic components, such as VEGF, the ligand of VEGFR, and inhibitors of angiogenesis (Zoccali et al., 2017).
Akagi et al., 1999 show that the expression of collagen XVI in human skin fibroblast is elevated in localized and systemic scleroderma. This suggests that collagen XVI may play a role in the development of fibrosis, although this has not been investigated in more detail yet. Collagen XVI expression is also upregulated in intestinal subepithelial myofibroblasts (ISEMFs) from Crohn's disease

tissue. *In vitro*, collagen XVI promotes cell spreading, formation, and maturation of focal adhesion contacts on ISEMFs, which themselves are known to produce and deposit collagen I, III, IV, and V (Ratzinger et al., 2010). Ratzinger et al., 2010 assume that collagen XVI may contribute to sustaining the fibrotic response in Crohn's disease by stabilizing ISEMFs and thereby promoting their persistence in the intestinal tract. Serum Pro-C16 is elevated in patients with ulcerative colitis (Jensen et al., 2018). The expression of collagen XVI in the kidney and possible changes in expression in renal fibrosis have not been investigated yet.

5.2.2 Collagen XIX

For collagen XIX, it could be shown that the gene expression was reduced in the UUO fibrosis model. In kidneys, Oudart et al., 2013 could detect three bands (70, 50, and 45 kDa) in western blot, corresponding to proteolytic products of collagen XIX. The proteolytic products with a molecular size of 50 and 40 kDa could be detected with the antibody used in this work. It could be shown that collagen XIX and the level of proteolytic products were lowered in most models. Since no data on collagen XIX in fibrosis models is available, an interpretation of these results is difficult to make.
Oudart et al., 2017 showed that the short NC1(XIX) C-terminal domain inhibits the migration and invasion of melanoma cells. It also exerts a strong anti-angiogenic effect by inhibiting MMP-14 and VEGF expression. The role of the other proteolytic products of collagen XIX is unknown, not only in fibrosis models.
The collagen XIX staining pattern near the macula densa, seems very interesting, especially considering that collagen XIX is important for neuromuscular transmission in the esophagus (Sumiyoshi et al., 2004). However, Myers et al., 1997 showed a different staining pattern. They observed collagen XIX staining in numerous basement membranes and the glomerular mesangium but it was absent in the GBM. Additionally, they showed that collagen XIX colocalizes with collagen IV and XV in the Bowman's capsule and all vascular basement membranes. It also could be stained in the tubular basement membrane. Collagen XIX seemed to be associated with types IV, XV, and XVIII collagens (Myers et al., 1997). A clear explanation for the difference is currently unclear, potentiall reason could be the different antibodies and tissues (with different fixations) that were used.

5.3 Network forming collagens and collagen VIII

The function of collagen IV in the development and maintenance of renal fibrosis has been extensively studied, since, among other things, the absence of collagen IV is responsible for Alport syndrome (confer Section B.2) (Rheault et al., 2004; Cosgrove et al., 1996; Chen & Miner, 2012). Accordingly, it will not be discussed in detail in this work.

In healthy kidneys, all arteries and arterioles express collagen VIII. It is not expressed in the kidney interstitium (Kittelberger et al., 1990). *Col8a1* is expressed in the rat renal cortex and cultured glomerular mesangial, epithelial, and endothelial cells. It is a normal constituent of the rat glomerulus as well as large intrarenal arteries (Rosenblum et al., 1993). The pattern of the immunohistochemistry staining performed for this thesis fitted very well to these results, even if a very discrete staining was measurable in the interstitium of healthy kidneys.

Collagen VIII is elevated in diseases associated with angiogenesis and vascular remodeling (Larsen et al., 2016). It does not only play an important role in myocardial remodeling as displayed in Section 1.2.2 but also seems to be involved in the development of renal fibrosis. In renal cells of diabetic mice and kidneys of patients with diabetic nephropathy, the expression of collagen VIII is enhanced (Loeffler et al., 2012; Gerth et al., 2007). In line with these results, the analyzed murine renal fibrosis models showed an increase in both gene expression and protein levels at a late stage.

When collagen VIII is incubated with pepsin, it forms pepsin-resistant fragments, which have a molecular size of 50 kDa (Kapoor et al., 1988). This fragment has been detected by the antibody used in this thesis. Interestingly, it is downregulated in the I/R and adenine day 21 model and has not been yet described in the kidney.

TGF-β1 is a major cytokine in diabetic nephropathy. In cell culture, collagen VIII significantly modulates the effect of TGF-β1 on mesangial cells and may, therefore, play a role in the pathogenesis of diabetic nephropathy (Loeffler et al., 2011). This observation could be confirmed in the animal model. Diabetic Col8α1/α2 knockout mice have a milder phenotype than their wild-type counterparts (Hopfer et al., 2009; Loeffler et al., 2012). Loeffler et al., 2012 postulate, that collagen VIII could be one of the major inducers of EMT-like changes in kidneys of diabetic wild-type mice. It would be very interesting to see if collagen VIII has a similar functional role in the investigated fibrosis models.

5.4 Transmembrane collagens

The analysis of gene expression of transmembrane collagens showed that *Col17a1* was significantly increased in all fibrosis models. Collagen XVII is described by Hurskainen et al., 2012 as a component of the glomerular filtration barrier. Knockout mice not only show the already known skin disease pattern of epidermolysis bullosa but also an increased glomerular amount in the cortex and effacement of podocyte foot processes. *Col25a1*, significantly reduced in the UUO model, has not been described in the kidney yet but mostly in the brain (Karsdal, 2016). The results of the Geo2R array analysis as well as the results of Pavkovic et al., 2019 underlined that collagen XXV is probably also expressed in the kidney, to a low level, and that, at least in the UUO model, the *Col25a1* gene expression is lowered.

5.4.1 Collagen XXIII

In the RT-qPCR, no regulation of collagen XXIII was shown. In both adenine time points *Col23a1* could not be detected, which indicates a very low gene expression, as already published by Koch et al., 2006. For protein analysis, Koch et al., 2006 detected only the 68 kDa full-length form in the kidney, while the antibody used here detected the 52 kDa form (splice form COL23A1-201 in the human protein atlas). Veit et al., 2007 detected a full-length form and a smaller shedded form. The protein detected here could correspond to the shedded form of collagen XXIII, but exact molecular masses were not indicated in the publication. The 52 kDa form of collagen XXIII was reduced in all analyzed models. The splice variant COL23A1-202 (Human Protein Atlas) with a protein size of 37 kDa was elevated. This variant has not yet been described in the kidney.
The role of collagen XXIII in the kidney remains completely unclear. Le Roux et al., 2010 showed that antibodies against collagen XXIII in patients sera are a specific biomarker for transplant glomerulopathy biomarkers versus interstitial fibrosis/tubular atrophy.

5.5 Multiplexins and other collagens

5.5.1 Multiplexins and collagen VII

The role of multiplexins is already well described in the literature. Collagen XV is expressed in the kidney and accumulates in fibrotic kidneys, where it is also functionally involved in the development and maintenance of kidney fibrosis (Hagg et al., 1997). For example, Zaferani et al., 2014 described that collagen XV and XVIII influence leukocyte influx in renal I/R. The influence of endostatin, a fragment of collagen XVIII, in the development of renal fibrosis has already been described in detail (refer reviews of Heljasvaara et al., 2017; Karsdal et al., 2017). The significant increase of gene expression of *Col15a1* in all and *Col18a1* in most murine renal fibrosis models fits well with these results.
Muda et al., 2001 show that collagen VII is expressed *de novo* in human glomerular sclerosis in areas of glomerular and tubular scarring. This goes well with the significant upregulation of *Col7a1* in the analyzed murine fibrosis model.

5.5.2 Collagen VI

Collagen VI is one of the most abundant proteins in the glomerular ECM (Hobeika et al., 2017; Fenton et al., 2017). It is also located in the renal vasculature, especially in the adventitia (Stribos et al., 2017). In healthy human kidneys, the α1α2α3-form of collagen VI is expressed on the endothelial side of the GBM, in the mesangial matrix and the interstitium (Zhu et al., 1994). This staining pattern could also be observed in immunohistochemical staining in healthy human kidney. A similar staining pattern was observed in murine kidneys. Gara et al., 2011 have analyzed the distribution of the different collagen 6 α-chains in more detail. In adult mouse kidney, the α3 chain is widely distributed in the cortical and medullar region. The α4 and α5 chains are restricted to the glomeruli, where they are associated with the basement membrane. The collagen VI α6 chain is absent in the cortical region and glomeruli. The α3 and α5 chains are expressed in the adult kidney capsule, whereas the α4 and α6 chains are only weakly expressed.
The increased gene expression and protein levels observed in murine kidney fibrosis models are consistent with the results of previous publications. Nerlich et al., 1994 show that collagen VI is increased in diabetic nephropathy. In the late stage of diabetic glomerulopathy, collagen VI forms a main part of the

Kimmelstiel-Wilson lesions and is a marker for nodular glomerulosclerosis. Intraglomerular mesangial and epithelial cells do overexpress *COL6A1* and contribute to glomerulosclerosis (Razzaque et al., 2015). The increased collagen VI staining in the renal fibrotic interstitium is concomitant with an increased appearance of myofibroblasts, the likely cellular source of collagen VI (Mak et al., 2014). Similar to collagen V, collagen VI is upregulated in the GBM of Alport mice (Kashtan & Kim, 1992) and IgG4-related kidney disease, where it is predominantly localized in the cortex and perivascular (Hara et al., 2016). Wu et al., 2001 showed that in idiopathic membranous nephropathy the accumulation of collagen VI in the interstitium is one of the most important prognostic factors.
Higher levels of serum endotrophin, a fragment of collagen VI, are associated with an increased risk of progression to end-stage renal disease and an increased mortality in CKD (Fenton et al., 2017). The serum level of endotrophin correlates with the eGFR in renal transplant recipients (Stribos et al., 2017).
In conclusion, in murine fibrosis models, the fibrillar collagens strongly increase. Together with other proteins, they form the scar tissue of the fibrotic kidneys. The amount of most investigated collagens correlates positively with the development of fibrosis. This applies to collagen V, the FACITs (except collagen XIX), the network forming collagens, the multiplexins, as well as the other investigated collagens. The exception is collagen XXIII, which correlates negatively with the development of fibrosis. Further investigations are needed to analyze the role of such downregulated collagens in the kidney.

Chapter 6
Summary

In summary, a comprehensive analysis of collagen expression in fibrotic murine kidneys was performed. First, published, publicly available array data were analyzed using Geo2R, and the data provided by Pavkovic et al., 2019 were reanalyzed for collagens. A general trend towards upregulation of collagen in fibrosis was observed. Exceptions were *Col27a1* (fibril-regulating collagens), *Col19a1, Col20a1, Col22a1* (FACITs), *Col4a3, Col4a4,* and *Col4a5* (network forming collagens) and *Col23a1* (transmembrane collagen), whose expressions were either not regulated or significantly decreased.
In a second step, exemplary collagens from the different families (fibrillar collagens, FACITs, network-forming collagens, transmembrane collagens, multiplexins and other collagens) were analyzed in detail. In the analysis of fibrillar collagens it was shown, as previously published, that the mRNA expression and protein level of collagen I and III were significantly increased in all three investigated murine fibrosis models. Collagen V, a fibril regulating collagen, was significantly increased in the late stages of fibrosis. Fibril-associated collagens with interrupted triple helices (FACITs) were shown to have increased gene expression of *Col12a1, Col14a1*, and *Col16a1*. This could be confirmed for collagen XVI also on the protein level. Collagen XIX was downregulated in some fibrosis models.
Collagen VIII, the network forming collagen that was studied in detail, showed an increased mRNA expression and protein level in the late stages of the fibrosis models. Only one 50 kDa proteolytic fragment, which has not yet been described in the kidney, was significantly downregulated. The transmembrane collagens, except for *Col17a1,* did not show a clear regulation in the murine fibrosis models investigated. For collagen XXIII, the protein level was lowered in fibrotic kidneys. Also, a 37 kDa splice variant of the protein could be detected, which had not been described in the kidney before. The gene expression of the multiplexins *Col15a1* and *Col18a1* was increased. Collagen VI, a beaded-filament forming collagen, which was studied in detail, also showed an increased expression on both mRNA and protein level.
Taken together, a previously unavailable overview of the changes in collagens in renal fibrosis was given, which will serve as a basis for a further analysis of possible functions of these collagens in renal fibrosis.

Bibliography

Akagi, Atsushi, Shingo Tajima, Akira Ishibashi, Noriko Yamaguchi, and Yutaka Nagai (1999). "Expression of type XVI collagen in human skin fibroblasts: Enhanced expression in fibrotic skin diseases". In: *Journal of Investigative Dermatology* 113.2, pp. 246–250. ISSN: 0022202X. DOI: 10.1046/j.1523-1747.1999.00663.x.

Alberts, Bruce, Alexander Johnson, Julian Lewis, David Morgan, Martin Raff, Keith Roberts, and Peter Walter (2014). *Molecular Biology of the Cell*. New York, p. 1465. ISBN: 9780815344322. DOI: 10.1017/CBO9781107415324.004.

Avila-Casado, M. Carmen, Teresa I Frtoul, and Sumant S Chugh (2011). "HIV-Associated Nephropathy: Experimental Models". In: *Experimental Models for Renal Diseases: Pathogenesis and Diagnosis*. Ed. by GA Herrera. Karger. Vol. 169. Basel, pp. 270–285. DOI: 10.1159/000320212.

Banyard, Jacqueline, Lere Bao, and Bruce R. Zetter (2003). "Type XXIII collagen, a new transmembrane collagen identified in metastatic tumor cells". In: *Journal of Biological Chemistry* 278.23, pp. 20989–20994. ISSN: 00219258. DOI: 10.1074/jbc.M210616200.

Banyard, Jacqueline, Lere Bao, Matthias D. Hofer, David Zurakowski, Kristin A. Spivey, Adam S. Feldman, Lloyd M. Hutchinson, Rainer Kuefer, Mark A. Rubin, and Bruce R. Zetter (2007). "Collagen XXIII expression is associated with prostate cancer recurrence and distant metastases". In: *Clinical Cancer Research* 13.9, pp. 2634–2642. ISSN: 10780432. DOI: 10.1158/1078-0432.CCR-06-2163.

Baues, Maike, Barbara M. Klinkhammer, Josef Ehling, Felix Gremse, Marc A.M.J. van Zandvoort, Chris P.M. Reutelingsperger, Christoph Daniel, Kerstin Amann, Janka Bábíčková, Fabian Kiessling, Jürgen Floege, Twan Lammers, and Peter Boor (2020). "A collagen-binding protein enables molecular imaging of kidney fibrosis in vivo". In: *Kidney International* 97.3, pp. 609–614. ISSN: 15231755. DOI: 10.1016/j.kint.2019.08.029.

Bedal, Konstanze B. (2015). "Funktionelle Aspekte von Kollagen XVI und seiner NC11-Domäne bei der Progression des oralen Plattenepithelkarzinoms". PhD thesis, p. 144.

Benninghoff & Drenckhahn, Detlev (2008). *Taschenbuch Anatomie*. Ed. by Detlev Drenckhahn and Jens Waschke. 1st. München: Urban&Fischer, p. 624. ISBN: 978-3.437-41194-6.

Bertelli, Roberta, Frederico Valenti, Roberta Oleggini, Gianluca Caridi, Paola Altieri, Domenico A. Coviello, Gerardi Botti, Roberto Ravazzolo, and Gian Marco Ghiggeri (2002). "Cell-specific regulation of 1(III) and 2(V) collagen by TGF-1 in tubulointerstitial cell models". In: *Nephrology Dialysis Transplantation* 13.3, pp. 573–579. ISSN: 0931-0509. DOI: 10.1093/ndt/13.3.573.

Birk, David E. (2001). "Type V collagen: Heterotypic type I/V collagen interactions in the regulation of fibril assembly". In: *Micron* 32.3, pp. 223–237. ISSN: 09684328. DOI: 10.1016/S0968-4328(00)00043-3.

Birk, David E, John M Fitch, Joanne P Babiarz, Kathleen J Doane, and Thomas F Linsenmayer (1990). "Collagen fibrillogenesis in vitro: interaction of types I and V collagen regulates fibril diameter." In: *Journal of cell science* 95, pp. 649–57. ISSN: 0021-9533. DOI: 2384532.

Blenman, Kim RM., Byian Duan, Zhiwei Xu, Suigui Wan, Mark A. Atkinson, Terence R. Flotte, Byron P. Croker, and Laurence Morel (2006). "IL-10 regulation of lupus in the NZM2410 murine model". In: *Laboratory Investigation* 86.11, pp. 1136–1148. ISSN: 00236837. DOI: 10.1038/labinvest.3700468.

Boor, Peter and Jürgen Floege (2015). "Renal allograft fibrosis: Biology and therapeutic targets". In: *American Journal of Transplantation* 15.4, pp. 863–886. ISSN: 16006143. DOI: 10.1111/ajt.13180.

Boor, Peter, Tammo Ostendorf, and Jürgen Floege (2010). "Renal fibrosis: novel insights into mechanisms and therapeutic targets". In: *Nature Reviews Nephrology* 6.11, pp. 643–656. ISSN: 1759-5061. DOI: 10.1038/nrneph.2010.120.

Bowen, Jessica M, Glenda J Sobey, Nigel P Burrows, Marina Colombi, Mark E Lavallee, Fransiska Malfait, and Clair A Francomano (2017). "Ehlers – Danlos Syndrome , Classical Type". In: *American Journal of Medical Genetics Part C* Seminars i, pp. 1–13. DOI: 10.1002/ajmg.c.31548.

Breitkopf, Daniel Maximilian (2020). *Notch-3 and a novel YB-1 modification alter the pathophysiology and immune cell balance in systemic lupus erythematosus*. Aachen, pp. 1–90.

Breuls, R. G M, Darinka D. Klumpers, Vincent Everts, and Theo H. Smit (2009). "Collagen type V modulates fibroblast behavior dependent on substrate stiffness". In: *Biochemical and Biophysical Research Communications* 380.2, pp. 425–429. ISSN: 0006291X. DOI: 10.1016/j.bbrc.2009.01.110.

Buchtler, Simone, Alexandra Grill, Stefanie Hofmarksrichter, Petra Stöckert, Gabriela Schiechl-brachner, Manuel Rodriguez Gomez, Sophia Neumayer, Kathrin Schmidbauer, Yvonne Talke, Barbara M Klinkhammer, Peter Boor, Alexander Medvinsky, Kerstin Renner, Hayo Castrop, and Matthias Mack (2018). "Cellular Origin and Functional Relevance of Collagen I Production in the Kidney". In: *Journal of the American Society of Nephrology* 29.29, pp. 1–15. DOI: 10.1681/ASN.2018020138.

Bülow, Roman David and Peter Boor (2019). "Extracellular Matrix in Kidney Fibrosis: More Than Just a Scaffold". In: *Journal of Histochemistry and Cytochemistry* 67.9, pp. 643–661. ISSN: 15515044. DOI: 10.1369/0022155419849388.

Cescon, Matilde, Francesca Gattazzo, Peiwen Chen, and Paolo Bonaldo (2015). "Collagen VI at a glance". In: *Journal of Cell Science* 128.19, pp. 3525–3531. ISSN: 0021-9533. DOI: 10.1242/jcs.169748.

Chakravarti, Shukti, Terry Magnuson, Jonathan H. Lass, Karl J. Jepsen, Christian LaMantia, and Heidi Carroll (1998). "Lumican regulates collagen fibril assembly: Skin fragility and corneal opacity in the absence of lumican". In: *Journal of Cell Biology* 141.5, pp. 1277–1286. ISSN: 00219525. DOI: 10.1083/jcb.141.5.1277.

Charras, Guillaume and Erik Sahai (2014). "Physical influences of the extracellular environment on cell migration". In: *Nature Reviews Molecular Cell Biology* 15.12, pp. 813–824. ISSN: 14710080. DOI: 10.1038/nrm3897.

Chen, Ying Maggie and Jeffrey H Miner (2012). "Glomerular basement membrane and related glomerular disease." In: *Translational research : the journal of laboratory and clinical medicine* 160.4, pp. 291–7. ISSN: 1878-1810. DOI: 10.1016/j.trsl.2012.03.004. URL: http://www.sciencedirect.com/science/article/pii/S1931524412001259.

Chilian, William M., Patricia E. Shamhart, Dorothee Weihrauch, Ravi K. Adapala, Daniel J. Luther, J. Gary Meszaros, Cheryl Hodnichak, Paolo Bonaldo, and Charles K. Thodeti (2012). "Absence of Type VI Collagen Paradoxically Improves Cardiac Function, Structure, and Remodeling After Myocardial Infarction". In: *Circulation Research* 110.6, pp. 851–856. ISSN: 0009-7330. DOI: 10.1161/circresaha.111.252734.

Colombatti, Alfonso, Maria Teresa Mucignat, and Paul Bonaldo (1995). "Secretion and matrix assembly of recombinant type VI collagen". In: *Journal of Biological Chemistry* 270.22, pp. 13105–13111. ISSN: 00219258. DOI: 10.1074/jbc.270.22.13105.

Cosgrove, Dominic, Daniel T. Meehan, James A. Grunkemeyer, Jody M. Kornak, Robinlyn Sayers, William J. Hunter, and Gina C. Samuelson (1996). "Collagen COL4A3 knockout: A mouse model for autosomal Alport syndrome". In: *Genes and Development* 10.23, pp. 2981–2992. ISSN: 08909369. DOI: 10.1101/gad.10.23.2981.

Crowley, Steven D. and Thomas M. Coffman (2014). "The inextricable role of the kidney in hypertension". In: *Journal of Clinical Investigation* 124.6, pp. 2341–2347. ISSN: 15588238. DOI: 10.1172/JCI72274.

Cui, Xiangqin, Juling Zhou, Jing Qiu, Martin R. Johnson, and Michal Mrug (2009). "Validation of endogenous internal real-time PCR controls in renal tissues". In: *American Journal of Nephrology* 30.5, pp. 413–417. ISSN: 02508095. DOI: 10.1159/000235993.

Eble, Johannes A., Anja Kassner, Stephan Niland, Matthias Mörgelin, Joachim Grifka, and Susanne Grässel (2006). "Collagen XVI harbors an integrin $\alpha 1\beta 1$ recognition site in its C-terminal domains". In: *Journal of Biological Chemistry* 281.35, pp. 25745–25756. ISSN: 00219258. DOI: 10.1074/jbc.M509942200.

Farris, Alton B. and Robert B. Colvin (2012). "Renal interstitial fibrosis". In: *Current Opinion in Nephrology and Hypertension* 21.3, pp. 289–300. ISSN: 1062-4821. DOI: 10.1097/MNH.0b013e3283521cfa.

Fenton, Anthony, Mark D. Jesky, Charles J. Ferro, Jacob Sørensen, Morten A. Karsdal, Paul Cockwell, and Frederica Genovese (2017). "Serum endotrophin, a type VI collagen cleavage product, is associated with increased mortality in chronic kidney disease". In: *PLoS ONE* 12.4, pp. 1–14. ISSN: 19326203. DOI: 10.1371/journal.pone.0175200.

Fichard, Agnès, Jean Philippe Kleman, and Florence Ruggiero (1995). "Another look at collagen V and XI molecules". In: *Matrix Biology* 14.7, pp. 515–531. ISSN: 0945053X. DOI: 10.1016/S0945-053X(05)80001-0.

Fitzgerald, Jamie, Cathleen R, Fiona H. Zhou, and Uwe Hansen (2008). "Three novel collagen VI chains, alpha4(VI), alpha5(VI), and alpha6(VI)." In: *The Journal of biological chemistry* 283.29, pp. 20170–80. ISSN: 0021-9258. DOI: 10.1074/jbc.M710139200.

Frantz, Christian, Kathleen M. Stewart, and Valerie M. Weaver (2010). "The extracellular matrix at a glance". In: *Journal of Cell Science* 123.24, pp. 4195–4200. ISSN: 0021-9533. DOI: 10.1242/jcs.023820.

Franzke, Claus Werner, Peter Bruckner, and Leena Bruckner-Tuderman (2005). "Collagenous transmembrane proteins: Recent insights into biology and pathology". In: *Journal of Biological Chemistry* 280.6, pp. 4005–4008. ISSN: 00219258. DOI: 10.1074/jbc.R400034200.

Freitas, Eduarda Correa, Mayara Souza de Oliveira, and Odirlei André Monticielo (2017). "Pristane-induced lupus: considerations on this experimental model". In: *Clinical Rheumatology* 36.11, pp. 2403–2414. ISSN: 14349949. DOI: 10.1007/s10067-017-3811-6.

Gara, Sudheer Kumar, Paolo Grumati, Stefano Squarzoni, Patrizia Sabatelli, Anna Urciuolo, Paolo Bonaldo, Mats Paulsson, and Raimund Wagener (2011). "Differential and restricted expression of novel collagen VI chains in mouse". In: *Matrix Biology* 30.4, pp. 248–257. ISSN: 0945053X. DOI: 10.1016/j.matbio.2011.03.006.

Genovese, Federica, Alba A Manresa, Diana Leeming, Morten A. Karsdal, and Peter Boor (2014). "The extracellular matrix in the kidney: a source of novel non-invasive biomarkers of kidney fibrosis?" In: *Fibrogenesis & Tissue Repair* 7.1, p. 4. ISSN: 1755-1536. DOI: 10.1186/1755-1536-7-4.

Genovese, Federica, Peter Boor, Marios Papasotiriou, Diana J. Leeming, Morten A. Karsdal, and Jürgen Floege (2016). "Turnover of type III collagen reflects disease severity and is associated with progression and microinflammation in patients with IgA nephropathy". In: *Nephrology Dialysis Transplantation* 31.3, pp. 472–479. ISSN: 14602385. DOI: 10.1093/ndt/gfv301.

Gerth, Jens, C. D. Cohen, U. Hopfer, M. T. Lindenmeyer, M. Sommer, H. J. Gröne, and G. Wolf (2007). "Collagen type VIII expression in human diabetic nephropathy". In: *European Journal of Clinical Investigation* 37.10, pp. 767–773. ISSN: 00142972. DOI: 10.1111/j.1365-2362.2007.01864.x.

Gordon, Marion K. and Rita A. Hahn (2010). "Collagens". In: *Cell and Tissue Research* 339.1, pp. 247–257. ISSN: 0302766X. DOI: 10.1007/s00441-009-0844-4.

Grande, Joseph P (2011). "Experimental Models of Lupus Nephritis". In: *Experimental Models for Renal Diseases: Pathogenesis and Diagnosis*. Ed. by GA Herrera. Karger. Vol. 169. Basel, pp. 183–197.

Grässel, Susanne, Christine Unsöld, Heike Schäcke, Leena Bruckner-Tuderman, and Peter Bruckner (1999). "Collagen XVI is expressed by human dermal fibroblasts and keratinocytes and is associated with the microfibrillar apparatus in the upper papillary dermis". In: *Matrix Biology* 18.3, pp. 309–317. ISSN: 0945053X. DOI: 10.1016/S0945-053X(99)00019-0.

Hagg, Paivi M Pasi, Paivi M Pasi Hagg, Sirkku Peltonen, Helena Autio-Harmainen, Taina Pihlajaniemi, P M O Hägg, P M O Hägg, Sirkku Peltonen, Helena Autio-Harmainen, and Taina Pihlajaniemi (1997). "Location of type XV collagen in human tissues and its accumulation in the interstitial matrix of the fibrotic kidney." In: *The American journal of pathology* 150.6, pp. 2075–2086. ISSN: 00029440.

Hang, Le Ming, Shozo Iui, and Frank J. Dixon (1981). "(NZW x BXSB)F1 hybrid. A model of acute lupus and coronary vascular disease with myocardial infarction." In: *Journal of Experimental Medecine* 154, pp. 216–221. DOI: 10.1084/jem.154.1.216.

Hara, Satoshi, Mitsuhiro Kawano, Ichiro Mizushima, Kenichi Harada, Takuma Takata, Takako Saeki, Yoshifumi Ubara, Yasuharu Sato, and Michio Nagata (2016). "Distribution and components of interstitial inflammation and fibrosis in IgG4-related kidney disease: analysis of autopsy specimens". In: *Human Pathology* 55, pp. 164–173. ISSN: 15328392. DOI: 10.1016/j.humpath.2016.05.010.

Heljasvaara, Ritva, Mari Aikio, Heli Ruotsalainen, and Taina Pihlajaniemi (2017). "Collagen XVIII in tissue homeostasis and dysregulation — Lessons learned from model organisms and human patients". In: *Matrix Biology* 57-58, pp. 55–75. ISSN: 15691802. DOI: 10.1016/j.matbio.2016.10.002.

Hill, Nathan R, Samuel T Fatoba, Jason L Oke, Jennifer A Hirst, A O Callaghan, Daniel S Lasserson, and F D Richard Hobbs (2016). "Global Prevalence of Chronic Kidney Disease – A Systematic Review and Meta-Analysis". In: *PLoS ONE* 11, pp. 1–18. DOI: 10.5061/dryad.3s7rd.Funding.

Hobeika, Liliane, Michelle T. Barati, Dawn J. Caster, Kenneth R. McLeish, and Michael L. Merchant (2017). "Characterization of glomerular extracellular matrix by proteomic analysis of laser-captured microdissected glomeruli". In: *Kidney International* 91.2, pp. 501–511. ISSN: 15231755. DOI: 10.1016/j.kint.2016.09.044.

Hopfer, Ulrike, Helmut Hopfer, Catherine Meyer-Schwesinger, Ivonne Loeffler, Naomi Fukai, Bjorn R. Olsen, Rolf A.K. Stahl, and Gunter Wolf (2009). "Lack of type VIII collagen in mice ameliorates diabetic nephropathy". In: *Diabetes* 58.7, pp. 1672–1681. ISSN: 00121797. DOI: 10.2337/db08-0183.

Hou, Guangpei, Diane Mulholland, Margaret Anna Gronska, and Michelle Patricia Bendeck (2000). "Type VIII collagen stimulates smooth muscle cell migration and matrix metalloproteinase synthesis after arterial injury". In: *American Journal of Pathology* 156.2, pp. 467–476. ISSN: 00029440. DOI: 10.1016/S0002-9440(10)64751-7.

Hurskainen, Tiina, Jyri Moilanen, Raija Sormunen, Claus Werner Franzke, Raija Soininen, Stefanie Loeffek, Laura Huilaja, Matti Nuutinen, Leena Bruckner-Tuderman, Helena Autio-Harmainen, and Kaisa Tasanen (2012). "Transmembrane collagen XVII is a novel component of the glomerular filtration barrier". In: *Cell and Tissue Research* 348.3, pp. 579–588. ISSN: 14320878. DOI: 10.1007/s00441-012-1368-x.

Hynes, Richard O (2009). "Extracellular matrix: not just prety fibrils". In: *Science* 326.5957, pp. 1216–1219. DOI: 10.1126/science.1176009.Extracellular.

Illidge, Chris, Cay Kielty, and Adrian Shuttleworth (1998). "The α1(VIII) and α2(VIII) chains of type VIII collagen can form stable homotrimeric molecules". In: *Journal of Biological Chemistry* 273.34, pp. 22091–22095. ISSN: 00219258. DOI: 10.1074/jbc.273.34.22091.

Inoguchi, Kazuhito, Hidekatsu Yoshioka, Mohammed Khaleduzzaman, and Yoshifumi Ninomiya (1995). "The mrna for α1(XIX) collagen chain, a new member of FACITs, contains a long unusual 3′ untranslated region and displays many unique splicing variants". In: *Journal of Biochemistry* 117, pp. 137–146. ISSN: 0021924X. DOI: 10.1093/oxfordjournals.jbchem.a124700.

Iozzo, Renato V. and Liliana Schaefer (2015). "Proteoglycan form and function: A comprehensive nomenclature of proteoglycans". In: *Matrix Biology* 42, pp. 11–55. ISSN: 15691802. DOI: 10.1016/j.matbio.2015.02.003.

Jacobson, Orit, Xuefeng Yan, Gang Niu, Ido D Weiss, Lawrence P Szajek, Baozhong Shen, Dale O Kiesewetter, and Xiaoyuan Chen (2015). "PET Imaging of Tenascin-C with a Radiolabeled Single-Stranded DNA Aptamer". In: *Journal of Nuclear Medicine* 56.4, pp. 616–622. DOI: 10.2967/jnumed.114.149484.

Jensen, Christina, Signe H. Nielsen, Joachim H. Mortensen, Jens Kjeldsen, Lone G. Klinge, Aleksander Krag, Henrik Harling, Lars N. Jørgensen, Morten A. Karsdal, and Nicholas Willumsen (2018). "Serum type XVI collagen is associated with colorectal cancer and ulcerative colitis indicating a pathological role in gastrointestinal disorders". In: *Cancer Medicine* 7.9, pp. 4619–4626. ISSN: 20457634. DOI: 10.1002/cam4.1692.

Jha, Vivekanand, Guillermo Garcia-Garcia, Kunitoshi Iseki, Zuo Li, Saraladevi Naicker, Brett Plattner, Rajiv Saran, Angela Yee Moon Wang, and Chih Wei Yang (2013). "Chronic kidney disease: Global dimension and perspectives". In: *The Lancet* 382.9888, pp. 260–272. ISSN: 01406736. DOI: 10.1016/S0140-6736(13)60687-X.

Jia, Ting, Hannes Olauson, Karolina Lindberg, Risul Amin, Karin Edvardsson, Bengt Lindholm, Göran Andersson, Annika Wernerson, Yves Sabbagh, Susan Schiavi, and Tobias E. Larsson (2013). "A novel model of adenine-induced tubulointerstitial nephropathy in mice". In: *BMC Nephrology* 14.1. ISSN: 14712369. DOI: 10.1186/1471-2369-14-116.

Jöbsis, G. Joost, H. Keizers, Jeroen P. Vreijling, Marianne de Visser, Marcy C. Speer, Ruud A. Wolterman, Frank Baas, and Pieter A. Bolhios (1996). "Type VI collagen mutations in Bethlem myopathy, an autosomal dominant myopathy with contractures". In: *Nat Genet.* 14.3, pp. 353–6. ISSN: 1061-4036. DOI: 10.1038/ng0496-417.

Kapoor, R., L. Y. Sakai, S. Funk, E. Roux, P. Bornstein, and E. H. Sage (1988). "Type VIII collagen has a restricted distribution in specialized extracellular matrices". In: *Journal of Cell Biology* 107.2, pp. 721–730. ISSN: 00219525. DOI: 10.1083/jcb.107.2.721.

Karsdal, Morten A. (2016). *Biochemistry of Collagens, Laminins and Elastin*. Ed. by Morten A. Karsdal. 1st ed. London: Elsevier Inc., pp. 1–238. ISBN: 9780128098479.

Karsdal, Morten A, Federica Genovese, Emilie A Madsen, Tina Manon-jensen, and Detlef Schuppan (2016). "Collagen and tissue turnover as a function of

age: Implications for fibrosis". In: *Journal of Hepatology* 64, pp. 103–109. DOI: 10.1016/j.jhep.2015.08.014.

Karsdal, Morton A., S. H. Nielsen, D. J. Leeming, L. L. Langholm, M. J. Nielsen, T. Manon-Jensen, A. Siebuhr, N. S. Gudmann, S. Rønnow, J. M. Sand, S. J. Daniels, J. H. Mortensen, and D. Schuppan (2017). "The good and the bad collagens of fibrosis – Their role in signaling and organ function". In: *Advanced Drug Delivery Reviews* 121, pp. 43–56. ISSN: 18728294. DOI: 10.1016/j.addr.2017.07.014.

Kashtan, Clifford E. and Youngki Kim (1992). "Distribution of the α1 and α2 chains of collagen IV and of collagens V and VI in Alport syndrome". In: *Kidney International* 42.1, pp. 115–126. ISSN: 00852538. DOI: 10.1038/ki.1992.269.

Kassner, Anja, Uwe Hansen, Nicolai Miosge, Dieter P. Reinhardt, Thomas Aigner, Leena Bruckner-Tuderman, Peter Bruckner, and Susanne Grässel (2003). "Discrete integration of collagen XVI into tissue-specific collagen fibrils or beaded microfibrils". In: *Matrix Biology* 22.2, pp. 131–143. ISSN: 0945053X. DOI: 10.1016/S0945-053X(03)00008-8.

Kirschner, Janbernd, Ingrid Hausser, Yaqun Zou, Gudrun Schreiber, Hans Jürgen Christen, Susan C. Brown, Ingrun Anton-Lamprecht, Francesco Muntoni, Folker Hanefeld, and Carsten G. Bönnemann (2005). "Ullrich congenital muscular dystrophy: Connective tissue abnormalities in the skin support overlap with Ehlers-Danlos syndromes". In: *American Journal of Medical Genetics* 132 A.3, pp. 296–301. ISSN: 15524825. DOI: 10.1002/ajmg.a.30443.

Kittelberger, Reinhold, Paul F Davis, David W Flynn, Nicholas S Greenhill, Reinhold Kittelberger, Paul F Davis, David W Flynn, and Nicholas S Greenhill (1990). "Distribution of Type Viii Collagen in Tissues : An Immunohistochemical Study". In: *Connective Tissue Research* 24, pp. 303–318. DOI: 10.3109/03008209009152157.

Koch, Manuel, Guido Veit, Sigmar Stricker, Pinaki Bhatt, Stefanie Kutsch, Peihong Zhou, Elina Reinders, Rita A. Hahn, Rich Song, Robert E. Burgeson, Donald R. Gerecke, Stefan Mundlos, and Marion K. Gordon (2006). "Expression of type XXIII collagen mRNA and protein". In: *Journal of Biological Chemistry* 281.30, pp. 21546–21557. ISSN: 00219258. DOI: 10.1074/jbc.M604131200.

Kuncio, Gerald S., Eric G Neilson, and Thomas Haverty (1991). "Mechanisms of tubulointerstitial fibrosis". In: *Kidney International* 39, pp. 550–556. ISSN: 10466673. DOI: 10.1681/ASN.2010080793.

Lai, Char Huei and Mon Li Chu (1996). "Tissue distribution and developmental expression of type XVI collagen in the mouse". In: *Tissue and Cell* 28.2, pp. 155–164. ISSN: 00408166. DOI: 10.1016/S0040-8166(96)80004-8.

Lameire, Norbert and Wim Van Biesen (2010). "Epidemiology of peritoneal dialysis: A story of believers and nonbelievers". In: *Nature Reviews Nephrology* 6.2, pp. 75–82. ISSN: 17595061. DOI: 10.1038/nrneph.2009.210.

Larsen, Lise, Niels Ulrik Brandt Hansen, Morten Asser Karsdal, Jannie Marie Bülow Sand, Nicholas Willumsen, and Diana Julie Leeming (2016). "Type VIII

collagen is elevated in diseases associated with angiogenesis and vascular remodeling". In: *Clinical Biochemistry* 49.12, pp. 903–908. ISSN: 00099120. DOI: 10.1016/j.clinbiochem.2016.05.023.

Le Roux, Sarah, A. Devys, C. Girard, J. Harb, and M. Hourmant (2010). "Biomarkers for the diagnosis of the stable kidney transplant and chronic transplant injury using the ProtoArray technology". In: *Transplantation Proceedings* 42.9, pp. 3475–3481. ISSN: 00411345. DOI: 10.1016/j.transproceed.2010.09.006.

Li, Yi, Jun Li, Yat Ming Woo, Zan Shen, Hong Yao, Yijun Cai, Marie Chia mi Lin, and Wai Sang Poon (2017). "Enhanced expression of Vastatin inhibits angiogenesis and prolongs survival in murine orthotopic glioblastoma model". In: *BMC Cancer* 17.1, pp. 1–10. ISSN: 14712407. DOI: 10.1186/s12885-017-3125-8.

Loeffler, Ivonne, Ulrike Hopfer, Dirk Koczan, and Gunter Wolf (2011). "Type VIII Collagen Modulates TGF- 1-induced Proliferation of Mesangial Cells". In: *Journal of the American Society of Nephrology* 22.4, pp. 649–663. ISSN: 1046-6673. DOI: 10.1681/asn.2010010098.

Loeffler, Ivonne, Marita Liebisch, and Gunter Wolf (2012). "Collagen VIII influences epithelial phenotypic changes in experimental diabetic nephropathy". In: *AJP: Renal Physiology* 303.5, F733–F745. ISSN: 1931-857X. DOI: 10.1152/ajprenal.00212.2012.

MacBeath, Jonathan R. E., Cay M. Kielty, and C. Adreian Shuttleworth (1996). "Type VIII collagen is a product of vascular smooth-muscle cells in development and disease." In: *The Biochemical journal* 319, pp. 993–8. ISSN: 0264-6021. DOI: 10.1042/bj3190993.

Mack, Matthias (2018). "Inflammation and fibrosis". In: *Matrix Biology* 68-69, pp. 106–121. ISSN: 15691802. DOI: 10.1016/j.matbio.2017.11.010.

Mak, Ki M., Priya Sehgal, and Cynthia K. Harris (2014). "Type VI Collagen: Its Biology and Value as a Biomarker of Hepatic Fibrosis". In: *Austin Biomark. Diagn.* 1-9.2, pp. 443–469.

Mak, Ki M., Chien Yi M. Png, and Danielle J. Lee (May 2016). "Type V Collagen in Health, Disease, and Fibrosis". In: *The Anatomical Record* 299.5, pp. 613–629. ISSN: 19328486. DOI: 10.1002/ar.23330.

Malfait, Fransiska, Delfien Syx, Florence Ruggiero, Sofie Symoens, Sylvie Ricard-Blum, Marjolijn Renard, Anne De Paepe, Christelle Bonod-Bidaud, Paul Coucke, Lut Van Laer, Efrat Kessler, and Elisabeth Vaganay (2010). "Identification of binding partners interacting with the α1-N-propeptide of type V collagen". In: *Biochemical Journal* 433.2, pp. 371–381. ISSN: 0264-6021. DOI: 10.1042/bj20101061.

Martinez-Hernandez, Antonio, Steffen Gay, and Edward J. Miller (1982). "Ultrastructural localization of type V collagen in rat kidney". In: *Journal of Cell Biology* 92.2, pp. 343–349. ISSN: 00219525. DOI: 10.1083/jcb.92.2.343.

Mason, Roger M. and Nadia Abdel Wahab (2003). "Extracellular matrix metabolism in diabetic nephropathy". In: *Journal of the American Society of Nephrology* 14.5, pp. 1358–1373. ISSN: 10466673. DOI: 10.1097/01.ASN.0000065640.77499.D7.

Mathian, Alexis, Arthur Weinberg, Mike Gallegos, Jacques Banchereau, and Sophie Koutouzov (2005). "IFN-alpha Induces Early Lethal Lupus in Preautoimmune (New Zealand Black x New Zealand White)F1 but Not in BALB/c Mice". In: *The Journal of Immunology* 174.5, pp. 2499–2506. ISSN: 0022-1767. DOI: 10.4049/jimmunol.174.5.2499.

Mecham, Robert P. (2011). *The Extracellular Matrix: an Overview*. Ed. by Robert P. Mecham. Springer-V. New York, pp. 1–425. ISBN: 9783642165542.

Melenovsky, Vojtech, Ludek Cervenka, Ondrej Viklicky, Janka Franekova, Tereza Havlenova, Matej Behounek, Martin Chmel, and Jiri Petrak (2018). "Kidney response to heart failure: Proteomic analysis of cardiorenal syndrome". In: *Kidney and Blood Pressure Research* 43.5, pp. 1437–1450. ISSN: 14230143. DOI: 10.1159/000493657.

Merlini, L., E. Martoni, P. Grumati, P. Sabatelli, S. Squarzoni, Anna Urciuolo, A. Ferlini, F. Gualandi, and Paolo Bonaldo (2008). "Autosomal recessive myosclerosis myopathy is a collagen VI disorder". In: *Neurology* 71.16, pp. 1245–1253. ISSN: 0028-3878. DOI: 10.1212/01.wnl.0000327611.01687.5e.

Mettouchi, Amel (2012). "The role of extracellular matrix in vascular branching morphogenesis." In: *Cell adhesion & migration* 6.6, pp. 528–34. ISSN: 1933-6926. DOI: 10.4161/cam.22862.

Muda, Andrea Onetti, Laura Ruzzi, Silvia Bernardini, Anna Teti, and Tullio Faraggiana (2001). "Collagen VII expression in glomerular sclerosis". In: *Journal of Pathology* 195.3, pp. 383–390. ISSN: 00223417. DOI: 10.1002/path.962.

Myers, Jeanne C., Hongyun Yang, Joseph A. D'Ippolito, Asaf Presente, Michael K. Miller, and Arnold S. Dion (July 1994). "The triple-helical region of human type XIX collagen consists of multiple collagenous subdomains and exhibits limited sequence homology to alpha 1(XVI)." In: *The Journal of biological chemistry* 269.28, pp. 18549–57. ISSN: 0021-9258.

Myers, Jeanne C., Deqin Li, Alexandra Bageris, Valsamma Abraham, Arnold S. Dion, and Peter S. Amenta (1997). "Biochemical and immunohistochemical characterization of human type XIX defines a novel class of basement membrane zone collagens." In: *The American journal of pathology* 151.6, pp. 1729–1740. ISSN: 00029440.

Naba, Alexandra, Karl R. Clauser, Huiming Ding, Charles A. Whittaker, Steven A. Carr, and Richard O. Hynes (2016). "The extracellular matrix: Tools and insights for the "omics" era". In: *Matrix Biology* 49, pp. 10–24. ISSN: 15691802. DOI: 10.1016/j.matbio.2015.06.003.

National Kidney Foundation (2002). "K/DOQI Clinical Practice Guidelines for Chronic Kidney Disease: Evaluation, Clasification and Stratification". In: *Am J Kidney Dis.* 39.(suppl. 1), pp. 1–266. ISSN: 1541-7891. DOI: 10.1634/theoncologist.2011-S2-45.

Nerlich, Andreas G., Erwin D. Schleicher, Irmgard Wiest, Ulrich Specks, and Rupert Timpl (1994). "Immunohistochemical localization of collagen VI in diabetic glomeruli". In: *Kidney International* 45.6, pp. 1648–1656. ISSN: 00852538. DOI: 10.1038/ki.1994.216.

O'Connel, Joe (2002). "The Basics of RT-PCR". In: *Journal of Clinical Pathology* 193. Ed. by N King and Joe O'Connel, pp. 19–25. ISSN: 1431-8784. DOI: 10.1007/0-387-28390-0.

Oudart, Jean-Baptiste, Sylvie Brassart-Pasco, E. Luczka, Aurelie Dupont-Deshorgue, G. Bellon, Sergei P. Boudko, Hans Peter Bächinger, Jean-Claude Monboisse, François-Xavier Maquart, and Laurent Ramont (2013). "Analytical methods for measuring collagen XIX in human cell cultures, tissue extracts, and biological fluids". In: *Analytical Biochemistry* 437.2, pp. 111–117. ISSN: 00032697. DOI: 10.1016/j.ab.2013.03.007.

Oudart, Jean Baptiste, Jean Claude Monboisse, François Xavier Maquart, Bertrand Brassart, Sylvie Brassart-Pasco, and Laurent Ramont (2017). "Type XIX collagen: A new partner in the interactions between tumor cells and their microenvironment". In: *Matrix Biology* 57-58, pp. 169–177. ISSN: 15691802. DOI: 10.1016/j.matbio.2016.07.010. URL: http://dx.doi.org/10.1016/j.matbio.2016.07.010.

Papasotiriou, Marios, Federica Genovese, Barbara M. Klinkhammer, Uta Kunter, Signe H. Nielsen, Morten A. Karsdal, Jürgen Floege, and Peter Boor (2015). "Serum and urine markers of collagen degradation reflect renal fibrosis in experimental kidney diseases". In: *Nephrology Dialysis Transplantation* 30.7, pp. 1112–1121. ISSN: 14602385. DOI: 10.1093/ndt/gfv063.

Parker, Matthew W, Daniel Rossi, Mark Peterson, Karen Smith, White Eric S. Silkström Kristina, John E. Connett, Crag A. Henke, Ola Larsson, and Peter B Bitterman (2014). "Fibrotic extracellular matrix activates a profibrotic positive feedback loop". In: *The Journal of Clinical Investigation* 124.4, pp. 1622–1635. DOI: 10.1172/JCI71386.1622.

Pavkovic, Mira, Lorena Pantano, Cory V. Gerlach, Sergine Brutus, Sarah A. Boswell, Robert A. Everley, Jagesh V. Shah, Shannan H. Sui, and Vishal S. Vaidya (2019). "Multi omics analysis of fibrotic kidneys in two mouse models". In: *Scientific Data* 6.92, pp. 1–9. DOI: 10.1038/s41597-019-0095-5.

Peng, Wen, Jie Zhao, Li Wang, Aili Cao, Minqian Jiang, and Xia Chen (2015). "Renal Tubulointerstitial Fibrosis: A Review in Animal Models". In: *Journal of Integrative Nephrology and Andrology* 2.3, p. 75. ISSN: 2225-1243. DOI: 10.4103/2225-1243.161428.

Plenz, Gabriele A M, Mario C Deng, Horst Robenek, and Wolfgang Vo (2003). "Vascular collagens : spotlight on the role of type VIII collagen in atherogenesis". In: *Atherosclerosis* 166, pp. 1–11. DOI: 10.1016/s0021-9150(01)00766-3.

Rabe, Michael and Franz Schaefer (2016). "Non-transgenic mouse models of kidney disease". In: *Nephron* 133.1, pp. 53–61. ISSN: 22353186. DOI: 10.1159/000445171.

Ramont, Laurent, Sylvie Brassart-Pasco, Jessica Thevenard, Aurélie Deshorgue, Lydie Venteo, Jean Yves Laronze, Michel Pluot, Jean-Claude Monboisse, and François-Xavier Maquart (2007). "The NC1 domain of type XIX collagen inhibits in vivo melanoma growth". In: *Molecular Cancer Therapeutics* 6.2, pp. 506–514. ISSN: 1535-7163. DOI: 10.1158/1535-7163.mct-06-0207.

Rasmussen, Daniel Guldager Kring, Anthony Fenton, Mark Jesky, Charles Ferro, Peter Boor, Martin Tepel, Morten Asser Karsdal, Federica Genovese, and Paul Cockwell (2017). "Urinary endotrophin predicts disease progression in patients with chronic kidney disease". In: *Scientific Reports* 7.1, pp. 1–11. ISSN: 2045-2322. DOI: 10.1038/s41598-017-17470-3.

Ratzinger, Sabine, Johannes A. Eble, Anja Pasoldt, Alfred Opolka, Gerhard Rogler, Joachim Grifka, and Susanne Grässel (2010). "Collagen XVI induces formation of focal contacts on intestinal myofibroblasts isolated from the normal and inflamed intestinal tract". In: *Matrix Biology* 29.3, pp. 177–193. ISSN: 0945053X. DOI: 10.1016/j.matbio.2009.11.004.

Razzaque, Mohammed S., T. Koji, Y. Horita, M. Nishihara, T. Harada, P. K. Nakane, and T. Taguchi (1995). "Synthesis of type III Collagen and type IV collagen by tubular epithelial cells in diabetic nephropathy". In: *Pathology Research and Practice* 191.11, pp. 1099–1104. ISSN: 03440338. DOI: 10.1016/S0344-0338(11)80654-0.

Razzaque, Mohammed S., Takehiko Koji, Takashi Harada, and Takashi Taguchi (2015). "Identification of Type VI Collagen Synthesizing Cells in Human Diabetic Glomerulosclerosis Using Renal Biopsy Sections". In: *Analytical Cellular Pathology* 15.3, pp. 175–181. ISSN: 0921-8912. DOI: 10.1155/1997/280571.

Rheault, Michelle N., Stefan M. Kren, Beth K. Thielen, Hector A. Mesa, John T. Crosson, William Thomas, Yoshikazu Sado, Clifford E. Kashtan, and Yoav Segal (2004). "Mouse model of X-linked Alport syndrome". In: *Journal of the American Society of Nephrology* 15.6, pp. 1466–1474. ISSN: 10466673. DOI: 10.1097/01.ASN.0000130562.90255.8F.

Ricard-Blum, Sylvie (2011). "The Collagen Family". In: *Cold Spring Harbor Perspectives in Biology* 3.1, pp. 1–19. ISSN: 19430264. DOI: 10.1101/cshperspect.a004978.

Ricard-Blum, Sylvie, Georges Baffet, and Nathalie Théret (2018). "Molecular and tissue alterations of collagens in fibrosis". In: *Matrix Biology* 68-69, pp. 122–149. ISSN: 15691802. DOI: 10.1016/j.matbio.2018.02.004.

Rockey, Don C., P. Darwin Bell, and Joseph A. Hill (2015). "Fibrosis — A Common Pathway to Organ Injury and Failure". In: *New England Journal of Medicine* 372.12, pp. 1138–1149. ISSN: 0028-4793. DOI: 10.1056/nejmra1300575.

Rodríguez-Iturbe, Bernado, Richard J. Johnson, and Jaime Herrera-Acosta (2005). "Tubulointerstitial damage and progression of renal failure". In: *Kidney International* 68.Supplement 99, S82–S86. DOI: 10.1111/j.1523-1755.2005.09915.x.

Romagnani, Paola, Giuseppe Remuzzi, Richard Glassock, Adeera Levin, Kitty J. Jager, Marcello Tonelli, Ziad Massy, Christoph Wanner, and Hans Joachim Anders (2017). "Chronic kidney disease". In: *Nature Reviews Disease Primers* 3, pp. 1–24. ISSN: 2056676X. DOI: 10.1038/nrdp.2017.88.

Rosenblum, N. D., D. M. Briscoe, M. J. Karnovsky, and B. R. Olsen (1993). "Alpha 1-VIII collagen is expressed in the rat glomerulus and in resident glomerular cells". In: *American Journal of Physiology-Renal Physiology* 264.6, F1003–F1010. ISSN: 1931-857X. DOI: 10.1152/ajprenal.1993.264.6.f1003.

Roy, Suvra and Vikash Kumar (2014). "A Practical Approach on SDS PAGE for Separation of Protein". In: *International Journal of Science and Research* 3.8, pp. 955–960. ISSN: 2319-7064.

Schaefer, Liliana (2018). "Decoding fibrosis: Mechanisms and translational aspects". In: *Matrix Biology* 68-69.2017, pp. 1–7. ISSN: 15691802. DOI: 10.1016/j.matbio.2018.04.009.

Schaefer, Liliana and Roland M. Schaefer (2010). "Proteoglycans: From structural compounds to signaling molecules". In: *Cell and Tissue Research* 339.1, pp. 237–246. ISSN: 0302766X. DOI: 10.1007/s00441-009-0821-y.

Schlondorff, Detlef and Bernhard Banas (2009). "The Mesangial Cell Revisited: No Cell Is an Island". In: *Journal of the American Society of Nephrology* 20.6, pp. 1179–1187. ISSN: 1046-6673. DOI: 10.1681/ASN.2008050549.

Schmid, Thomas M, Rose G Popp, and Thomas F Linsenmayer (1990). "Hypertrophic cartilage matrix". In: *Annals New York Academy of Sciences* 580, pp. 64–73. ISSN: 0077-8923. DOI: 10.1111/j.1749-6632.1990.tb17918.x.

Shen, Zan, Chen Yao, Zifeng Wang, Lu Yue, Zheping Fang, Hong Yao, Feng Lin, Hui Zhao, Yuan Jue Sun, Xiu Wu Bian, Wenqi Jiang, Xiaomei Wang, Yi Li, Gang Lu, Wai Sang Poon, Hsiang Fu Kung, and Marie Chia Mi Lin (2016). "Vastatin, an Endogenous Antiangiogenesis Polypeptide That Is Lost in Hepatocellular Carcinoma, Effectively Inhibits Tumor Metastasis". In: *Molecular Therapy* 24.8, pp. 1358–1368. ISSN: 15250024. DOI: 10.1038/mt.2016.56.

Sherratt, Michael J., C. Adrian Shuttleworth, Simon Stephan, Cay M. Kielty, and Nigel Hodson (2004). "Expression and Supramolecular Assembly of Recombinant α1(VIII) and α2(VIII) Collagen Homotrimers". In: *Journal of Biological Chemistry* 279.20, pp. 21469–21477. ISSN: 0021-9258. DOI: 10.1074/jbc.m305805200.

Skorecki, Karl, Glenn M. Chertow, Philip A. Marsden, and Maarten W. Taal, eds. (2016). *Brenner & Rector's the Kidney*. 10th. Philadelphia: Elsevier, p. 3341.

Skrbic, Biljana, Johannes L. Bjørnstad, Henriette S. Marstein, Cathrine R. Carlson, Ivar Sjaastad, Ståle Nygård, Sigrid Bjørnstad, Geir Christensen, and Theis Tønnessen (2013). "Differential regulation of extracellular matrix constituents in myocardial remodeling with and without heart failure following pressure overload". In: *Matrix Biology* 32.2, pp. 133–142. ISSN: 0945053X. DOI: 10.1016/j.matbio.2012.11.011.

Skrbic, Biljana, Kristin V.T. Engebretsen, Mari E. Strand, Ida G. Lunde, Kate M. Herum, Henriette S. Marstein, Ivar Sjaastad, Per K. Lunde, Cathrine R. Carlson, Geir Christensen, Johannes L. BjØrnstad, and Theis TØnnessen (2015). "Lack of collagen VIII reduces fibrosis and promotes early mortality and cardiac dilatation in pressure overload in mice". In: *Cardiovascular Research* 106.1, pp. 32–42. ISSN: 17553245. DOI: 10.1093/cvr/cvv041.

Smyth, Gordon K (2004). "Linear Models and Empirical Bayes Methods for Assessing Differential Expression in Microarray Experiments". In: *Statistical Applications in Genetics and Molecular Biology* 3.1, pp. 1–25. ISSN: 1544-6115. DOI: 10.2202/1544-6115.1027.

Smyth, Gordon K, Matthew Ritchie, and Natalie Thorne (2010). *Linear Models for Microarray Data User ' s Guide*. Tech. rep. Melbourne, Australia: Bioinformatics Division, The Walter and Eliza Hall Institute of Medical research, pp. 1–99. DOI: 10.1093/nar/gkv007.

Soylemezoglu, O., G. Wild, A. J. Dalley, S. MacNeil, A. Milford-Ward, C. B. Brown, and A. M. El Nahas (1997). "Urinary and serum type III collagen: Markers of renal fibrosis". In: *Nephrology Dialysis Transplantation* 12.9, pp. 1883–1889. ISSN: 09310509. DOI: 10.1093/ndt/12.9.1883.

Spivey, Kirstin A., Jacqueline Banyard, Luisa M. Solis, Ignacio I. Wistuba, Justine A. Barletta, Leena Gandhi, Henry A. Feldman, Scott J. Rodig, Lucian R. Chirieac, and Bruce R. Zetter (2010). "Collagen XXIII: A Potential Biomarker for the Detection of Primary and Recurrent Non-Small Cell Lung Cancer". In: *Cancer Epidemiology Biomarkers & Prevention* 19.5, pp. 1362–1372. ISSN: 1055-9965. DOI: 10.1158/1055-9965.EPI-09-1095.

Spivey, Kristin A., I. Chung, J. Banyard, I. Adini, H. A. Feldman, and B. R. Zetter (2012). "A role for collagen XXIII in cancer cell adhesion, anchorage-independence and metastasis". In: *Oncogene* 31.18, pp. 2362–2372. ISSN: 09509232. DOI: 10.1038/onc.2011.406.

Stalteri, Maria A. and Andrew P. Harrison (2007). "Interpretation of multiple probe sets mapping to the same gene in Affymetrix GeneChips". In: *BMC Bioinformatics* 8, pp. 1–15. ISSN: 14712105. DOI: 10.1186/1471-2105-8-13.

Stribos, Elisabeth G.D., Signe Holm Nielsen, Susanne Brix, Morten Asser Karsdal, Marc A. Seelen, Harry Van Goor, Stephan J.L. Bakker, Peter Olinga, Henricus A.M. Mutsaers, and Federica Genovese (2017). "Non-invasive quantification of collagen turnover in renal transplant recipients". In: *PLoS ONE* 12.4, pp. 1–11. ISSN: 19326203. DOI: 10.1371/journal.pone.0175898.

Sumiyoshi, Hideaki, Kazuhito Inoguchi, Mohammed Khaleduzzaman, and Yoshifumi Ninomiya (1997). "Ubiquitous Expression of the a1(XIX) Collagen Gene (Col19a1) during Mouse Embryogenesis Becomes Restricted to a Few Tissues in the Adult Organism". In: *The Journal of Biological Chemistry* 272.4, pp. 17104–17111. DOI: 10.1074/jbc.272.27.17104.

Sumiyoshi, Hideaki, Friedrich Laub, Hidekatsu Yoshioka, and Francesco Ramirez (2001). "Embryonic expression of type XIX collagen is transient and confined to muscle cells". In: *Developmental Dynamics* 220.2, pp. 155–162. ISSN: 10588388. DOI: 10.1002/1097-0177.

Sumiyoshi, Hideaki, Niv Mor, Sui Y. Lee, Stephen Doty, Scott Henderson, Shizuko Tanaka, Hidekatsu Yoshioka, Satish Rattan, and Francesco Ramirez (2004). "Esophageal muscle physiology and morphogenesis require assembly of a collagen XIX-rich basement membrane zone". In: *Journal of Cell Biology* 166.4, pp. 591–600. ISSN: 00219525. DOI: 10.1083/jcb.200402054.

Sun, Qinxue, Maike Baues, Barbara M. Klinkhammer, Josef Ehling, Sonja Djudjaj, Natascha I. Drude, Christoph Daniel, Kerstin Amann, Rafael Kramann, Hyojin Kim, Julio Saez-Rodriguez, Ralf Weiskirchen, David C. Onthank, Rene M. Botnar, Fabian Kiessling, Jürgen Floege, Twan Lammers, and Peter Boor

(2019). "Elastin imaging enables noninvasive staging and treatment monitoring of kidney fibrosis". In: *Science Translational Medicine* 11.486, pp. 1–14. ISSN: 19466242. DOI: 10.1126/scitranslmed.aat4865.

Suvarna, S. Kim, Christopher Layton, and John D. Bancroft (2013). *Bancroft's Theory and Practice of Histological Techniques*. 7th ed. Churchill Livingstone Elsevier, p. 603. ISBN: 9780702042263.

Tomasek, James J., Giulio Gabbiani, Boris Hinz, Christine Chaponnier, and Robert A. Brown (2002). "Myofibroblasts and mechano: Regulation of connective tissue remodelling". In: *Nature Reviews Molecular Cell Biology* 3.5, pp. 349–363. ISSN: 14710072. DOI: 10.1038/nrm809.

Tzortzaki, Eleni G., Jay A. Tischfield, Amrik Sahota, Nikolaos M. Siafakas, Marion K. Gordon, and Donald R. Gerecke (2003). "Expression of FACIT Collagens XII and XIV during Bleomycin-Induced Pulmonary Fibrosis in Mice". In: *Anatomical Record - Part A Discoveries in Molecular, Cellular, and Evolutionary Biology* 275.2, pp. 1073–1080. ISSN: 0003276X. DOI: 10.1002/ar.a.10120.

Veit, Guido, Elena P. Zimina, Claus Werner Franzke, Stefanie Kutsch, Udo Siebolds, Marion K. Gordon, Leena Bruckner-Tuderman, and Manuel Koch (2007). "Shedding of collagen XXIII is mediated by furin and depends on the plasma membrane microenvironment". In: *Journal of Biological Chemistry* 282.37, pp. 27424–27435. ISSN: 00219258. DOI: 10.1074/jbc.M703425200.

Veit, Guido, Daniela Zwolanek, Beate Eckes, Stephan Niland, Jarmo Käpylä, Manon C. Zweers, Akemi Ishada-Yamamoto, Thomas Krieg, Jyrki Heino, Johannes A. Eble, and Manuel Koch (2011). "Collagen XXIII, novel ligand for integrin α 2β 1in the epidermis". In: *Journal of Biological Chemistry* 286.31, pp. 27804–27813. ISSN: 00219258. DOI: 10.1074/jbc.M111.220046.

Vleming, LJ., JJ. Baelde, RG. Westendorp, MR. Daha, LA van Es, and Bruijn JA. (1994). "Progression of chronic renal disease in humans is associated with the deposition of basement membrane components and decorin in the interstitial extracellular matrix". In: *Clinical nephroplogy* 44.4, pp. 211–219. DOI: 8575119.

Walker, John M. (1996). "The Bicinchoninic Acid (BCA) Assay for Protein Quantitation". In: *The Protein Protocols Handbook*. Totowa, NJ: Humana Press, pp. 11–14. ISBN: 1-59259-169-8. DOI: 10.1007/978-1-60327-259-9{_}3.

Webster, Angela C., Evi V. Nagler, Rachael L. Morton, and Philip Masson (Mar. 2017). "Chronic Kidney Disease". In: *The Lancet* 389.10075, pp. 1238–1252. ISSN: 01406736. DOI: 10.1016/S0140-6736(16)32064-5.

Welsch, Ulrich (2006). *Lehrbuch Histologie*. Ed. by Ulrich Welsch. 2nd. München: Urban&Fischer, p. 676. ISBN: 978-3-437-44430-2.

Wenstrup, Richard J., Jane B. Florer, Eric W. Brunskill, Sheila M. Bell, Inna Chervoneva, and David E. Birk (2004). "Type V collagen controls the initiation of collagen fibril assembly". In: *Journal of Biological Chemistry* 279.51, pp. 53331–53337. ISSN: 00219258. DOI: 10.1074/jbc.M409622200.

Wu, Qiong, Kiichiro Jinde, Makoto Nishina, Ryoji Tanabe, Masayuki Endoh, Yoshikazu Okada, Hideto Sakai, and Kiyoshi Kurokawa (2001). "Analysis of prognostic predictors in idiopathic membranous nephropathy". In: *American Journal of*

Kidney Diseases 37.2, pp. 380–387. ISSN: 02726386. DOI: 10.1053/ajkd.2001.21319.

Wynn, Thomas A and Thirumalai R Ramalingam (2012). "Mechanisms of fibrosis: therapeutic translation for fibrotic disease." In: *Nature medicine* 18.7, pp. 1028–40. ISSN: 1546-170X. DOI: 10.1038/nm.2807.

Xu, Ren, Zhong Yin Yao, Li Xin, Qian Zhang, Tsai Ping Li, and Ren Bao Gan (2001). "NC1 domain of human type VIII collagen (α 1) inhibits bovine aortic endothelial cell proliferation and causes cell apoptosis". In: *Biochemical and Biophysical Research Communications* 289.1, pp. 264–268. ISSN: 0006291X. DOI: 10.1006/bbrc.2001.5970.

Yang, Hai-Chun, Yiqin Zuo, and Agnes B. Fogo (2010). "Models of chronic kidney disease". In: *Drug Discov Today Dis Models* 7.1-2, pp. 13–19. ISSN: 1740-6757. DOI: 10.1016/j.ddmod.2010.08.002.Models.

Zaferani, Azadeh, Ditmer T. Talsma, Saleh Yazdani, Johanna W.A.M. Celie, Mari Aikio, Ritva Heljasvaara, Gerjan J. Navis, Taina Pihlajaniemi, and Jacob Van Den Born (2014). "Basement membrane zone collagens XV and XVIII/proteoglycans mediate leukocyte influx in renal ischemia/reperfusion". In: *PLoS ONE* 9.9. ISSN: 19326203. DOI: 10.1371/journal.pone.0106732.

Zeisberg, Michael and Eric G Neilson (2010). "Mechanisms of Tubulointerstitial Fibrosis". In: *Journal of the American Society of Nephrology* 21, pp. 1819–1834. DOI: 10.1681/ASN.2010080793.

Zeisberg, Michael, Mary A. Soubasakos, and Raghu Kalluri (2005). "Animal Models of Renal Fibrosis". In: *Fibrosis Research*. Vol. 117. Totowa, NJ: Humana Press, pp. 261–272. DOI: 10.1385/1-59259-940-0:261.

Zhu, Dan, Youngki Kim, Michael W. Steffes, Thomas J. Groppoli, Ralph J. Butkowski, and S. Michael Mauer (1994). "Application of electron microscopic immunocytochemistry to the human kidney: distribution of type IV and type VI collagen in normal human kidney." In: *Journal of Histochemistry & Cytochemistry* 42.5, pp. 577–584. ISSN: 0022-1554. DOI: 10.1177/42.5.8157929.

Zoccali, Carmine, Raymond Vanholder, Ziad A. Massy, Alberto Ortiz, Pantelis Sarafidis, Friedo W. Dekker, Danilo Fliser, Denis Fouque, Gunnar H. Heine, Kitty J. Jager, Mehmet Kanbay, Francesca Mallamaci, Gianfranco Parati, Patrick Rossignol, Andrzej Wiecek, and Gerard London (June 2017). "The systemic nature of CKD". In: *Nature Reviews Nephrology* 13.6, pp. 344–358. ISSN: 1759-5061. DOI: 10.1038/nrneph.2017.52.

Appendix A
Material

A.1 Devices

All used devices are listed in Table A.1.

TABLE A.1: Devices

Device	Supplier
ABI Prism 7300 sequence detection system	Life technologies (Darmstadt, DE)
Accu-jet© pro Pipettierhelfer	Brand GmbH + co KG (Wertheim, DE)
Autoclave sterilizer	H & P Labortechnik (München, DE)
Behrotest peristaltic pump capacity 0,4-2l/h	Behr Labor-Technik (Düsseldorf, DE)
Casy Modell TTC System	Roche Diagnostics GmBH (Mannheim, DE)
Centrifuge 4K15	Sigma Laborzentrifugen (Osterode, DE)
Electrosurgical Unit, Kauter Erbotom Acc 450	Erbe (Tübingen, DE)
Entwickler Crurix 60	AGFA (Mortsel, BE)
Fluoview FV1000 Multiphoton Microscope	Olympus (Hamburg, DE)
Homogeniser RZR 2020	Heidolph (Schwabach, DE)
Hotplate MR 3001	Heidolph (Schwabach, DE)
Leica Histo-Embedder	Leica Instruments GmbH (Nussloch, DE)
Light- and fluorescence microscope BZ-9000	Keyence (Osaka, JP)
Microplate Readers-Photometer Tecan sunrise	Tecan (Männedorf, CH)
Micro-serrefine	Fine Science Tools GmbH (Heidelberg, DE)
NanoDrop 2000	Peqlab (Erlangen, DE)
NuPAGE Novex Electrophoreses-System	Invitrogen (Carlsbad, USA)
PCR System T3000 Thermocycler	Biometra (Göttingen, DE)
Pipettes	Eppendorf (Hamburg, DE)
Pixma MG5350 Printer	Canon (Tokio, JP)
PowerPac™ 200 High-Current Power Supply	Biorad (München, DE)
PowerPac™ 3000 High-Current Power Supply	Biorad (München, DE)
Razor Favorita 2	Aesculap© (Stuhl, DE)
Rocking Platform WT12	Biometra by Analytik Jena AG (Jena, DE)
Rotations microtome CUT5062	Leica Instruments GmbH (Nussloch, DE)
Slide Scanner Nanozoomer 2.0.-HT	Hamamatsu (Osoka, JP)

Surgical Microscope Wild M650	Wild Heerbrug (Heerbrug, CH)
Thermocycler	Landgraf (Langenhagen, DE)
Tabletop centrifuge Tischzentrifuge 5415D	Eppendorf (Hamburg, DE)
TC-1000 Temperature Controller	CWE Inc. (Ardamore USA)
Ultrasound Sonorex RK100H	Bandelin electronics (Berlin, DE)
Vascular clamp	Fine Science Tools GmbH (Heidelbaerg, DE)
Vibrator mill, Schwinglmühle MM 400	Retsch (Haan, DE)
Water bath for paraffin section	Barnstead (Electrothermal) (Iowa, USA)
Water bath GFL 1083	GFL (Burgwedel, DE)
Western Blot system	Biorad (München, DE)
XCell SureLock™ Mini-Cell Electrophoresis System	Thermo-Fischer Scientific (Rockford, USA)

A.2 Consumables

All consumables are listed in Table A.2.

TABLE A.2: Consumables

Consumables	Supplier
Amersham Hyperfilm™	GE Healthcare (Little Chalfont, UK)
Amersham Protran© Nitrocellulose membrane 0,45 µm	GE Healthcare (Little Chalfont, UK)
Adenin 0.2% diet	Altromin International (Lage, DE)
Cellstar© Serological Pipettes (5, 10, 25 ml)	Greiner bio-one (Kremsmünster, AT)
Coverslips	Roth (Karlsruhe, DE)
Cryo-tube, Cryovial, 2 ml	Simport (Saint-Michel-de-Bellechasse, CA)
EDTA-tube	Sarstedt AG + Co KG (Nümbrecht, DE)
Embedding cassettes	Sakura (Staufen, DE)
Feather Disposable scalpel No 15	Feather Safety Razor Co LTD (Osaka, JP)
Glass capillary blood collection, heparinised Ø 0,8 mm	Hilgenberg (Masfeld, DE)
Glove, Nitril powder-free	Sempercare (Wien, AT)
Microtube 1,5 ml, 2 ml	Sarstedt AG & Co KG (Nümbrecht, DE)
Needle, 21 G 1/2, 27G G 1/2, 30 G	BD Microbalance (Bedford, USA)
Nu Page 4-12 % Bis Tris-Gel 1,5 mm x 10 well	Novex by life technologies (Calsbad, CA)
Nu Page 4-12 % Bis Tris-Gel 1,5 mm x 15 well	Novex by life technologies (Calsbad, CA)
Operation sets	FST (Heidelberg, DE)
Pipette tips	Eppendorf (Hamburg, DE)
Pipette tips	Greiner bio-one (Kremsmünster, AT)

QIAshredder	Qiagen (Hilden, DE)
Safe-Lock tubes	Eppendorf (Hamburg, DE)
Slides Superfrost Plus	Menzel GmbH (Braunschweig, DE)
Suture Mersilene 5.0	Ethicon (Norderstedt, DE)
Tubes 15 ml, 50 ml	Greiner bio-one (Kremsmünster, AT)
Venofix© Safety (G23, G21)	B. Braun (Melsungen, DE)
Whatman-Filter papers	Biorad (München, DE)

A.3 Reagents

All reagentsare listed in Table A.3.

TABLE A.3: Reagents

Reagents	Supplier
0.9 % saline solution	B. Braun (Meisungen, DE)
2-Mercaptoethanol	Sigma-Aldrich Chemie (Steinheim, DE)
4‘,6 Diamidino-2-phenylindole (DAPI)	Roche Diagnostics (Mannheim, DE)
Acetic acid	Calbiochem (Darmstadt, DE)
Albumin bovine fraction V	SERVA Electrophoresis GmbH (Heidelberg, DE)
Antigen Unmasking Solution, Citric Acid based	Vector Laboratories (Burlingame, USA)
Avidin/Biotin Blocking Kit	Vector Laboratories (Burlingame, USA)
BC Assay Protein Quantitation Kit	Optima Interchim (Montlucon, FR)
BSA standard for Protein assay	Optima Interchim (Montlucon, FR)
Chloroform	VWR (Leuwen, BE)
Complete Tablets, Mini, EDTA free, EASYpack	Roche Diagnostics GmbH (Mannheim, DE)
Developer G153	AGFA Healthcare (Mortsel, BE)
Diaminobenzidin-Substrat (DAB)	Sigma-Aldrich Chemie (Steinheim, DE)
Dimethylbutane	Roth (Karlsruhe, DE)
Demethylformalide	Merck (Darmstadt, DE)
Dimethylsulfoxide (DMSO)	ICN Biochemicals (Clevland, Ohio, USA)
Dinatriumhydrogenphosphat	Merck (Darmstadt, DE)
Dithiothreitol (DTT)	Biorad (München, DE)
DNeasy© Blood & Tissue Kit	Qiagen (Hilden, DE)
dNTP	Roth (Karlsruhe, DE)
Eosin	Roth (Karlsruhe, DE
Ethanol 100 %	Apotheke des Universitätsklinikums der RWTH Aachen (Aachen, DE)
Ethanol 70 %	Apotheke des Universitätsklinikums der RWTH Aachen (Aachen, DE)
Ethyl cinnamate	Sigma-Aldrich Chemie (Steinheim, DE)
Ethylendiamintetraacetat (EDTA)	Sigma-Aldrich Chemie (Steinheim, DE)

EMSURE©ACS, ISO, Reag. Ph EUR Ethanol	Merck (Darmstadt, DE)
Glycin	Roth (Karlsruhe, DE)
Glycerol	Merck (Darmstadt, DE)
First Strand Buffer	Invitrogen (Carlsbad, USA)
Heparin-Natrium Braun 25 000 IE / 5 ml	B. Braun (Meisungen, DE)
Histokitt	Roth (Karlsruhe, DE)
Hydrochloric acid (HCl) 1N	Applichem (Darmstadt, DE)
Hydrogen peroxide (H_2O_2) 30%	Calbiochem (Darmstadt, DE)
Immu-Mount	Thermo Electron Corp. (Pittsburgh, USA)
Isoflurane Florene	Abott (Wiesbaden, DE)
Ketamin Rompun, 10 %	Ceva Sante Animale (Düsseldorf, DE)
L-Glutamin	Gibco© lifetechnologies (Paisley, UK)
Lumi light western blotting substrate	Roche Diagnostics (Mannheim, DE)
Mayer's haematoxylin solution	Calbiochem (Darmstadt, DE)
MES SDS Running Buffer (20x) NuPAGE	Invitrogen (Carlsbad, USA)
MOPS SDS Running Buffer (20x) NuPAGE	Invitrogen (Carlsbad, USA)
Methanol	VWR (Fontenay-sous-Bois, FR)
Methyl green	Sigma-Aldrich Chemie (Steinheim, DE)
M-MLV-RT	Invitrogen (Carlsbad, USA)
Monopotassium phosphate (KH_2PO_4)	Merck (Darmstadt, DE)
Nickel(II)chloride	Sigma-Aldrich Chemie (Steinheim, DE)
NP-40	Roche Diagnostics GmBH (Mannheim, DE)
Non-fat milk powder	Roth (Karlsruhe, DE)
Paraffin	Roth (Karlsruhe, DE)
Paraformaldehyde (PFA)	Sigma-Aldrich Chemie (Steinheim, DE)
Periodic acid	Sigma-Aldrich Chemie (Steinheim, DE)
Phenylmethylsulfonyl Fluoride (PMSF)	Merck (Darmstadt, DE)
PhosSTOP™(phosphatase inhibitor tablets)	Roche Diagnostics GmBH (Mannheim, DE)
Picric acid, 1i2 %	Waldeck GmbH Chroma (Münster, DE)
Pierce ECL Western Blotting Substrate	Thermo-Fischer Scientific (Rockford, USA)
Potassium chloride	Merck (Darmstadt, DE)
Protease & Phosphatase Inhibitor Cocktail, EDTA free	Thermo-Fischer Scientific (Rockford, USA)
qPCR core kit	Eurogentec (Seraing, BE)
Random-primer	Roche Diagnostics GmbH (Mannheim, DE)
Rapid Fixer G354	AGFA Healthcare (Mortsel, BE)
Roti©-Block	Roth (Karlsruhe, DE)
RNA Lysis Solution	Stratec (Berlin, DE)
RNAlater Solution	Ambion Inc. (Austin, USA)
RNAsin recombinant	Promega (Mannheim, DE)
RNeasy© Mini Kit (250)	Qiagen (Hilden, DE)
Rotiblock	Roth (Karlsruhe, DE)

Schiff's Reagent	Merck (Darmstadt, DE)
Sodium acetate	Calbiochem (Darmstadt, DE)
Sodium chloride	VWR (Leuven, BE)
Sodium dodecyl sulfate (SDS)	Biorad (München, DE)
Sodium Hydroxide solution (10 N)	Calbiochem (Darmstadt, DE)
Sodium orthovanadate	Sigma-Aldrich Chemie (Steinheim, DE)
Spectra™ Multicolor Broad Range Protein Ladder	Thermo-Fischer Scientific (Rockford, USA)
Spectra™ Multicolor High Range Protein Ladder	Thermo-Fischer Scientific (Rockford, USA)
Sucrose	Sigma-Aldrich Chemie (Steinheim, DE)
Sulphuric acid	Roth (Karlsruhe, DE)
SYBR Green I	Eurogentec (Seraing, BE)
Temgesic	Reckitt Benckiser Healthcare (Slough, UK)
Tris	Biorad (München, DE)
Tris-HCl	Roth (Karlsruhe, DE)
Triton X-100	Sigma-Aldrich Chemie (Steinheim, DE)
Tween-20	Biorad (München, DE)
VECTASTAIN© Elite© ABC-HRP Kit	Vector Laboratories (Burlingame, USA)
Xylazine, 2 %	Medistar GmbH (Bernburg, DE)
Xylene	Roth (Karlsruhe, DE)

A.4 Software

In Table A.4 the used software is indicated. For a better readability, the different materials will not be refered explicitly in the following.

TABLE A.4: Software

Software	Manufacturer
7300 Systems SDS v1.4.	Applied Biosystems (Foster City, USA)
Geo2R	NCBI (Bethesda, USA)
Graph Pad Prism 6	GraphPad Software, Inc. (LaJolla, USA)
Heatmapper	Wishart Research Group (Alberta, CA)
Image J	Wayne Rasband, NIH Bethesda (MD, USA)
Imaris Software, Version 8.4.1	Bitplane AG (Zurich, SZ)
Keyence BZ II Viewer	Keyence (Neu-Isenburg, DE)
Keyence BZ II Analyzer	Keyence (Neu-Isenburg, DE)
Libre Office calc	The Document Foundation (Berlin, DE)
Magellan™Version 6	Tecan, Newcastle (UK)
ND-1000 V3.8	Thermo-Fischer Scientific (Wilmington, USA)
NDP-view	Hamamatsu Photonics (Hamamatsu, JP)
Texmaker	Pacal Brachet - GNU General Public License Version 2

Appendix B
mRNA-Array

B.1 Used mRNA-Arrays

TABLE B.1: DataSets used for analysis with Geo2R

Series accession number	Title	Disease model	Ref. Figure 4.1	Control Goup (n)	Deseased Group (n)
GSE35226	Systems approach identifies HIPK2 as a critical regulator of kidney tubulointerstitial fibrosis	HIV-associated nephropathy[1]	A	WT-mice (6)	TG26-mice (6)
GSE85409	Transcriptional effects of Pentraxin-2 in fibrotic disease of the kidney	Alport model	B	WT (3)	Alport (3)
GSE32583	Expression data from lupus NZB/W, NZM2410, NZW/BXSB mouse kidneys prenephritic and nephritic	Lupus nephritis	C.1	control (16 weeks) (8)	NZB/W-Hybrids nephritic (23 weeks) (6)
			C.2	control (16 weeks) (8)	NZB/W-Hybrids nephritic (36 weeks) (10)
			C.3	NZM2410 (5)	NZM2410 mice 30 w nephritic (5)
			C.4	NZW/BXSB (non-proteinuric) (6)	NZW/BXSB mice nephritic (18 - 21 weeks) (6)
GSE86444	Characterization of mouse models of lupus nephritis	Lupus nephritis (NZB x NZW F1 with IFNa)	D.1	untreated (3)	interferon-induced lupus 1 w (5)
			D.2	untreated (3)	interferon-induced lupus 3 w (5)
			D.3	untreated (3)	interferon-induced lupus 5 w(5)
			D.4	untreated (3)	interferon-induced lupus 7 w(5)
			D.5	untreated (3)	interferon-induced lupus 9 w(5)
		Lupus nephritis (SFN1 with Pristane)	D.6	untreated (9)	pristrane-induced lupus 14 w(9)

[1]Only the glomerula were analyzed

GSE87024	Tubular epithelial NF-κB activity regulates acute ischemic kideny injury	I/R (17.5 min)	E.1 E.2 E.3	sham (3) sham (3) sham (3)	6 h after I/R (3) 12 h after I/R (3) 6 d after I/R (3)
GSE87023	Tubular epithelial NF-κB activity regulates acute ischemic kideny injury	I/R (17,5 min)	F	sham (6)	I/R 1 d (6)
GSE39548	Transcriptome Analysis of Renal Ischemia/Reperfusion Injury and its Modulation by Ischemic Pre-Conditioning or Hemin treatment	I/R (45 min)	G	sham (4)	I/R 6 h (4)
GSE52004	Acute cellular injury responses in mouse renal ischemic reperfusion injury	I/R bilateral (28 min)	H	sham (2)	I/R (1 d) (4)
GSE36496	Murine Kidney Tissue: Unilateral ureteral obstructed mice vs. Sham control	UUO	I.1 I.2 I.3	sham (3) sham (2) sham (2)	UUO d2 (3) UUO d5 (3) UUO d9 (3)
GSE42303	TIMP2 and TIMP3 have divergent roles in early renal tubulointerstitial injury	UUO d3	J	sham (3)	UUO d3 (3)
GSE38117	Exploring new pathways involved during experimental renal fibrogenesis in the Unilateral Ureteral Obstruction	UUO d8	K	contralateral kidney (3)	UUO d8 (3)
GSE96102	Murine Kidney Tissue: Reversible unilateral ureteral obstructed mice (RUUO) vs. Sham control	reversible UUO	L.1 L.2 L.3	sham (sd: 1d [2], ct: 0d[3] (5)) sham (sd:5, ct: 0) (5) sham (sd:5, ct: 10) (5)	UUO (sd: 1d, ct: 0d) (5) UUO (sd: 5, ct: 0d) (6) UUO (sd: 5, ct: 10d) (5)
GSE96101	Murine Kidney Tissue: Unilateral ureteral obstructed (UUO) mice vs. Sham control	UUO	M.1 M.2 M.3 M.4 M.5 M.6	Sham (6) Sham (6) Sham (6) Sham (6) Sham (6) Sham (5)	UUO (7 h) (6) UUO 12h (6) UUO d1 (6) UUO d3 (6) UUO d5 (6) UUO d7 (5)
GSE121190	Expression Profiling of Fibroblasts in Chronic and Acute Disease Models [4]	UUO (d14)	N	Sham (3)	UUO (3)
GSE54015	Expression data from male and female Schlager hypertensive (BPH/2J) and normotensive (BPN/3J) kidneys	Hypertension (female) Hypertension (male)	O.1 O.2	BPN/3J normotensive (6) BPN/3J normotensive (6)	BPH/2J hypertensive (6) BPH/2J hypertensive (6)

[2]sd: stress (obstruction) duration
[3]ct: collection time after end of stress (obstruction)
[4]Only fibroblasts were analyzed

GSE121190	Expression Profiling of Fibroblasts in Chronic and Acute Disease Models[5]	FA	P.1	control (3)	FA d3 (3)
			P.2	control (3)	FA d7 (3)
			P.3	control (3)	FA d14 (3)

Some animal models or points in time did not yield any significant results and were therefore not included in the Figure. All this arrays are listed in the following:

- Model of lupus nephritis (GSE86444):
  - Interferon-induced lupus nephritis timepoint: week 2: n(control) = 3, n(interferon-induced lupus week 2) = 5
  - Pristrane-induced lupus nephritis: The time points week 2, 4, 8 and 12 showed no significant change in collagen gene expression.
- UUO
  - UUO (GSE36496) n(contralateral) = 3, n(UUO d1) = 3
  - reversible UUO (GSE96102): no significant results were seen for one day of obstruction and collection 10 and 28 days after end of obstruction, as well as for five days of obstruction and collection 28 days after end of obstruction
  - UUO (GSE96101): For very early times after UUO such as 30 min, 1 h, 3 h or 5 h after obstruction, no significant changes in gene expression could be observed.

B.2 Animal models in mRNA-Arrays

These are the animal models used in the analyzed datasets.

Transgenic models

HIV-associated nephropathy (HIVAN). The infection of renal cells by HIV-1 leads to interstitial fibrosis and enhanced glomerular matrix synthesis. HIVAN is the most common cause of renal failure in HIV-1-seropositive patients. This form of renal fibrosis can be studied with the transgenic mouse line TgN(pNL43d14)26Lom ("Tg26") (Avila-Casado et al., 2011).

[5] Only fibroblasts were analyzed

Alport model (Col4a3$^{-/-}$). The Alportsyndrome is an X-linked genetic disease which causes a progressive disorder of basement membranes. Typical symptoms are deafness, anterior lenticonus and progressive glomerulopathy resulting in end-stage kidney disease (Rheault et al., 2004). It is mostly caused by mutations in the COL4A5 gene. The knockout of COL4A3 produces a very similar autosomal form of the disease (Cosgrove et al., 1996).

Spontaneous models of lupus nephritis. Lupus nephritis is a complex chronic autoimmune disease that affects multiple organs. For 50 – 80 % of the patients with lupus, glomerulonephritis can be observed. The kidney involvement is critical for the prognosis of these patients (Grande, 2011). Several mice strains spontaneously develop lupus nephritis.

NZB/W-Hybrids. The NZB-parent strain develops antibodies against thymocitep and red blood cells. The NZW-parent strain develops mesangial glomerulonephritis. The NZB/NZW-hybrids develop high-titer antibodies and an immune complex-mediated glomerulonephritis very simmilar to the human lupus nephritis (Grande, 2011).

NZM2410 mice. This strain develops a highly penetrant lupus-like disease (Blenman et al., 2006).

NZW/BXSB mice. These mice develop an early systemic lupus erythematosus-like disease (Hang et al., 1981).

Hypertension. The kidney plays a major role in blood pressure control via the renin-angiotensin-system. On the other hand, chronic hypertension leads to CKD (Crowley & Coffman, 2014). Schlager BPH-mice are a genetical hypertension model.

Non-surgical models

Lupus nephritis

Pristane-induced lupus. When pristrane is administered into mice abdominal cavity, they develop symptoms similar to those of lupus erythematosus (Freitas et al., 2017).

Interferon-induced lupus. Interferon activates the immunsystem. When given to mice susceptible to lupus, like the NZB/W-hybrids, it induces an early lethal lupus (Mathian et al., 2005).

Folic acid nephropathy. The intraperitoneal administration of a high dose of folic acid is a potent inductor of tubular damage and consequently renal fibrosis. Folic acid crystals are formed in the tubules and folic acid also has a direct nephrotoxic potential (Rabe & Schaefer, 2016).

Surgical methods

Unilateral uretal obstruction model (Section 3.3.1)

Ischemia reperfusion model (Section 3.3.2)

B.3 R-script used in Geo2R

The following R script, used for the comparison of WT-mice vs. Tg26-mice in GSE35226, illustrates how the results were calculated.

```
# Version info: R 3.2.3, Biobase 2.30.0, GEOquery 2.40.0,
limma 3.26.8
# R scripts generated  Thu Apr 26 11:16:51 EDT 2018

################################################################
#   Differential expression analysis with limma
library(Biobase)
library(GEOquery)
library(limma)

# load series and platform data from GEO

gset <- getGEO("GSE35226", GSEMatrix =TRUE, AnnotGPL=TRUE)
if (length(gset) > 1) idx <- grep("GPL1261", attr(gset, "names"))
else idx <- 1
gset <- gset[[idx]]

# make proper column names to match toptable
fvarLabels(gset) <- make.names(fvarLabels(gset))

# group names for all samples
gsms <- "111111000000"
sml <- c()
for (i in 1:nchar(gsms)) { sml[i] <- substr(gsms,i,i) }
```

```
# log2 transform
ex <- exprs(gset)
qx <- as.numeric(quantile(ex, c(0., 0.25, 0.5, 0.75, 0.99, 1.0),
na.rm=T))
LogC <- (qx[5] > 100) ||
          (qx[6]-qx[1] > 50 && qx[2] > 0) ||
          (qx[2] > 0 && qx[2] < 1 && qx[4] > 1 && qx[4] < 2)
if (LogC) { ex[which(ex <= 0)] <- NaN
  exprs(gset) <- log2(ex) }

# set up the data and proceed with analysis
sml <- paste("G", sml, sep="")    # set group names
fl <- as.factor(sml)
gset$description <- fl
design <- model.matrix(~ description + 0, gset)
colnames(design) <- levels(fl)
fit <- lmFit(gset, design)
cont.matrix <- makeContrasts(G1-G0, levels=design)
fit2 <- contrasts.fit(fit, cont.matrix)
fit2 <- eBayes(fit2, 0.01)
tT <- topTable(fit2, adjust="fdr", sort.by="B", number=250)

tT <- subset(tT, select=c("ID","adj.P.Val","P.Value","t","B",
"logFC","Gene.symbol","Gene.title"))
write.table(tT, file=stdout(), row.names=F, sep="\t")


################################################################
#   Boxplot for selected GEO samples
library(Biobase)
library(GEOquery)
```

Appendix C
Antibodies that could not be established

C.1 Immunohistochemistry

All antibodies were tested in a standardized manner, with different fixation methods and antigen retrieval methods. The fixations methods with their specific characteristics are described in Table C.1. Following antigen-retrieval methods were used:

- Heat-mediated antigen retrieval methods:
  - Citrate antigen retrieval with a citric acid based antigen unmasking solution (Vector, 3x5 minutes in the microwave),
  - Tris-EDTA pH9 (see 3.5.2, 5 minutes in the microwave),
- Enzymatic antigen retrieval
  - Proteinase K
  - Fast Enzyme
- HCl (see Table C.2)

TABLE C.1: Methods for tissue Fixation

Method	Specifics
Methacarn	no antigen retrieval needed
Formalin	3x5 minutes citrate antigen retrieval
Cryo-sections	Fixation for 10 minutes in -20°C acetone
	Fixation for 10 minutes in -20°C methanol

TABLE C.2: Hydrochloric Acid (HCl) solution

10 N HCl	20 ml
A. dest	80 ml
pH	0.6-0.9

When the antibodies showed too much unspecific staining, reducing the background with an avidin-biotin block or blocking with serum (1/5000) was tried.

Despite all efforts some antibodies could not be stained in murine kidneys (see Table C.3).

TABLE C.3: Not-established antibodies in IHC

Name	Host species	Supplier	Catalog-Nr.
Collagen VII	rabbit (polyclonal)	Sigma-Aldrich (Steinheim)	SAB4500390
Collagen XIII	sheep (polyclonal)	R&D systems (Wiesbaden-Norderstadt)	AF4627
Collagen XV	rabbit (polyclonal)	Antibodies Online (Aachen)	ABIN965912
Collagen XVI	rabbit (polyclonal)	Thermo-Fischer Scientific (Rockford, USA)	PA5-38893
Collagen XXIII	rabbit (polyclonal)	Abcam (Cambridge, UK)	ab204578
Lumican	rabbit (monoclonal)	Abcam (Cambridge, UK)	ab168348

C.2 Western blot

To get a distinct signal, different blocking methods were tested while establishing antibodies for western blot (see Table C.4). Nevertheless, for the antibodies listed in Table C.5 no specific or no signal could be obtained for urea-kidney-lysates.

TABLE C.4: Blocking methods used for establishing WB

Bovine serum albumine (BSA)	1-3%
Milk powder (NFDM)	3-5%
Rotiblock	10%

TABLE C.5: Not established antibodies in WB.

Name	Host species	Supplier	Catalog-Nr.
Collagen VII	rabbit (polyclonal)	Sigma Aldrich (Steinheim)	SAB4500390
Collagen XIII	sheep (polyclonal)	R&D systems (Wiesbaden-Norderstadt)	AF4627
Collagen XV	rabbit (polyclonal)	Antibodies Online (Aachen)	ABIN965912

Acknowledgements

In the following, I would like to thank all persons who contributed to the success of the experiments carried out in this doctoral thesis and without whose support my thesis would not have been completed in this form.
First and foremost, I would like to mention Prof. Dr. Peter Boor and Dr. Barbara Klinkhammer, who have provided me with excellent support over all the years since the beginning of my doctoral thesis and with whom I was always able to discuss solutions to problems. Their expertise, optimism, patience and motivation were essential for the success of this work.
I would like to thank Prof. Dr. Jürgen Floege for the opportunity to write my dissertation in his department and for the interest in my project. I would also like to thank him and Prof. Dr. Joachim Jankowski for taking over the review of this dissertation.
Without my dear colleagues who always supported me with constructive ideas and gave me technical support my thesis would not look the same. Thanks goes to Dr. rer. nat. Sonja Djudjaj, PHD Dickson Wong, Jana Baues, Dr. rer. nat. Eva Miriam Buhl, Dr. med. Roman Bülow, Patrick Droste, Katja Ermert, Christina Gianussis, Ting Jia, Gertrud Minartz, Simon Otten, Sophie Reichelt, Marie Cherelle Timm, Tong Xu.
Finally, I would like to thank my family and Daniel for their mental support during the doctorate as well as for the proofreading of this dissertation.

Erklärung § 5 Abs. 1 zur Datenaufbewahrung

Hiermit erkläre ich, dass die dieser Dissertation zu Grunde liegenden Originaldaten bei meinem Betreuer, Universitätsprofessor Dr. med. Peter Boor, PhD, Institut für Pathologie des Universitätsklinikums Aachen, hinterlegt sind.

Paula Marie Tyra

Eidesstattliche Erklärung gemäß § 5 Abs. (1) und § 11 Abs. (3) 12. der Promotionsordnung

Hiermit erkläre ich, Paula Marie Tyra, an Eides statt, dass ich folgende in der von mir selbstständig erstellten Dissertation „Collagen expression in renal fibrosis“ dargestellten Ergebnisse erhoben habe.
Bei der Durchführung der Arbeit hatte ich folgende Hilfestellungen, die in der Danksagung angegeben sind.

	Paula Marie Tyra	Prof. Peter Boor (Doktorvater)	Dr. rer nat. Barbara Klinkhammer (praktische Betreuung)	Technische AssistentenInnen (Jana Baues, Christina Ginaussis, Simon Otten, Cherelle Timm)	Summe (%)
Studiendesign Konzeption	50	30	20		100
In vivo Experimente			80	20	100
Bereitstellung von histologische Schnitten				100	100
Durchführung der experimentellen Versuche (alle ausgenommen *in vivo* Versuchen)	95			5	100
Statistische Auswertung	100				100
Interpretation der Datenauswertung	60	20	20		100

_____
Paula Marie Tyra

Als Betreuer der obigen Dissertation bestätige ich die Angaben von Paula Tyra

_____
Universitätsprofessor Dr. med. Peter Boor, PhD